A ZERO LIQUID DISCHARGE METHOD FOR CO-DISPOSING COAL FLY ASH AND FLUE GAS DESULFURIZATION (FGD) BRINES: ZERO VALENT IRON REDUCTION AND SOLIDIFICATION/STABILIZATION

A Dissertation
Presented to
The Academic Faculty

by

Wenlong Zhang

In Partial Fulfillment
of the Requirements for the Degree
Doctor of Philosophy in the
School of Civil and Environmental Engineering

Georgia Institute of Technology
May 2019

A ZERO LIQUID DISCHARGE METHOD FOR CO-DISPOSING COAL FLY ASH AND FLUE GAS DESULFURIZATION (FGD) BRINES: ZERO VALENT IRON REDUCTION AND SOLIDIFICATION/STABILIZATION

Approved by:

Dr. Ching-Hua Huang, Advisor
School of Civil and Environmental Engineering
Georgia Institute of Technology

Dr. Yongsheng Chen
School of Civil and Environmental Engineering
Georgia Institute of Technology

Dr. Susan Burns
School of Civil and Environmental Engineering
Georgia Institute of Technology

Dr. Yuanzhi Tang
School of Earth and Atmospheric Engineering
Georgia Institute of Technology

Dr. Kimberly Kurtis
School of Civil and Environmental Engineering
Georgia Institute of Technology

Date Approved: [March 27th, 2019]

ACKNOWLEDGEMENTS

I thank Dr. Ching-Hua Huang for her tremendous effort for guiding me through this process. I thank her for giving me the chance to fulfill my dream of obtaining my Ph.D. I thank her help and encouragement not only on my research, but also on my family. I thank her for being such a great role model as a teacher.

I thank my parents and parents in law for supporting my study and my family during this process.

I thank my wife for everything she has done.

I thank my three children, Abbie, Anna, and Allen, for all the joy and hope you brought to me.

I thank Dr. Yongsheng Chen, Dr. Kimberly Kurtis, Dr. Yuanzhi Tang, and Dr. Susan Burns for their guidance in this work.

I thank Dr. Guangxuan Zhu for his support on the analytical instruments.

I thank Jay Renew, Kirk Ellison and Benjamin Gallagher for all the research ideas and supports.

I thank Environmental Research and Education Foundation (EREF), Southern Company, and Georgia Power for research funding.

TABLE OF CONTENTS

LIST OF TABLES

LIST OF FIGURES

LIST OF SYMBOLS AND ABBREVIATIONS

ABMet	Advanced Biological Metals Removal
AFm	Alumina, ferric oxide, mono-sulfate
AFm-Cl	Friedel's salt
Aft	Alumina, ferric oxide, tri-sulfate
AFt-SO4	Ettringite
AIP	Activated Iron Process
As(III)	Arsenite
As(V)	Arsenate
ASTM	American Society of Testing and Materials
BCFA	Bituminous coal fly ash
CCP	Coal combustion products
CCR	Coal combustion residuals
CFA	Coal fly ash
Cr(VI)	Chromate
CSF	Chemical speciation fingerprint
C-S-H	Calcium silicate hydrate
DBPs	Disinfection Byproducts
EIA	Energy Information Administration
ELG	Effluent Limitation Guidelines
FE-SEM	Field emission scanning electron microscopy
FGD	Flue gas desulfurization
FS	Friedel's salt

GR	Green rust
HAA5	Haloacetic acids
IC	Ionic chromatography
ICP-OES	Inductively coupled plasma-optical emission spectroscopy
K	Hydraulic conductivity
LDH	Layered double hydroxides
MATs	Mercury and Air Toxics Standards
MCL	Maximum contaminant level
Monophase	AFm phase
MSWI	Municipal solid waste incineration
mZVI	Micron-sized zero-valent iron
nZVI	Nano zero-valent iron
PC	Portland cement
PI	Principal investigator
QXRD	Quantitative x-ray diffraction
S/S	Solidification/stabilization or solidified/stabilized
SCFA	Sub-bituminous coal fly ash
Se(IV)	Selenite
Se(VI)	Selenate
TCLP	Toxicity characteristic leaching procedure
TDS	Total dissolved solids
TTHM	Total trihalomethane
TVA	Tennessee Valley Authority
U.S.	United States
USEPA	United States Environmental Protection Agency

XAFS	X-ray absorption fine structure
XRD	X-ray diffraction
XRF	X-ray fluorescence
ZLD	Zero liquid discharge
ZVI	Zero-valent iron

SUMMARY

The United States coal-fired power industry is facing new challenges related to the management and treatment of coal combustion residuals (CCRs) and flue gas desulfurization (FGD) wastewater due to more stringent regulations on these wastes and growing needs for better environmental stewardship. The United State Environmental Protection Agency (USEPA) has determined that the wastes generated from the wet FGD systems and coal ash-handling systems contribute the largest proportion of contaminant loading from coal-fired power plants to the environment. To address these challenges, the coal-fired power industry is in urgent need of new strategies for treatment of CCRs and wastewater to meet the discharge limits required by new regulations. Among treatment options, the zero liquid discharge (ZLD) method by combining concentration of FGD wastewater to brine and treatment of the brine with coal fly ash (CFA) through a solidification/stabilization (S/S) process has gained significant interests. This ZLD method is attractive because it has the potential of treating both wastes (CCRs and FGD wastewater) in the same process, eliminating the need for wastewater discharge, and maximizing water recycling at the power plants. A limited amount of previous research has demonstrated this co-disposal S/S process to be a promising ZLD method for effective heavy metal immobilization. However, it was also found that oxidized forms of heavy metals, such as selenate (Se(VI)) and chromate (Cr(VI)), remain challenging to treat due to their high mobility and require improvement on their immobilization efficiency. Furthermore, the impacts of reaction conditions during the S/S process and the mineralogy of the S/S solids on the performance of this ZLD method in contaminant immobilization

need to be better understood in order to optimize this method to achieve the highest effectiveness.

The first part of this thesis investigated the performance of aged, micron-sized zero-valent iron (ZVI) in treating the simulated and real FGD hot brines for enhanced heavy metal removal. The results demonstrated that high temperature and Mg^{2+} are the dominant factors that will enhance ZVI's reactivity for the removal of selenate, arsenate, cadmium, and chromate in brine matrices. At 80°C, almost 100% of arsenate (1 mg/L) and chromate (1 mg/L) can be removed in less than 5 minutes using 4.17 g/L of ZVI in simulated brines, while selenate (25 mg/L) and cadmium (5 mg/L) can be completely removed within 30 minutes. Once the ZVI is corroded, the formation of green rust (GR) leads to the removal of heavy metals. Mg^{2+} ions naturally present in FGD brines play an important role in the depassivation of aged ZVI. The main contribution of this work is addressing the knowledge gap regarding the removal of heavy metals by ZVI in high salt and high temperature conditions. This work demonstrates that ZVI is an effective material for removing heavy metals in hot FGD brines generated through thermal evaporation at power plants, and the ZVI treatment should be considered post evaporation of FGD wastewater.

The second part of this thesis investigated the S/S process for the co-disposal of FGD brine and CFA for heavy metal and chloride immobilization by evaluating the effects of different CFAs (bituminous (BCFA) and sub-bituminous (SCFA)) and activating agents (Portland cement (PC) and lime), as well as the pretreatment of brines by ZVI on the S/S process. The pre-treatment of FGD brine by ZVI enhanced the retainment of heavy metals (Se(VI), As(V), Cd(II) and Cr(VI) when BCFA was used but not when SCFA was used, primarily because the SCFA S/S solids already performed quite well without ZVI

pretreatment. The formation of Friedel's salt was critical in the retainment of heavy metals and chloride. S/S solids made with SCFA contained a higher amount of Friedel's salt because SCFA contained a higher content of lime and reactive aluminate than BCFA. With the same type of CFA, using lime as the activating agent provided more alkalinity that PC, which could further enhance the formation of Friedel's salt. The main contributions of this work include demonstrating the effects of different S/S recipes and identifying the importance of Friedel's salt for the contaminant immobilization. The results of this work suggest that optimizing the mineralogy in the S/S solids is a promising approach to enhance the performance of the S/S process.

The third part of this thesis investigated the optimization of mineralogy in co-disposed FGD brines and BCFA to improve heavy metal and chloride immobilization. The results demonstrated that enhancing the formation of Friedel's salt in the S/S solids greatly reduced the leaching of contaminants (Se and chloride). S/S solids made with 10% lime, 2.5% sodium aluminate, 30-35% of FGD brine and 52.5-57.5% of BCFA (by mass) could retain the majority of halides (>50%), selenate (>90%), arsenate (>99%) and chromate (>99%) from the brine after nine weeks of long-term leaching tests. In terms of enhancing the formation of Friedel's salt, aluminate addition along with an adequate amount of lime was most important. The main contribution of this work is further demonstrating that optimizing the mineralogy in the S/S solids could enhance the performance of the S/S process in contaminant immobilization. The results of this work also suggest that the hydraulic conductivity of the S/S solids could be another important factor for contaminant leaching because it could affect the stability of Friedel's salt under leaching condition.

Meanwhile, it could also govern the immobilization of halides because the halide concentration from the brine exceeds the binding capacity of Friedel's salt.

The fourth part of this thesis aimed to better understand the process of Friedel's salt in removing heavy metals by investigating the effects of various anions on the removal of selenate and chromate by Friedel's salt. The results from sorption and desorption tests indicated that the uptake of Cr(VI) by Friedel's salt was more favorable than Se(VI). Sulfate and carbonate demonstrated a stronger hindering effect than nitrate and chloride for the uptake of both heavy metals by Friedel's salt. The stability of Friedel's salt in the S/S solids over the long-term leaching conditions was also an important factor that needed to be considered. This study also demonstrated that the slow transformation from Friedel's salt to stratlingite is a possibility since the CFA can provide reactive silicate and aluminate which are required for this transformation to occur. The main contributions of this work include providing more insights into the effects of various anions on the uptake mechanism of Friedel's salt for Se(VI) and Cr(VI), and revealing the transformation from Friedel's salt to stratlingite over the long term.

CHAPTER 1. INTRODUCTION

1.1 SCOPE OF THE WORK

The overall objective of this study was to investigate and optimize the ZLD method of co-disposal of FGD brines and CFAs through a S/S process. The research focused on two aspects in achieving high efficiency for the immobilization of heavy metals and halides from the FGD brines and CFAs. The first aspect was the utilization of an iron-based reduction process as a pretreatment for the FGD brines to enhance removal of heavy metals, particularly for heavy metal oxyanions. Then, the treated FGD brines were applied in the S/S process with CFAs under different conditions and the overall heavy metal and halide immobilization efficiency by the S/S solids was evaluated by different leaching methods. The second aspect was the investigation of the mineral phases in the S/S solids formed and their roles in heavy metal and halide immobilization, and of potential strategies to enhance the formation such mineral phases in the S/S process. To obtain a fundamental understanding of the key mineral, Friedel's salt, in facilitating heavy metal and chloride immobilization, pure form of this mineral was synthesized and studied for its mechanisms in Se(VI) and Cr(VI) uptake under different conditions. Overall, the results were used to identify the optimal approach and conditions for a successful ZLD method that will generate S/S solids with minimized leaching potential of heavy metal and halide contaminants.

In the first approach, aged zero valent iron (ZVI) was applied to pretreat the FGD brine for heavy metals removal. The chemistry, speed and effectiveness of this pretreatment process were evaluated, and the reaction conditions were optimized. The

results suggested that aged ZVI was an effective material to remove the heavy metals in the hot FGD brine. Once the reaction conditions of this pretreatment process were optimized, the pretreated FGD brine was applied in the S/S process to evaluate the impact of this pretreatment process by comparing the heavy metal retainment between S/S processes with and without the pretreatment of brine by ZVI. The results suggested that the ZVI pretreatment of brine enhanced the performance of S/S solids made with BCFA, but not with SCFA since the SCFA S/S solids already performed well without the pretreatment. Friedel's salt was identified as the key mineral phase which was responsible for the retainment of oxyanion heavy metals as well as halides.

In the second approach, the mineral formation in the S/S solids made with BCFA, especially Friedel's salt and ettringite, was optimized through adjusting the mixing recipe for the generation of S/S solids. The results suggested that the addition of reactive aluminate with an adequate amount of lime enhanced the formation of Friedel's salt, and the S/S solids with higher Friedel's salt formation generally retained more selenate, chromate, and halides. Ettringite formation only enhanced the retainment of borate, but not the other contaminants being studied. To further understand the role and fate of Friedel's salt in the S/S solids, pure Friedel's salt was synthesized and its performance on selenate and chromate removal was evaluated at different high salt conditions contributed by different anions. Slow transformation from Friedel's salt to stratlingite was also observed when Friedel's salt was exposed to reactive aluminate and silicate for three months, and this transformation only enhanced the desorption of selenate on the surface of the Friedel's salt, but not inside the interlayers.

1.2 OUTLINE OF THESIS

This thesis includes a general introduction of the topics, followed by four chapters of specific research foci, and the conclusions for the overall work. Chapter 1 provides an overview of the FGD wastewater, ZLD approach, ZVI on heavy metal removal, S/S process, CFA, and mineralogy of S/S solids.

Chapter 2 evaluates the performance of aged ZVI on heavy metals removal (Se, As, Cd, and Cr) in the FGD brine. The optimized reaction conditions were also applied to treat the real FGD brine. The reacted ZVI was also characterized by XRD to determine the mechanism for heavy metal removal.

Chapter 3 evaluates the immobilization of heavy metals by the S/S solids made with BCFA or SCFA with PC or lime as the activating agent. The impact of brine pretreatment by ZVI on the overall S/S process was also evaluated. Short-term leaching tests (USEPA 1311 AND 1313) and the long-term leaching test (USEPA 1315) were applied to evaluate the leaching of heavy metals from different S/S solids. The mineralogy of S/S solids before and after the leaching tests were characterized by XRD and SEM to determine the most likely phases for heavy metal immobilization.

Chapter 4 optimizes the mineralogy of S/S solids made with BCFA through adjusting the mixing recipes. The roles of Friedel's salt and ettringite on the retainment of heavy metals and halides were evaluated. The weight percentages of Friedel's salt and ettringite were obtained by quantitative XRD analyses, and they were correlated to the long-term leaching trends of heavy metals and halides.

Chapter 5 evaluates the selenate and chromate removal by Friedel's salt under the impacts of different anions. The slow transformation from Friedel's salt to stratlingite was

observed, and the impact of this transformation on selenate removal was also evaluated. XRD was applied to monitor the phase change over time to evaluate the fate of Friedel's salt when exposed to different anions.

Chapter 6 provides the overall conclusions of this work and recommendations for future research directions regarding these topics.

1.3 BACKGROUND KNOWLEDGE

1.3.1 FGD Wastewater

The FGD-purge wastewaters at coal-fired power plants contain significant concentrations of heavy metals (e.g. Se, As, Cr, Cd and Hg) and large amounts of salts (e.g. Cl^-, Ca^{2+}, Mg^{2+}, Na^+ and SO_4^{2-}),[1] which will contaminate receiving water bodies if discharged without proper treatment. Table 1.1 presents the concentration range of all the significant elements in the FGD wastewater. At present, the most commonly used FGD technology is the wet limestone/lime-gypsum system.[2] Limestone ($CaCO_3$) or lime ($Ca(OH)_2$) is used as the absorber for SO_2 in flue gas. Along with SO_2, heavy metals are also removed and accumulated in the FGD slurry. In a forced oxidation FGD system, air is pumped up through the FGD tower to completely oxidize SO_3^{2-} to SO_4^{2-} which precipitates as $CaSO_4 \cdot 2H_2O$ (gypsum), a salable product for wallboard or soil amendment.[3] The forced oxidation systems are more common and the USEPA noted that it expected the majority of new wet FGD systems constructed at coal plants to be of the forced oxidation type.[4] However, heavy metals including Se and Cr can be oxidized into Se(VI) and Cr(VI) along with SO_3^{2-} in these forced oxidation systems. [5] Moreover, FGD wastewater also contains significant concentrations of Ca^{2+} (from the alkaline sorbent) and Cl^- (from the coal). Thus,

FGD wastewater from forced oxidation FGD systems can be difficult to treat. To reduce the amount of toxic metals and other pollutants discharged from coal plants, the USEPA released the Steam Electric Power Effluent Limitation Guidelines (ELG) in 2015, which set stringent limits on As, Hg, Se and other pollutants' release to the environment from FGD wastewater.[6] The revised guidelines set the strict discharge limits for Se (12 µg/L), As (8 µg/L) and Hg (356 ng/L) at the maximum 30-day average limits. However, due to the technical difficulty and financial burden to comply with this regulation, implementation of the ELG has been postponed for another two years.

Table 1.1. Concentration range of typical FGD wastewater.[7]

Parameter	Concentration (mg/L)	Parameter	Concentration (mg/L)
TSS	250 – 25,000	**Boron**	1 - 10
TDS	15,000 – 35,000	**Cadmium**	0.05 – 0.1
pH	4 – 7	**Chromium**	0.3 – 1.0
Chloride	10,000 – 25,000	**Cobalt**	0.1 – 0.8
COD	200 – 500	**Copper**	0.2 – 0.8
Ammonia	20 – 60	**Iron**	80 – 400
Nitrate	30 – 120	**Mercury**	0.01 – 0.8
Calcium	300 – 5,000	**Nickel**	2 – 7
Magnesium	50 – 4,000	**Lead**	0.5 – 1.5
Sulfate	3,000 – 5,000	**Zinc**	0.5 – 1.0
Fluoride	40 - 100	**Manganese**	3 – 20
Aluminum	20 - 200	**Selenium**	1 – 4
Arsenic	0.5 – 0.8	**Vanadium**	2 - 15

1.3.2 Methods for Treating the FGD Wastewater

In terms of treating FGD wastewater, traditional technologies include chemical precipitation, which could be coupled with either biological treatment or zero-valent iron reduction-based treatment. The chemical precipitation process involves multi-stage chemical injections to generate hydroxide precipitates, iron co-precipitates and sulfide precipitates.[8] Advanced Biological Metal Removal (ABMet) designed by General Electric's has demonstrated successful treatment for selenate and nitrate in the FGD wastewater. [9-10] However, the biological process will be very sensitive to compositional fluctuations of the FGD wastewater, thus making its performance not reliable. Zero valent iron (ZVI)-based reduction processes, such as traditional ZVI and Siemens' Activated Iron Process™ (AIP), have been shown to remove arsenic, mercury, and selenium (including selenate) to low levels.[11-17] However, one of the major drawbacks of the ZVI process is that the ZVI surface becomes corroded with passive iron oxide layers when in contact with wastewater.[15-17] These layers can decrease the reactivity of the ZVI toward target contaminants by limiting the flow of electrons from the ZVI to target contaminants under the iron oxide.[15-17]

The ZLD options have gained significant interests from the coal-fired power industry because of the elimination of environmental wastewater discharge and water reuse maximization in power plants.[18] Potential ZLD technologies for FGD wastewater include traditional falling film evaporators/crystallizers, wastewater spray dryers, brine concentrators, and advanced membrane processes. At coal-fired power plants, thermal evaporation related technology could be the most convenient method to concentrate the FGD wastewater. Both Duke Energy's Mayo Plant near Roxboro, North Carolina and the Public Service of New Hampshire's Merrimac Station installed thermal evaporation

systems in ZLD strategies to treat FGD wastewater. The hot brine generated will contain significant amounts of heavy metals and high concentrations of salts. To our knowledge, the method regarding the heavy metal removal in hot brine conditions is still very rare in the field.

1.3.3 ZVI on Heavy Metals Removal

Heavy metals: Within the scope of this study, selenium, chromium, arsenic and cadmium were chosen as the targets of interest. Among all the heavy metals within the FGD wastewater, Se(VI) as in selenate is likely the most challenging heavy metal to be immobilized due to its complex redox chemistry and high mobility.[19-22] The United States Environmental Protection Agency (USEPA) has set a maximum contaminant level (MCL) of selenium at 50 ppb for drinking water. Se(IV) as in selenite can be immobilized more easily than Se(VI). However, it remains challenging to reduce selenate to selenite effectively in the complex FGD wastewater brine. While bioremediation methods have been applied to remove some selenium contaminated water using selenium reducing bacteria,[9, 23] the very high chloride and TDS concentrations in concentrated FGD brines will likely seriously inhibit the biological process. Chromium, particularly in the form of Cr(VI) as in chromate, is highly soluble and thus poses a larger threat to human health.[24] The USEPA regulated the MCL of chromium at 100 ppb in drinking water. Compared to the much less soluble Cr(III), Cr(VI) as in chromate is more soluble and thus brings a larger threat to human health. The removal of Cr(VI) can be achieved by reduction to Cr(III) followed by precipitation.[25-26] Arsenic is recognized as a highly toxic heavy metal with a regulated MCL of 10 ppb in drinking water. As(III) is more toxic than As(V) because As(III) can be transported into the cell by binding to specific proteins.[27] Due to arsenic's

high toxicity and accidents worldwide, a wide range of treatment methods have been developed including adsorption, oxidation, precipitation, coagulation and membrane separation.[28] Cadmium is also a toxic heavy metal with a regulated MCL of 5 ppb in drinking water.[29] Cd(II) could be removed from aqueous phase through various ways including precipitation, ion exchange, adsorption and solvent extraction.[30]

ZVI: ZVI has been shown to effectively remove a variety of contaminants such as selenate, chromate, nitrate, phosphate and chlorinated hydrocarbons.[19-22, 24, 31-38] ZVI is a moderately strong reducing agent which is readily available, non-toxic and inexpensive.[35] Although its reactivity on heavy metal removal has been well studied by many researchers, to our knowledge, it has not been tested in concentrated FGD wastewater brine. Huang et al. has conducted a successful field study using their hybrid ZVI system to immobilize heavy metals and nitrate in FGD wastewater;[21-22] however, the chemistry between FGD wastewater and its concentrated brines is expected to be quite different due to the significantly higher concentrations of salts and other components in the brines. Therefore, evaluating the effectiveness of ZVI on heavy metal removal in real FGD wastewater brine is an important study when associated with the development of ZLD method.

The reactivity of ZVI on heavy metals removal is owing to its corrosion intermediates containing Fe(+II)-Fe(+III) hydroxyl salts which are known as green rust (GR).[35, 39-41] Green rusts are layered double hydroxides (LDH) composed of positively charged octahedral layers of Fe(+II) and Fe(+III) hydroxides with interlayers containing water molecules and anions.[42-44] GRs with planar anions (e.g., Cl^-, Br^-, and CO_3^{2-}) are classified as Type 1 (GR-1), and those with tetrahedral anions (e.g., SO_4^{2-} and SeO_4^{2-}) are classified as Type 2 (GR-2).[39-40] The molecular formula of GR can generally be represented as

$[Fe(+II)_{(1-x)}Fe(+III)_x(OH)_2]^{+x}\cdot[(x/n)A^{-n}\cdot(m/n)H_2O]^{-2}$, where A represents the anion.[41-43] Green rusts have been reported for their capability of reducing a variety of contaminants including selenite,[41, 43-47] chromate,[26, 48-51] nitrate,[52-53] and chlorinated hydrocarbons.[54-56] Further oxidation of GR will lead to goethite (a-FeOOH), lepidocrocite (γ-FeOOH), maghemite (γ-Fe_2O_3), or magnetite (Fe_3O_4), depending on the pH, rate of oxidation and dehydration of GR.[45]

The electrochemical corrosion of ZVI can be affected by various factors such as temperature, pH, mixing, ZVI size, ionic strength, different levels of various anions and the coexistence of other heavy metals.[32, 35-38, 57-60] Lower starting pH promotes the corrosion of ZVI and helps the formation and release of Fe(II), which later involves in the formation of Fe(+II)-Fe(+III) hydroxyl layer that gives rise to the reactivity of ZVI.[32, 36] Different levels of various anions and metal ions could affect the composition of active layer around ZVI, which directly affects the reactivity of ZVI on contaminant removal.[35-36] In term of size of ZVI, nano-sized ZVI (nZVI) has the advantage over micron-sized ZVI (mZVI) because nZVI has larger reactive surface area, therefore leading to a faster remediation of contaminates.[60] At high temperatures, ZVI-based material is found to be more reactive in removing chromium, arsenic, and nitrate.[38, 61-62] This enhanced performance might be attributed to the enhanced diffusion of metal ions and enhanced formation of active sites.[63-64]

The mechanism of contaminant removal by ZVI in aqueous systems has been studied by various researchers.[24, 32, 35-36, 65-67] However, most of the studies were focused on one or a few contaminants in a fairly “clean” aqueous system compared to in a more complex FGD brine. Also, most studies were done under anoxic condition, especially for nZVI

because a passive iron oxide layer can easily form when the particles are exposed to air. It is well known that once the passive layer is formed, the reactivity of ZVI will be hindered unless the passive layer is destructed.

Removal of Se(VI) by ZVI: Zhang et al. studied the effect of different anions on the selenate removal by ZVI. [35] They observed the formation of GR-1 in the chloride solution, and GR-2 in the sulfate solution. The composition of GR-1 with chloride was shown as $[Fe(+II)_3Fe(+III)(OH)_8Cl]$,[40] and the composition of GR-2 with sulfate as $[Fe(+II)_4Fe(+III)_2(OH)_{12}]^{+2}[SO_4^{2-} \cdot 2H_2O]^{-2}$.[39] Both GR-1 and GR-2 were shown to remove selenate very effectively.[41, 44-46] Under anoxic condition, selenate can be reduced to elemental selenium inside the GR interlayer. Even under oxic condition, Refait et al. showed that the reduction from selenate to selenite was still thermodynamically possible in the presence of dissolved oxygen.[41] The removal of selenate by GR can both be described as a two-step process. The first step involves the uptake of selenate by iron (hydr)oxide through the interlayer anions exchange. Schellenger and Larese-Casanova observed a faster selenate uptake rate by GR-Cl than that by GR-SO_4.[44] The second step involves the reduction of Se(+VI) to its lower oxidation states. The rate of reduction will be dependent on structural Fe(+II) abundance, which relates to pH and the amount of oxidant in the solution. [35, 41, 44]

Removal of Cr(VI) by ZVI: Li et al. showed that nano ZVI particles can effectively remove chromium by reduction and immobilization; Cr(VI) was rapidly reduced to Cr(III) which was then immobilized on iron oxide layers on ZVI nano particles. [24] Similar to selenate, chromate is also reported to have a faster reduction rate with GR-Cl than GR-SO_4.[49] Chromium incorporated iron oxyhydroxide layer will form a Cr-Fe hydroxide

represented by a formula of $Cr_{0.67}Fe_{0.33}(OH)_3$ or $Cr_{0.67}Fe_{0.33}OOH$.[24] Chromate is thermodynamically more easily reduced than selenate according to their reduction potentials. This means that reductants such as GR capable of reducing selenate are expected to reduce chromate readily.

Removal of As(V) by ZVI: Kanel et al. studied the removal of arsenate in groundwater by nZVI and showed that As(V) could rapidly adsorbed to the nZVI surfaces by forming an inner-sphere surface complexation. Reduction from As(V) to As(III) could also happen by at a slow rate (25% reduction over 90 days). [68] Like other oxyanions, As(V) can be also easily reduced by various types of GRs.[69-71]

Removal of Cd(II) by ZVI: Li et al. studied the metal cation sequestration by nZVI and showed that Cd(II) can be immobilized at the nZVI surfaces by both adsorption and reduction to elemental Cd.[72] The same mechanism was also proposed by other studies,[73-74] but the formation of GR was not mentioned or observed. Although removal of Cd(II) by GR is not well reported in the literature, O'Loughlin et al. studied the reduction of several transition metal cations, including Ag(I), Au(III), Cu(II), and Hg(II) by GR, and showed that all these metal cations could be reduced to their zero-valent state.[75] Therefore, Cd(II) could be also immobilized by GR.

1.3.4 Solidification and Stabilization (S/S) with CFA

S/S: The S/S process includes the mixing of wastes (liquids, sludges, or solid waste) with Portland cement, Portland cement/coal fly ash, or coal fly ash/lime.[76-85] The USEPA regards S/S to be an established treatment technology for more than 57 wastes.[86-87] S/S has been shown by many studies to be a viable treatment process for many heavy metal bearing

solid wastes.[76-77, 80, 82-96] S/S consists of two processes: solidification (producing a solid product with improved physical properties) and stabilization (process of converting a contaminant of concern to its less mobile and less toxic forms).[76]

Fly ash has successfully replaced a portion of Portland cement in several S/S mixture applications.[80, 84-85, 90-92, 97-103] The combination of Portland cement and coal fly ash appear to optimize the S/S process. Portland cement/coal fly ash S/S mixtures trap metals into the matrix better than purely pozzolanic processes involving lime.[104] Replacement of a portion of Portland cement with fly ash has been shown to enhance S/S mixtures versus pure Portland cement mixes by forming a less permeable solid.[76, 104-105] Coal fly ash has been utilized in S/S mixtures to immobilize numerous waste streams which include significant concentrations of heavy metals typically found in fly ash including arsenic, mercury, selenium, cadmium, and chromium.[82, 85, 91-92, 96, 106-107]

Effect of CFA: The properties of CFA are highly influenced by the type of fuel (coal) and the combustion conditions.[108] In 2017, 774.6 million tons of coal was produced in the U.S., and approximately 45.6% of the coal produces BCFA and 45.4% produces SCFA, and about 92.8% of the total coal use was for energy production.[109] The most significant difference between these two CFAs is the higher CaO content in SCFA. SCFA with CaO contents >20% can be classified as cementitious materials.[110] Once mixed with water, the resulting slurry will be cured over time through pozzolanic reactions to generate the S/S solids. The properties of CFA will influence the performance of the S/S process for heavy metal immobilization. Our previous study[18] demonstrated that S/S solids using SCFA resulted in better retainment of Se(VI) than using BCFA due to higher formation of Friedel's salt, which is denoted as AFm phase and belongs to the family of layered double

hydroxides (LDHs). Friedel's salt is capable of binding heavy metal oxyanions [111-113] and chlorides.[114-116] The previous results that S/S solids using BCFA generated a negligible amount of Friedel's salt, which could be due to the lack of reactive aluminate in BCFA.[18] Meanwhile, the previous study also used PC as the activating agent with BCFA in the S/S process, which probably provided limited alkalinity for dissolving the glassy phases in BCFA. Alternatively, S/S processes using stronger activating agents such as hydrated lime or quick lime (i.e. $Ca(OH)_2$ and CaO) can provide more alkalinity for the pozzolanic reaction to proceed, which may facilitate the S/S in Friedel's salt formation and leach less heavy metals and chloride.[82, 107, 117-120] While BCFA is less effective than SCFA for Se^{VI} immobilization, unfortunately power plants that burn bituminous coal have more difficult FGD wastewater problems than sub-bituminous coal plants. Because bituminous coal contains higher sulfur content than sub-bituminous coal, bituminous FGD systems generate larger volume of wastewater with more concentrated salts and heavy metals.[121]

Proposed S/S process: The proposed S/S process of this work is shown in Figure 1.1. The FGD wastewater, named FGD blowdown, is concentrated into its brine form through thermal evaporator. The brine generated, with or without ZVI pretreatment, will be mixed with CFA (bituminous or subbituminous) and activating agent (PC or lime). Additional additives which could enhance the formation of certain mineral phases could be also added. The mixed slurry normally exhibits as a paste which can be pumped out of the mixer for curing, or directly sent to landfill.

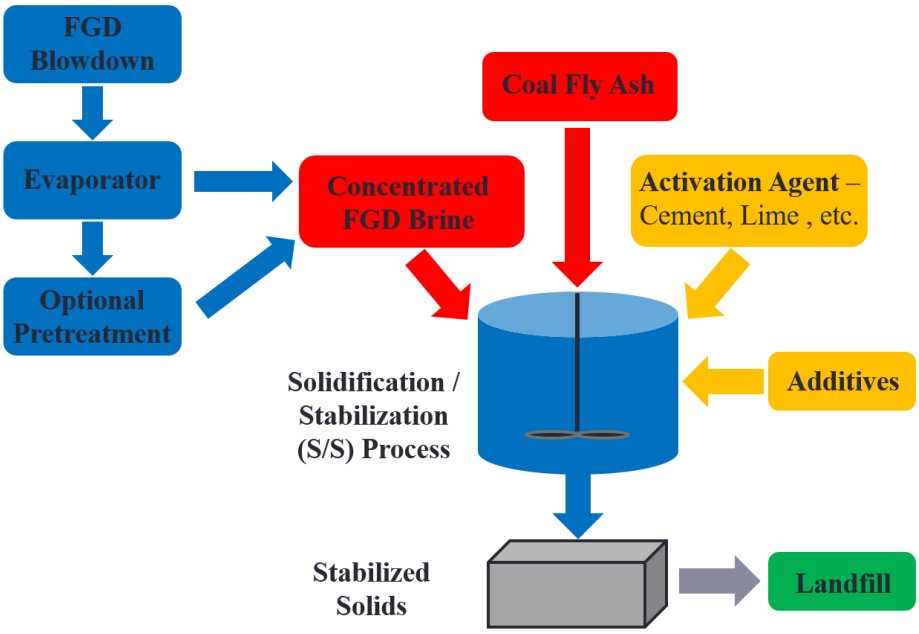

Figure 1.1. Proposed S/S process in this work

1.3.5 Mineral Phases for Heavy Metals/Halides Immobilization in S/S Solids

The three most important phases for heavy metal immobilization in S/S solids are monophase ($Ca_2(Al,Fe)(OH)_6 \cdot X \cdot xH_2O$), ettringite ($Ca_6Al_2(OH)_{12}(SO_4)_3 \cdot 26H_2O$), and calcium silicate hydrate (C-S-H).[81] C-S-H is the major hydration product of cement, with a Ca:Si ratio of 1.5-1.7.[122] It contains large micropores and specific surface area due to its highly disordered layered structure, thus has a strong potential for sorption.[123] Its calcium-rich surface could adsorb various anions. At Ca:Si ratios less than 1.2, the surface becomes negatively charged and thus prefers the adsorption of cations. Calcium (sulfo)aluminate hydrates (ettringite and monophase), which are about 10-20% of the total hydrated cement,[122] are also capable of adsorbing heavy metal cations, but it is quantitatively

unimportant compared to the cation immobilization by C-S-H and hydroxide precipitation in a cement system,[124] However, their capability of adsorbing anions by anion exchange makes them the important components for anionic contaminant removal.[123] Ettringite (an AFt phase) and monophase (an AFm phase), differ significantly in structure.[122] Ettringite has a column-like structure with interchannels containing anions and water molecules. Monophase has a lamellar structure of hexagonal plates, with interlayers containing anion and water molecules.[122] AFm-Cl is known as Friedel's salt.[125] Ettringite could be also transformed into its monophase as monosulfate ($3CaO{\cdot}CaSO_4{\cdot}12H_2O$) when sulfate is limited. Sulfate substituted ettringite and monophase by anions such as selenite, selenate, arsenate, and chromate have been reported.[124] The sorption of Se(VI) to AFm-SO_4, AFt-SO_4, and C-S-H was studied by Baur and Johnson through mineral synthesis and contact with Se(VI) in aqueous solution.[113] There was little sorption to C-S-H and weak sorption to AFt-SO_4 (Rd = 0.03), but strong sorption of Se(VI) to AFm-SO_4 (Rd = 2.06), indicating that cement rich in AFm-SO_4 would significantly immobilize Se(VI).[113] Through X-ray diffraction (XRD) analysis, the authors determined that Se(VI) sorption increased the $Ca_2[Al(OH)_6]^+$ layer spacing due to SeO_4^{2-} replacing for SO_4^{2-} as the primary mechanism of Se(VI) immobilization.[113] Another study by Wu *et al.* demonstrated that AFm-Cl effectively and rapidly removed Se(VI) from aqueous solutions through SeO_4^{2-} exchanging for Cl^- in the interlayers.[126] In general, AFm phases have shown significant affinity for immobilizing oxyanions, such as Se(VI), As(V) and Cr(VI), through anion exchange.[125-128]

Besides metal removal, AFm-Cl formation in S/S has been proposed to bind Cl^- in high salt waste.[129-131] Lampris *et al*. attempted to S/S municipal solid waste incineration

(MSWI) fly ash with Cl^- content of 130,000−220,000 ppm using PC with the aim to immobilize Cl^- through AFm-Cl formation.[130] In 72-day tank leaching tests, the authors observed Cl^- releases at 40-50% even with PC addition up to 50%.[130] In contrast, AFt phases have the ability to bind SO_4^{2-}, but not Cl^-.[131]

1.3.6 Environmental Risk of Bromide and Its Potential Removal by AFm phases

The recently finalized EPA regulations (e.g., Mercury and Air Toxics Standards, MATS) for coal-fired power plants regarding air emissions have resulted in more technologies being applied for air pollution control. For mercury control, the most common strategy is injecting bromide salts on the coal. The mercury in the coal will be present in three forms after combustion: particulate-bound mercury, elemental mercury (Hg^0), and oxidized mercury (Hg^{2+}).[132] While particulate-bound and oxidized mercury can be removed by electrostatic precipitation or cleaned up by the FGD system, respectively, elemental mercury is not water soluble and highly volatile and thus is difficult to be removed. By adding bromide salts into the coal combustion unit, bromide will be oxidized to bromine, which will oxidize the elemental mercury into $HgBr_2$ - a more water-soluble chemical that can be easily removed by the FGD system.[132]

Mercury ended up in the FGD wastewater will need to be further treated, whereas bromide is not regulated and commonly discharged into the environment. Therefore, it may be reasonable to expect that the bromide concentration in the downstream waterbodies may increase over time as more FGD systems and bromide-based mercury control measures are applied across coal-fired power plants to meet the EPA regulations. This elevated bromide concentration has the potential to increase the formation of brominated disinfection

byproducts (DBPs) at water treatment plants impacted by bromide discharge from upstream coal-fired power plants. The bromide present in the water can be readily oxidized to free bromine (HOBr) by free chlorine during water treatment processes, and the free bromine can react will organic precursors in water to generate brominated DBPs.

The brominated DBPs are of greater concerns than the chlorinated DBPs due to three reasons. First, the brominated DBPs pose greater health risks than chlorinated DBPs.[133-134] Second, the regulatory limits for total trihalomethane (TTHM) (< 80 µg/L) and total haloacetic acids (HAA_5) (< 60 µg/L) set by the drinking water standards are mass-based. Therefore, for the same molar concentration of precursors, brominated DBPs will have a higher mass concentration than chlorinated DBPs because bromine has a higher atomic weight than chlorine. Third, free bromine is more reactive than free chlorine; so more DBPs will be produced with same molar concentration of precursors. Due to these three reasons, it is important for upstream coal-fired power plants to consider bromide control measures if there are water treatment utilities at downstream.[132]

Our S/S process has demonstrated that chloride can be well retained by the solids made from sub-bituminous coal ash and FGD brines. Since Friedel's salt can uptake chloride, it is likely to uptake bromide also due to similar charge and properties of these two halides. So far, no literature could be found on bromide immobilization through S/S using coal ash. Therefore, it will add important new knowledge for the industry if the retainment of bromide can be evaluated as well with chloride in the optimization of the S/S process.

1.3.7 Boron from CCRs and the Role of Ettringite on Boron Removal

Ettringite has been demonstrated to immobilize borate more efficiently than other contaminants. Although boron is not currently regulated in ELG or drinking water standards and has shown limited adverse effect on humans, it is harmful for humans to take over a long time.[135] Boron leached from coal combustion residues (CCRs) is one of the major sources of boron in the environment. Several studies have demonstrated that the "$\delta^{11}B$" value can be used as a tracer for CCRs contaminated waterbodies.[136-138] The $\delta^{11}B$ value is defined as the fractional difference between ^{11}B and ^{10}B in the unit of parts per thousand.[136] A negative $\delta^{11}B$ value indicates that the sample is rich in ^{10}B or light boron. Williams and Hervig [138] measured boron isotopic ratios of different coals in the U.S. and found a wide range of negative $\delta^{11}B$ values (−70‰ to −1‰), indicating that the boron in coal is ^{10}B-enriched. This negative $\delta^{11}B$ signature is contrast with other waterbodies which have positive $\delta^{11}B$ values: meteoric boron (10−40‰), domestic wastewater (0−10‰), seawater (39‰), and saltwater intrusion and brines (>39‰). Davidson and Bassett [136] demonstrated the potential of using boron isotopes to identify the contamination of groundwater by fly ash leachate. The author states that boron is not involved in redox reactions at earth surface conditions, so isotopic ratio results are generally more easily interpreted. Ruhl et al. recently reported the boron isotopic ratios of leaching experiments on CCRs from various coal sources.[137] The resulting leachate had mostly negative $\delta^{11}B$ value from -17.6‰ to 6.3‰. The author also measured the boron isotopic ratios of water samples collected from ash-spill contaminated waterbodies, and the result has a distinctive negative $\delta^{11}B$ signature relative to the background waters. These results indicate that $\delta^{11}B$ value could be used as a CCR tracer.

Fate of boron from coal combustion: Coal combustion at high temperatures volatilizes most of the elements associated with the organic phases (including boron) and volatilizes elements associated with silicate phases in coal. The boron behavior during coal combustion is consider as a two-step process: volatilization and heterogeneous condensation.[135] During combustion, most boron compounds are volatilized to the gaseous phase. Some volatilized boron compounds are enriched into the clinker and coal fly ash, while the remaining boron will be completely absorbed by the wet FGD system since most boron compounds are water soluble. Noda et al.[135] recently studied the volatilization characteristics of boron compounds during coal combustion. The results from chemical equilibrium calculations and XAFS analysis suggest that the boron compound contained in the ash is mainly B_2O_3. Analysis of CCR indicates that there is no isotopic fractionation associated with the coal combustion process, and CCRs retain the $\delta^{11}B$-depleted signature measured in the coal.[138-139] Therefore, it is assumed that $\delta^{11}B$ value in coal and CCR remains the same. Boron is associated with the easily leachable fraction of elements that adsorbed onto the fly ash particles during cooling of exhaust gas.[140] Since there is no species-specific preferential leaching to water, no isotopic fractionation is expected during the leaching of boron from CCRs and thus the boron isotopic imprints of contaminated water would mimic the CCR composition.[137]

Leaching and intake of boron from coal ash: Boron is very often associated with smallest particles in the ash, accumulated on the water-soluble fraction of the particle surface, and therefore has very high leaching rate.[141-143] Cox et al. reported the leaching of boron (as borate or boric acid) from bottom ash and fly ash.[144] The boron content in fly ash was found as high as 1900 ppm and more than 50% was leachable into the water. However,

the boron content in bottom ash was 960 ppm and it was almost insoluble. Treating the fly ash for 30 min at 1200 ^{o}C reduce the leachable boron to 6%. The result indicates that boron is initially in two independent chemical states, one of which is insoluble, likely in the form of polyborate or borosilicate.

Jankowski at al. studied the mobility of As, B, Mo and Se from selected Australian fly ashes.[140] Long-term (144 h) batch leaching tests were performed using two acidic and two alkaline fly ashes and leaching solution with initial pH of 4, 7, and 10. The results suggest that boron has the highest relative mobility of all four elements, and decrease of B, As and Se in leaching solution in contact of alkaline coal fly ash could attribute to the formation of ettringite. At high pH values, boron can co-precipitate with $CaCO_3$.[145-146] There are also several studies that reported the formation of borate substituted ettringite.[147-149]

1.3.8 Factors Affecting the Mineralogy of S/S Solids

Effect of pH: The pH domain for the stability of various AFm and AFt phase have been reported.[150-154] In general, both phases are less stable when the pH is lower than 11 or higher than 13. At lower pH, $Ca(OH)_2$ in the framework tends to disolve, while at higher pH, $Al(OH)_3$ in the framework tends to dissolved. Clark and Brown stated that a high alkaline hydration solution promoted the formation of AFm phase over AFt phase.[150-151] The effects of pH on oxyanions substituted AFt and AFm phases have also been reported. Baur and Johnson reported that SeO_4^{2-}-substituted AFm phase was stable at pH >12.[152] Perkins and Palmer reported that during the synthesis of CrO_4^{2-}-substituted ettringite, CrO_4^{2-}-substituted monophase was also formed at pH 12; however, at pH >12.5,

monophase was the only form. They also reported that the stability domain of monophase could be lowered to pH 11 when there was excess free calcium in the system, which favored the formation of monophase.[153-154] These findings show that pH is an important factor on mineralogy of S/S solids, not only during the curing stage but also the exposure environment. The pH of the S/S mixture can be purposely increased to enhance the monophase formation. However, carbonation, acid rain and other factors in the environment could drop the pH of S/S solids and should be taken into consideration.

Effect of temperature: Temperature plays an important role in the early stage of S/S process. Damidot and Glasser studied the thermodynamics of $CaO–Al_2O_3–CaSO_4–H_2O$ system at different temperatures.[155] At <50ºC, the stability diagram shows that ettringite is favored over the monophase, with monophase covering only a small area. At 85 ºC, the monophase becomes more stable compared to that at 50 ºC, although ettringite is still favored if the sulfate concentration is high. Clark and Brown studied the formation of calcium sulfoaluminate at different temperatures (30–90 ºC) and different sulfate-to-aluminate ratios (3:1 and 1:1).[150-151] When the sulfate-to-aluminate ratio is 3:1, ettringite is the only phase formed at different temperatures. When the ratio becomes 1:1, increasing temperature enhances the formation of monophase.

Effect of competing ions: Competing ionic species in the S/S system is also an important factor to be considered, especially for waste containing heavy metals, like FGD wastewater brine. Not only anions exchange could occur during and after the formation of ettringite and monophase, cationic exchange could also occur. Zhang and Reardon studied the uptake of B, Cr, Mo and Se by ettringite and OH^--substituted hydrocalumite (monophase).[149] They found that the anion uptake rate by monophase is higher than

ettringite. Ettringite shows an anion preference in the order of $B(OH)_4^-$ > SeO_4^{2-} > CrO_4^{2-} > MoO_4^{2-}, while hydrocalumite shows an opposite trend. McCarthy also reported that, through the synthesis of borate- and selenate-substituted ettringite, >95% of the borate and selenate could be removed from the hydration solution.[156] Klemm and Bhatty reported that when arsenate, chromate and selenate are in the hydration solution, arsenate shows a greater affinity to form ettringite than selenate and chromate, while the latter oxyanions incorporate into ettringite at equal molar ratio. However, when sulfate is present, it dominates other oxyanions for the formation of ettringite. Sulfate could also replace oxyanions in the substituted ettringite.[157] Albino reported the formation Cd^{2+}- and Cr^{3+}-substituted ettringite during the synthesis experiments to incorporate various divalent and trivalent metals into ettringite.[158]

Impact of activating agents: The type of activating agent greatly impacts the mineralogy of S/S solid in terms of free calcium, aluminate and sulfate content. Commonly applied activation agents in S/S techniques include cement (PC, high-Al cement with sodium aluminate), lime (hydrated or quick lime) and gypsum.[117, 157] Cement and lime could greatly increase the pH, creating a high alkaline condition during the early stage of hydration which could enhance the formation of ettringite and monophase. The hydration of lime will also release significant amount of heat which helps converting ettringite to monophase. Quick lime could further increase the temperature of the system. The addition of aluminate and gypsum enhances the immobilization of heavy metals since they could speed up the formation of ettringite during the early stage when heavy metals are still mobile and easily incorporated into the ettringite.[157]

Impact of FGD brine chemistry: As mentioned in section 1.3.1, FGD brines contain high levels of TDS, with abundant Ca^{2+} and Cl^-. When the reaction condition allows the formation of monophase, the AFm-Cl phase (Friedel's salt) will be the dominant form. The sulfate concentration in the brine (plus from added gypsum if utilized) also needs to be considered since a high level of sulfate will hinder the formation of monophase, or compete with metal oxyanions for incorporation into ettringite or monophase. The acidic to neutral pH of FGD brines is not ideal for formation of ettringite or monophase; however, this is not a concern since the high alkaline property of CFA and activation agents will raise the pH during mixing and curing. During leaching of S/S solids, the excess free calcium could help maintain the monophase from converting to ettringite.

1.3.9 Permeability of S/S Solids

Permeability is an important characteristic to be analyzed for our stabilized solids because it is a good indication of how well the solids can retain the contaminants. Although ettringite and monophase are capable of retaining heavy metals and chloride, they are not stable once exposed to aqueous phase with pH less than 10.5. Previous leaching tests results also indicate that once the solid is crushed and being leached at neutral pH, both ettringite and monophase are destructed, resulting in the leaching of heavy metals. However, if the solid is not crushed, only the surface will be exposed to the extraction fluid. Therefore, the stability of ettringite and monophase in the inner part of the solid will greatly depend on the permeability of the solids, and a low permeability could be a key factor to the success of this ZLD method. The permeability of CFA based stabilized solids have been studied by several researchers. Ghosh reported that the addition of lime (4−10%) and gypsum (0.5−1.0%) lowered the hydraulic conductivity of stabilized BCFA (1.4% CaO) by more

than 500 times compared to the ash only system.[159] Mahlaba also reported that longer curing time and addition of lime decreased the permeability of the solids generated by BCFA and brine.[160] Bowders et al. reported that the permeability of BCFA stabilized solids could be lowered by the addition of 15% lime and cement by weight. Adding bentonite further decreased the permeability but increased the leaching of contaminants.[161]

1.3.10 Heavy Metal Removal by Friedel's salt

Friedel's salt ($Ca_4Al_2(OH)_{12}Cl_2(H_2O)_4$) is an AFm-Cl phase belongs to the family of layered double hydroxides (LDH). The AFm-X phase, or monophase, structure consists of positively charged $Ca_2[Al(OH)_6]^+$ layers, producing a net charge imbalance.[116] Anions (X), such as CO_3^{2-}, Cl^-, OH^-, and SO_4^{2-} occupy the space between the layers of $Ca_2[Al(OH)_6]^+$ to balance the mineral's charge.[116, 125] The exchange of anions in the interlayers with external anions is typically highly favored.[125] Friedel's salt has been shown to successfully remove various heavy metals such as selenate,[112] chromate,[111, 162] arsenate,[163-164] and various anion such as chloride,[116, 129-131] nitrate,[165] and nitrite.[166] Compared to other adsorbents, Friedel's salt is easy and cheap to synthesis and it has demonstrated a higher adsorption capacity than other types of LDHs for contaminants in various types of aqueous systems.[111-112, 162-164] Wu et al. demonstrated the effective removal of selenate by Friedel's salt with an uptake efficiency up to 1.37 mmol/g.[112] Dai et al. demonstrated the effective removal of chromate by Friedel's salt with an uptake efficiency up to 1.4 mmol/g.[111]

1.3.11 Stability of Friedel's salt

The stability of Friedel's salt and its phase change after uptaking the contaminants is also an important aspect to be considered in its application. Baur and Johnson reported that

SeO_4^{2-}-substituted AFm phase was stable in the cementitious system.[152] Perkins and Palmer reported that during the synthesis of CrO_4^{2-}-substituted ettringite, CrO_4^{2-}-substituted monophase was also formed at pH 12; however, at pH >12.5, monophase was the only form. They also reported that the stability domain of monophase could be lowered to pH 11 when there was excess free calcium in the system, which favored the formation of monophase.[153-154] Wu et.al showed that selenate substituted Friedel's salt is stable in water at a starting pH range of 4 -13 with an equilibrium pH around 11. At lower starting pH, $Ca(OH)_2$ in the framework of LDH is partially dissolved, while at higher staring pH, $Al(OH)_3$ in the framework of LDH is partially dissolved. However, under both cases, less than 3% of the selenate was desorbed, indicating the strong fixation of selenate by Friedel's salt. [112] Similar findings regarding chromate substituted Friedel's salt was also report by Dai et al. [111] The findings mentioned above indicated that AFm phases are likely more stable around pH 11-12.

In this work, we detected the transformation from Friedel's salt to stratlingite in the S/S solids after the USEPA 1315 long-term leaching test. After around 3 months, the Friedel's salt (which was 15% by weight in the solid) disappeared but stratlingite was detected. Stratlingite is also an AFm phase, but with aluminosilicate ion, expressed as $[AlSi(OH)_8 \cdot 0.25H_2O]^{-1}$, in the interlayer of the LDHs. It's commonly found in hydrated cement and concrete. Stratlingite is more difficult to synthesize than Friedel's salt and the its synthesis takes up to 4-6 weeks.[114, 167] Transformation from stratlingite to Friedel's salt when exposed to chloride solution has been shown in previous research. [114, 168-169] However, to the best of our knowledge, no research has demonstrated the transformation from Friedel's salt to stratlingite, or the heavy metals removal by stratlingite. In the S/S

solid generated in this study, coal fly ash could provide silicate and aluminate which are required for the formation of aluminosilicate ion in the stratlingite.

1.3.12 Leaching Procedures

USEPA 1311 [170]: USEPA 1311 leaching test (i.e. Toxicity Characteristic Leaching Procedure, TCLP) is a regulatory leaching test to determine whether the solid waste is hazardous or non-hazardous. TCLP is an equilibrium batch extraction test which sets the initial pH of the leachant to 2.88 or 4.93 using acetic acid. The size of the solid pieces must be less than 0.95 cm and the liquid to solid ratio is set to 20. The extraction time is usually 18 ± 2 hours.

USEPA 1313 [171]: The USEPA Method 1313 (i.e. Liquid-Solid Partitioning as a Function of Extract pH for Constituents in Solids Materials using a Parallel Batch Extraction Procedure) is similar to the TCLP test except that the final leachate pH is controlled at a target value, not the initial pH and nitric acid or sodium hydroxide is used. In order to achieve the targeting pH, preliminary titration tests are conducted to determine the amount of acid or based required. The liquid to solid ratio is set to 10 and the extraction time is usually 24 ± 2 hours.

USEPA 1315 [172]: The USEPA Method 1315 (i.e. Mass Transfer Rates of Constituents in Monolithic Materials Using a Semi-Dynamic Tank Leaching Procedure) is a long-term leaching procedure to evaluate the contaminant release from cylindrical monolith, instead of crushed solid in USEPA 1311 and 1313. In this method, the monolith is submersed into deionized water which needs to be refreshed following the designed

schedule. The ratio of the liquid volume to solid surface area ratio is set to 9 ± 1 mL/cm^2. The leaching test normally last for a total of 63 days.

CHAPTER 2. REMOVAL OF HEAVY METALS BY AGED ZERO-VALENT IRON FROM FLUE-GAS-DESULFURIZATION BRINE UNDER HIGH SALT AND TEMPERATURE CONDITIONS

2.1 ABSTRACT

To achieve zero liquid discharge, the flue-gas-desulfurization (FGD) wastewater at coal-fired power plants can be concentrated into brine through thermal evaporation to maximize water reuse; however, the hot brine generated requires further treatment prior to disposal. To address this need, this study investigates the performance of aged, micron-sized zero-valent iron (ZVI) for heavy metal removal in simulated and real FGD hot brines, which was scarcely studied previously. The effects of temperature, pH, total dissolved solids, ZVI dosage, major cations, nitrate and sulfate on the reactivity of ZVI in the brines were evaluated. Among many factors, higher temperature and Mg^{2+} exert the dominant influence. At 80°C, almost 100% of arsenate (1 mg/L) and chromate (1 mg/L) can be removed in < 5 minutes using 4.17 g/L of ZVI in simulated brines, while selenate (25 mg/L) and cadmium (5 mg/L) can be completely removed within 30 minutes. Mg^{2+} ions naturally present in FGD brines account for the depassivation of aged ZVI. X-ray diffraction results suggest that green rust is the reactive intermediate for selenate and cadmium removal. Overall, this study demonstrates that ZVI is an effective material for removing heavy metals in hot FGD brines generated through thermal evaporation at power plants.

2.2 INTRODUCTION

The United States coal-fired power industry is facing the challenge to improve wastewater treatment and discharge. The U.S. Environmental Protection Agency (USEPA) has determined that the wastes generated from wet flue-gas-desulfurization (FGD) systems and ash-handling systems contribute the most to the contaminant loading to the environment.[4] Because of the complexity of the wastewater and difficulties related to technology and maintenance, a special concern for the industry is treating the wastewater from wet FGD systems which contains significant concentrations of heavy metals (e.g. Se, As, Cr, Cd, and Hg) and large amounts of salts (e.g. Cl^-, Ca^{2+}, Mg^{2+}, Na^+, and $SO4^{2-}$).[1]

At present, the most commonly used FGD technology is the forced oxidation type wet scrubber,[2] which uses limestone ($CaCO_3$) or lime ($Ca(OH)_2$) as an absorber for SO_2. Forced oxidation FGD systems pump air into the scrubber to completely oxidize SO_3^{2-} to SO_4^{2-} which precipitates as $CaSO_4 \cdot 2H_2O$ (gypsum), a commercial product for wallboard or soil amendment.[3] However, heavy metals, including Se and Cr, are oxidized along with SO_3^{2-}. Once Se(IV) and Cr(III) are oxidized into Se(VI) and Cr(VI), their mobility (and toxicity) will increase, thus creating difficulties for their treatment. Moreover, FGD wastewater also contains significant concentrations of Ca^{2+} (from the alkaline sorbent) and Cl^- (from the coal). The recently released (but postponed) Steam Electric Power Effluent Limitation Guidelines (ELG Rule) by the USEPA set stringent limits on the release of As, Hg, Se and other pollutants into the environment from FGD wastewater,[173] motivating the coal-fired power industry to seek more treatment options.

The zero-liquid-discharge (ZLD) options have gained significant interest from the coal-fired power industry because of the elimination of environmental wastewater discharge and maximization of water reuse.[18] At coal-fired power plants, thermal evaporation related technologies could be the most reliable method to concentrate the FGD wastewater followed by a suitable solidification/stabilization process to treat the concentrated brines to form a solid for landfill disposal [18]. Both Duke Energy's Mayo Plant near Roxboro, North Carolina and the Public Service of New Hampshire's Merrimac Station installed thermal evaporation systems in ZLD strategies to treat FGD wastewater. Significant interests exist in these type technologies which will increase with increasing effluent limitations. While the volume of the wastewater is reduced substantially after thermal evaporation, the hot brines generated will contain significantly higher concentrations of heavy metals and salts which renders the treatment of this brine a new kind of challenge. Extensive literature search shows that the methods regarding the removal of heavy metals in hot brine conditions is scarce in the field and require more research to address this knowledge gap.

Studies have shown that zero-valent iron (ZVI) can effectively remove or stabilize a variety of contaminants such as selenate, chromate, nitrate, phosphate and chlorinated hydrocarbons in hazardous wastes or contaminated sites.[19-22, 24, 31-38, 174] Although the reactivity of ZVI for heavy metal removal has been well studied, to the best of our knowledge ZVI has not been studied for treatment in concentrated FGD wastewater brines. The previous work by Huang et al. has conducted a successful field study using a hybrid ZVI system to treat heavy metals and nitrate in FGD wastewater.[21-22] However, the chemistry of FGD wastewater versus its concentrated brines will be quite different due to

the significantly higher concentrations of metals, salts and other components in the brines. Therefore, evaluating the effectiveness of ZVI on heavy metal removal in real FGD wastewater brines is still lacking and such studies will yield valuable new scientific information that can be taken into consideration when designing the ZLD method at the coal-fired power plants.

Moreover, while the mechanisms of contaminant removal by ZVI have been extensively studied,[24, 32, 35-36, 65-67] most of the studies were focused on one or a few contaminants in a fairly "clean" aqueous system compared to in a more complex FGD brine. Also, most studies were conducted under anoxic condition, especially for nano-sized ZVI (nZVI), because a passive iron oxide layer can easily form when the particles are exposed to air. It is well known that once the passive layer is formed, the reactivity of ZVI will be hindered unless the ZVI is corroded and the passive layer is destructed. However, conducting the treatment of FGD brines by ZVI under anoxic conditions at the power plants is not desirable or very practical, and thus conditions to promote ZVI corrosion and passive layer destruction are needed.

The electrochemical corrosion of ZVI can be affected by various factors such as temperature, pH, mixing, ZVI size, ionic strength, different levels of various anions, and the coexistence of other heavy metals.[32, 35-38, 57-60] Lower starting pH promotes the corrosion of ZVI and helps the formation and release of Fe(+II), which later involves in the formation of Fe(+II)-Fe(+III) hydroxyl layers (e.g. green rusts (GR)) that give rise to the reactivity of ZVI for reduction of a variety of contaminants.[41, 47-49, 52, 55] Different levels of various anions and metal ions could affect the composition of the active layer around ZVI and compete with targeting contaminants.[35-36] At higher temperatures, ZVI-based materials

were found to be more reactive in removing chromium, arsenic, and nitrate than at room temperature.[38, 61-62] This enhanced performance might be attributed to the enhanced diffusion of metal ions and enhanced formation of active sites.[63-64] Therefore, removing heavy metals in FGD brines after the evaporation process could be very advantageous in a ZLD scenario where the concentrated brines will be at elevated temperatures.

The objective of this study was to evaluate the use of ZVI for heavy metal removal in concentrated FGD wastewater brines. Micron-sized, aged ZVI particles were selected in use because they are cheaper in costs and easier to handle compared to freshly made nZVI which requires anoxic condition to avoid passivation. Selenate, chromate, arsenate and cadmium were the main heavy metals of concern. The treatment of heavy metals by ZVI was conducted in both simulated and real FGD brines. The effects of a range of factors including temperature, pH, total dissolved solids (TDS), ZVI dosage, major cations, nitrate and sulfate on the treatment efficacy were systematically investigated to better understand the involved chemical reactions and mechanisms and to optimize the treatment process. The ZVI's characteristics and longevity over time were also evaluated. This study is among the first to evaluate the effectiveness of ZVI for heavy metal removal in concentrated FGD brines and reveals several important new findings. Results of this study will be useful to facilitate industries in the design and development of treatment options for mitigation of heavy metals in waste brines.

2.3 EXPERIMENTAL SECTION

2.3.1 Chemicals and materials

ZVI spherical particles (Figure 2.1) with a labeled size of 1-3 micron in diameter was purchased from Alfa Aesar (Haverhill, MA). The particles were stored in a closed amber borosilicate bottle under ambient condition at room temperature without special sealing for more than one year. These particles' surfaces were highly oxidized, and thus were termed aged ZVI. Figure 2.2 shows the SEM image of raw ZVI particles, indicating most particles were within 1-3 μm range in diameter. The surface composition of raw ZVI particles was analyzed by x-ray photoelectron spectroscopy (XPS) and shown in Figure 2.3. Without considering the carbon intrusion and minor impurities, the raw ZVI contained 71.4% of oxygen and 28.6% of iron, indicating the surface of the material was highly oxidized. This high oxygen content was contributed from the oxygen in the passive iron oxide layer on the ZVI which was formed due to exposure to air more than a year. Previous study indicated that after this aging time, minimum change in reactivity was expected [175]. ZVI particles with similar aging time were applied in the tests performed in this study.

Figure 2.1. Raw ZVI particles

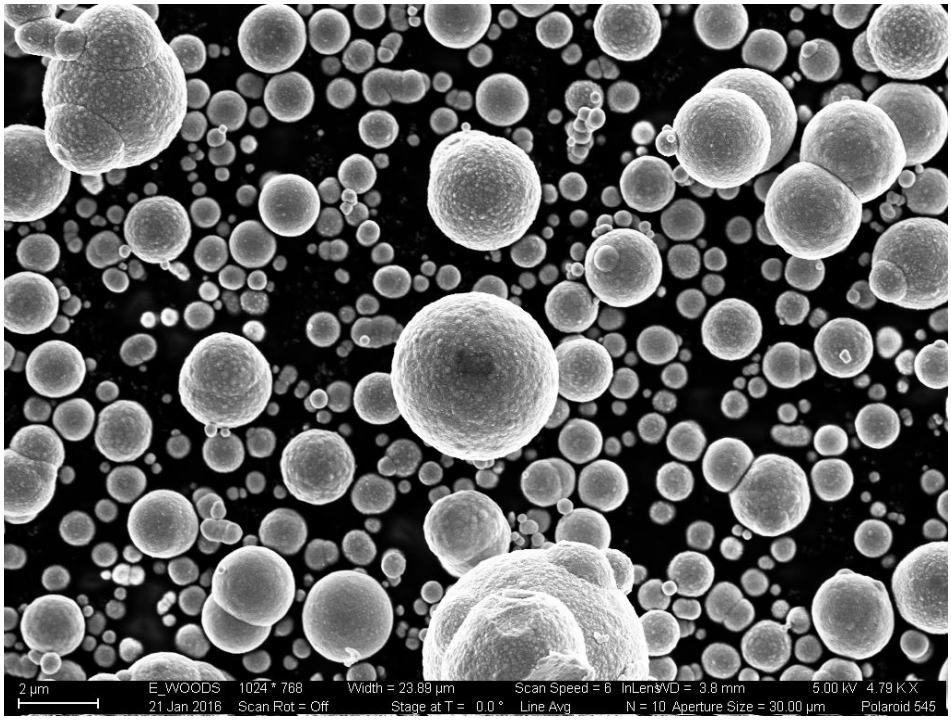

Figure 2.2. SEM image of raw ZVI particles

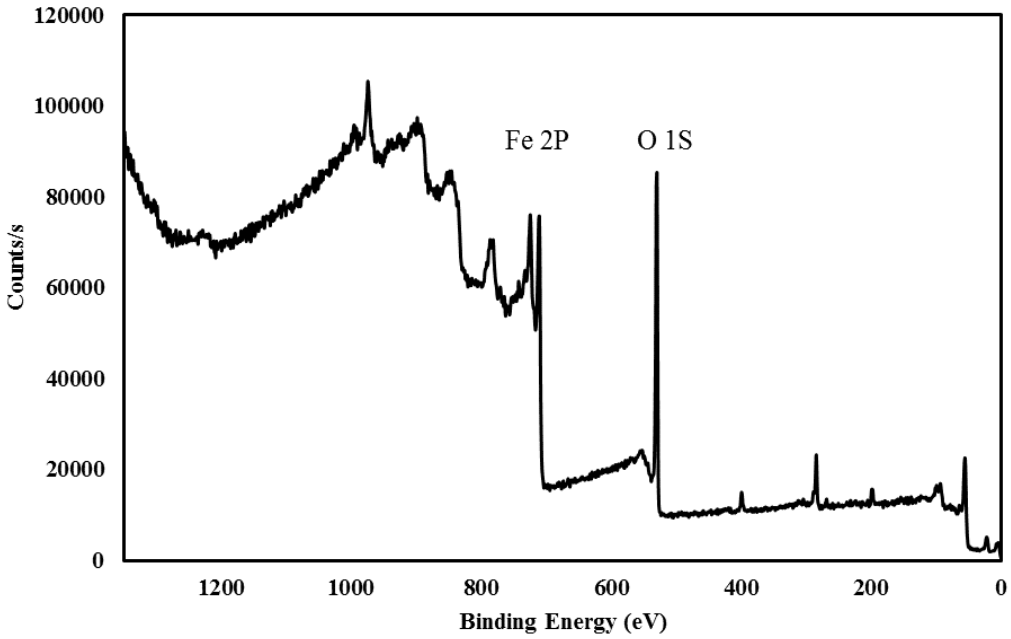

Figure 2.3. XPS scan of raw ZVI

All chemicals used for making the simulated FGD were in analytical grade and used as received. Sodium selenate (Na_2SeO_4), sodium arsenate heptahydrate ($Na_2HAsO_4 \cdot 7H_2O$), cadmium chloride ($CdCl_2$), sodium chromate (Na_2CrO_4), barium chloride dihydrate ($BaCl_2 \cdot 2H_2O$), and mercuric chloride ($HgCl_2$) were purchased from VWR (Radnor, PA). Calcium chloride dihydrate ($CaCl_2 \cdot 2H_2O$), sodium chloride (NaCl), magnesium nitrate hexahydrate ($Mg(NO_3)_2 \cdot 6H_2O$), magnesium chloride hexahydrate ($MgCl_2 \cdot 6H_2O$), magnesium sulfate heptahydrate ($MgSO_4 \cdot 7H_2O$), and sodium bromide (NaBr) were purchased from Fisher Scientific (Hampton, NH). All the solutions used in the experiments were prepared by dissolving the corresponding salts in ultrapure deionized (DI) water generated from a Milli-Q nanopure water purification system, and the resulted components' concentrations are shown in Table 2.1. Notice that selenate has the highest concentration among the heavy metals and its difficulty to be removed is well known. Therefore, initial tests regarding the optimization of reaction condition were done in the brine containing only 25 mg/L selenate and is named "selenate-only brine". The simulated brine with the addition of Se(+VI), As(+V), Cd(+II), Cr(+VI) and Hg(+II) is named "metal brine".

Table 2.1. Characteristics of simulated FGD brine, and real FGD brine (concentrations in mg/L)

Parameter	Simulated Brine	Real FGD Brine
pH	5.9	6.5
TDS	126,000	133,000
Chloride	80,000	77,800
Nitrate	0-600	1,300
Sulfate	0-1200	1,390
Bromide	1,312	240

Ca	57,580	38,439
Na	990	1,801
Mg	9,340	3,727
Se	25	3.1
As	1.0	ND
Cd	5.0	0.8
Cr	1.0	0.09
Fe	NA	0.7
Cu	NA	0.30
Hg	1.0	0.14
Pb	NA	0.08
Zn	NA	3.82
Mn	NA	12.5

NA: not added; ND: not detected

Real FGD wastewater was collected following the solid separation of the FGD blowout in a coal-fired power plant in the southeast of U.S. The real FGD brine was generated by heating 1.0 L of the real FGD wastewater using a heating plate with gentle magnetic stirring at 200°C until the volume of the final brine was about 10% of the original wastewater volume. During the process of concentrating the FGD wastewater into its brine through heating, the colorless FGD wastewater gradually turned yellow to brownish, with the formation of precipitates and crystal solids at the bottom. Images of real FGD brine generated from real FGD wastewater are shown in Figure 2.4. The real FGD brine was filtered (acid washed glass fiber filters with 0.7 μm pore size) to remove the precipitate before being characterized and tested.

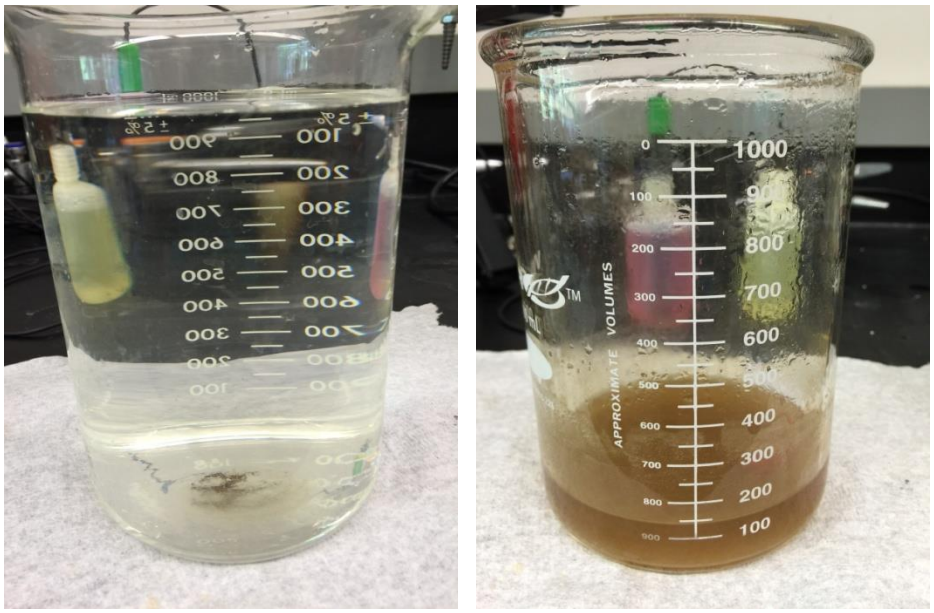

Figure 2.4. Real FGD wastewater (left) and brine after thermal evaporation (right)

2.3.2 Batch experiments and analytical methods

The effects of temperature, pH, TDS, ZVI dosage, nitrate and sulfate on selenate removal by ZVI was evaluated in the selenate-only brine. The starting pH (2.5, 3.0, 3.8, or 5.9) was adjusted by adding HCl. The pH throughout the reaction was not controlled. TDS (100%, 50% or 10%) was adjusted by diluting the brine with DI water before adding the selenate. The solution was preheated in a heating bath at constant temperature (25, 40, 60 or 80°C) which was maintained throughout the reaction. Nitrate concentration (0, 300, or 600 mg/L) and sulfate concentration (0, 300, 600, or 1200 mg/L) were adjusted by adding sodium nitrate or sulfate. ZVI powder (0.10, 0.25, 0.50 or 1.00 g) was added into the 60 mL brine-containing solution and the mixture was stirred by a magnetic stir bar (1.5" × 0.312") at 550 rpm. At this speed, most of the ZVI added was observed to be well dispersed in the mixture and this stirring condition was applied in all the tests performed in this study. Sample aliquots were taken at 0, 5, 10, 20, 30, and 60 min, filtered using a syringe filter

(0.22 μm) to remove solids, and the supernatant was diluted 10 times with 5% trace-metal-grade HNO3 for heavy metal measurement. The tests mentioned above suggested that temperature was a dominant factor for selenate removal, so the effect of temperature was also tested in the metal brine to evaluate its effect on the removal of other metals.

The longevity test of ZVI was conducted by adding 0.25 g or 0.10 g of ZVI into 60 mL of selenate-only brine or metal brine at pH 5.9 and 80°C. Samples were taken at 1-hour interval for 5-6 hours. Once an aliquot of samples was taken, additional heavy metals (equal to their initial concentration) were spiked and an aliquot of sample was taken immediately to confirm the concentration spiked in. The volume added compensated the volume loss from sampling. The corroded iron samples from sample aliquots were removed by the syringe filters and freeze dried before x-ray diffraction (XRD) analysis.

All the tests were conducted in duplicates with a fixed brine volume of 60 mL under ambient conditions without special prevention from contact with air. The pH was measured by an Orion Star^{TM} A111 bench top pH meter (Waltham, MA). The concentration of heavy metals was detected by inductively coupled plasmas – optical emission spectroscopy (ICP-OES) 8000 (Perkin Elmer, Waltham, MA). For the real FGD brine, the chloride, sulfate and nitrate concentrations were measure by ion chromatography (IC) (Dionex, Sunnyvale, CA). TDS was measured by drying 5 mL of the real brine in an aluminum crucible in the oven at 100 °C. The XPS (Thermo K-Alpha, Waltham, MA) and SEM (Zeiss Ultra60, Oberkochen, Germany) analysis of raw ZVI, and the XRD (Panalytical XPert PRO Alpha-1, Almelo, Netherlands) analysis of ZVI at different reaction conditions were conducted at the Department of IEN/IMAT Materials Characterization Facility at Georgia Tech.

2.4 RESULTS AND DISCUSSION

The simulated and real FGD brines shared comparable characteristics in major components (Table 2.1) such as high concentrations of TDS (126,000 vs. 133,000 mg/L), chloride (80,000 vs. 77,800 mg/L) and calcium (57,580 vs. 38,439 mg/L). The simulated brine was slightly more acidic (pH 5.9 vs. 6.5) and contained higher concentrations of Mg^{2+} and heavy metals than the real brine. The higher concentrations of heavy metals employed in the simulated brine was aimed to better evaluate the removal efficiency. Results from different experimental tests are discussed below.

2.4.1 Treatment efficiency of ZVI in selenate-only brine

2.4.1.1 Effects of pH and temperature

Figure. 5 and 6 show the effect of pH and temperature on selenate removal by 16.67 g/L of ZVI in selenate-only brine. Generally, higher temperature and lower pH led to higher removal of selenate. At 25°C (Figure 2.5a), removal of selenate was not observed, even at the lowest pH (2.5) tested. The color of the ZVI-brine mixture remained grey as the color of raw ZVI particles, because ZVI was not corroded. At 40 °C (Figure 2.5b), the percent removal of selenate increased with decreasing pH. The acidic condition enhanced the corrosion of the iron surfaces. However, at the lowest pH of 2.5, only about 30% of selenate was removed after 60 minutes.

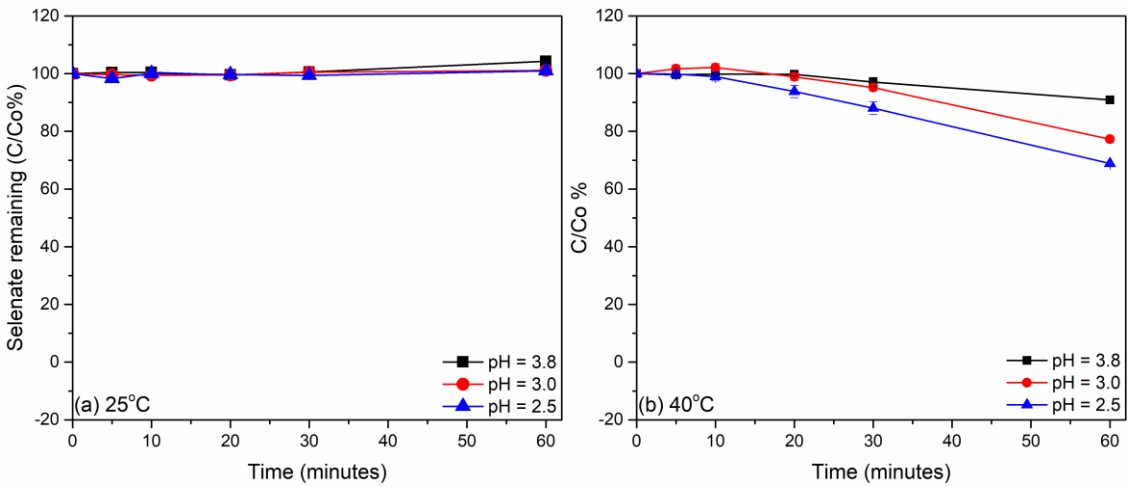

Figure 2.5. Effect of pH on selenate removal at 25°C (a) and 40°C (b) by 16.67 g/L ZVI in simulated brine.

By increasing the temperature to 60 °C and 80 °C (Figure 2.6), the effect of pH became negligible. At 60 °C, more than 90% of selenate could be removed within an hour. At 80 °C, more than 99% of selenate could be removed within 30 minutes regardless of the pH. Since the pH of the simulated brine and the real brine in this study was only slightly acidic (5.9-6.5), the above result suggests that lowering the pH of the brine to increase the removal rate is not in great need when the temperature is at 60 °C or higher.

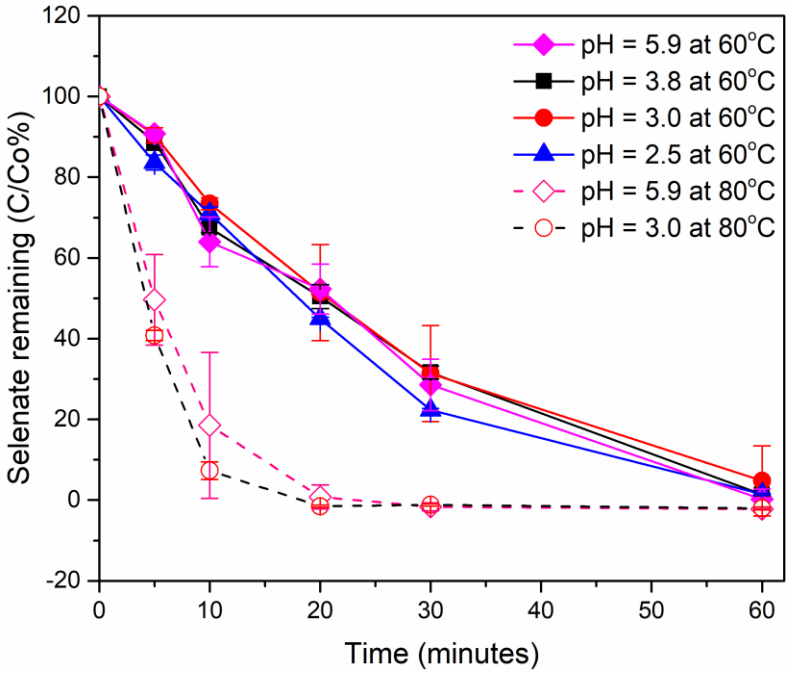

Figure 2.6. Effect of pH on selenate removal at 60°C and 80°C by 16.67 g/L ZVI in selenate-only brine.

At elevated temperature (60 °C and 80 °C), the color of the reacting mixture turned into dark green as the reaction proceeded. The dark green color was a strong indication of the formation of green rusts (GR) which were further confirmed by XRD (see Section 2.4.3.2). GR are layered double hydroxides (LDH) composed of positively-charged octahedral layers of Fe(+II) and Fe(+III) hydroxides with interlayer containing water molecules and anions.[42-44] Their molecular formula are generally represented as $[Fe(+II)_{(1-x)}Fe(+III)_x(OH)_2]^{+x}\cdot[(x/n)A^{-n}\cdot(m/n)H_2O]^{-2}$ where A represents the anion.[41-43] GR have been reported for their capability of reducing various contaminants including selenate,[41, 43-47] chromate,[26, 48-51] nitrate,[52-53] and chlorinated hydrocarbons.[54-56] However, GR is not stable in oxic condition. Further oxidation of GR will lead to goethite (a-FeOOH), lepidocrocite (γ-FeOOH), maghemite (γ-Fe_2O_3), or magnetite (Fe_3O_4), depending on the pH, rate of oxidation and dehydration of GR.[45]

The reaction suspension at 80°C (Figure 2.7) was dark green after one hour of reaction. When it was left in room temperature without stirring, the particles remained mostly dark green and settled to the bottom after one hour, and eventually turned orange-brown after 24 hours. This color change suggests that, although GR is unstable at oxic condition,[176] the high temperature condition most likely decreased the dissolved oxygen content in the brine which helped preserve the GR. Once the temperature cooled down, the dissolved oxygen level increased, and further oxidation of the GR occurred.

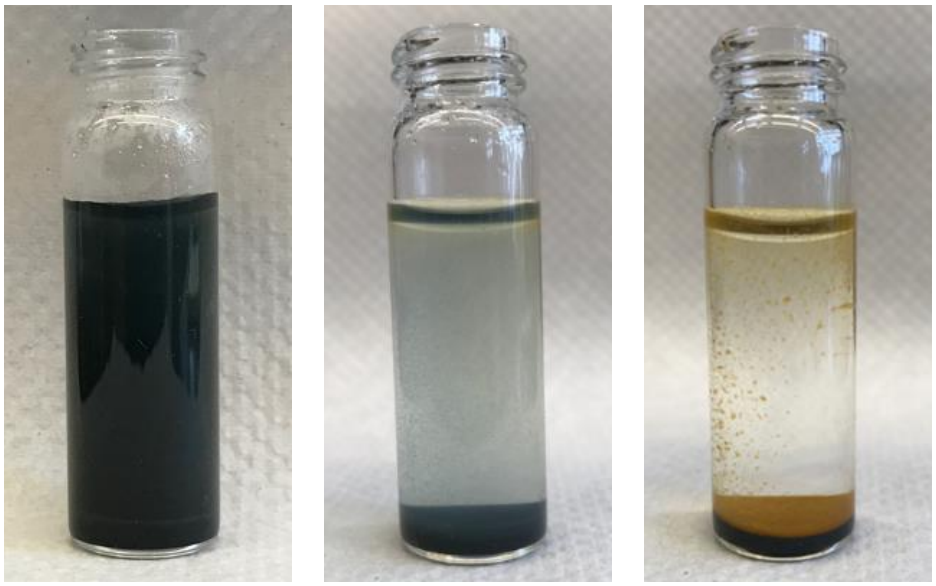

Figure 2.7. The change of color of the ZVI-brine mixture. The mixture was from after 1 hour of reaction of ZVI (4.17 g/L) and selenate (25 mg/L) in simulated FGD brine (pH 5.9) at 80°C. The mixture was taken out of the hot reactor and transferred into a small vial in the room temperature as shown in the picture. Left: the mixture taken out of the reactor right after the reaction; Middle: 1 hour after the mixture was taken out; Right: 24 hours after the mixture was taken out.

Since the simulated brine contained 80,000 mg/L of chloride, the GR formed was likely the chloride GR (i.e. GR-Cl). The formation of GR-Cl is important as Myneni et al. showed that it could trap selenate inside its interlayers by forming bidentate binuclear and edge-sharing complexes, and further reduce it to selenite.[45] Refait et al. studied the

reduction of selenate by GR-Cl under both oxic and anoxic conditions and similar color change was observed when GR-Cl was formed and further oxidized [41]. Zhang et al. studied the effect of different anions on the selenate removal by ZVI, and observed the formation of GR-Cl in the chloride-rich solution.[35] Selenate can be removed rapidly by adsorption once GR is formed and further reduced to selenite or even elemental selenium which stays inside the GR interlayers. Schellenger and Larese-Casanova studied the selenate uptake rate by GR-Cl under anoxic condition [44], and also proposed that selenate can be reduced to elemental selenium by incorporating into the interlayers followed by reduction. Therefore, the selenate in the FGD brine in this study is most likely removed by GR-Cl.

2.4.1.2 Effects of TDS and dosage

The effect of TDS on selenate removal by 1.00 g ZVI in 60 mL of simulated brine at pH 3.0 at both 25°C and 80°C was tested. At 25°C, selenate was not removed at all. At 80°C (Figure 2.8), the dilution of brine had only modest impact on selenate removal; the lower the TDS, the faster the removal rate. The slightly faster removal rate in more diluted brine could be attributed to less competition between selenate and other anions for the reactive sites [177-178].

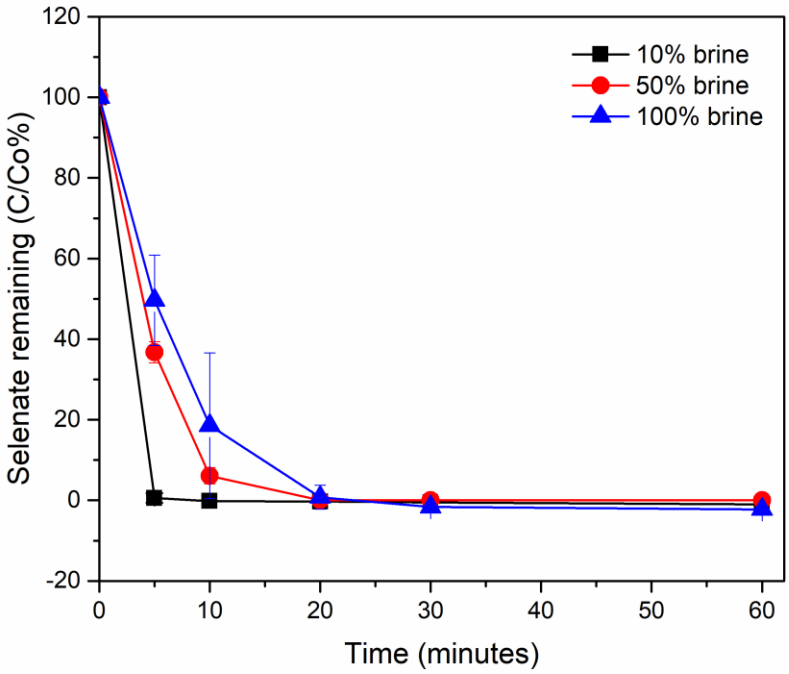

Figure 2.8. Effect of brine dilution on selenate removal by 16.67 g/L ZVI in selenate-only brine. The brine was at pH 3.0 and 80°C.

The effect of ZVI dosage on selenate removal was tested at both 60 °C and 80 °C in pH 3.0 simulated brine (60 mL) to find the optimal dosage for the treatment. At 60°C (Figure 2.9a), ZVI dosages of 0.25, 0.50 and 1.00 g had similar selenate removal rates, but 0.10 g ZVI led to a slower removal rate. At 80°C (Figure 2.9b), ZVI dosages of 0.25, 0.50 and 1.00 g could still achieve the similar percent removal of selenate within 30 min. Again, 0.10 g ZVI led to a slower removal rate. A lower dosage of ZVI resulted in fewer reactive sites for selenate, therefore leading to a slower removal rate. ZVI dosage is an important factor when considering the cost of treatment. In this test, increasing the temperature could reduce the dosage of ZVI required to achieve the similar selenate removal rate to that under higher ZVI dosages but a lower temperature at pH 3.0.

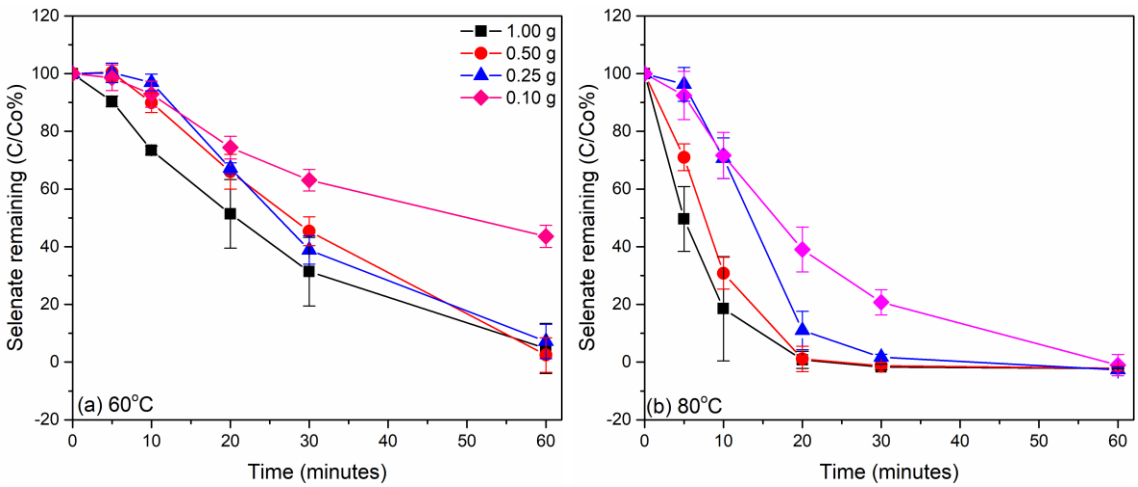

Figure 2.9. Effect of ZVI dosage (1.67-16.67 g/L) on selenate removal at different temperatures: (a) 60°C; (b) 80°C in selenate-only brine at pH 3.0.

2.4.2 Treatment efficiency of ZVI in multi-metal simulated brine

2.4.2.1 Effects of temperature on heavy metal removal in metal brine

Based on the results shown above, temperature was the dominant factor on ZVI's reactivity for selenate removal compared to other studied factors. The co-removal of selenate, arsenate, cadmium and chromate by 4.17 g/L ZVI was further studied in metal brine at 25°C-80°C and pH 5.9 (Figure 2.10). At 25°C and 40°C, ZVI was not corroded since the mixture's color did not change (remained grey). Selenate and cadmium were not removed at all at these two temperatures (Figure 10a and 10b). At 25°C, 50% of arsenate and 60% of chromate were removed within an hour, while at 40°C, they could be completely removed. At 60°C and 80°C (Figure 10c and 10d), almost 100% removal of arsenate (1 mg/L) and chromate (1 mg/L) could be achieved in less than 5 minutes. Selenate (25 mg/L) and cadmium (5 mg/L) could be completely removed within 60 minutes at 60°C and within 30 minutes at 80°C.

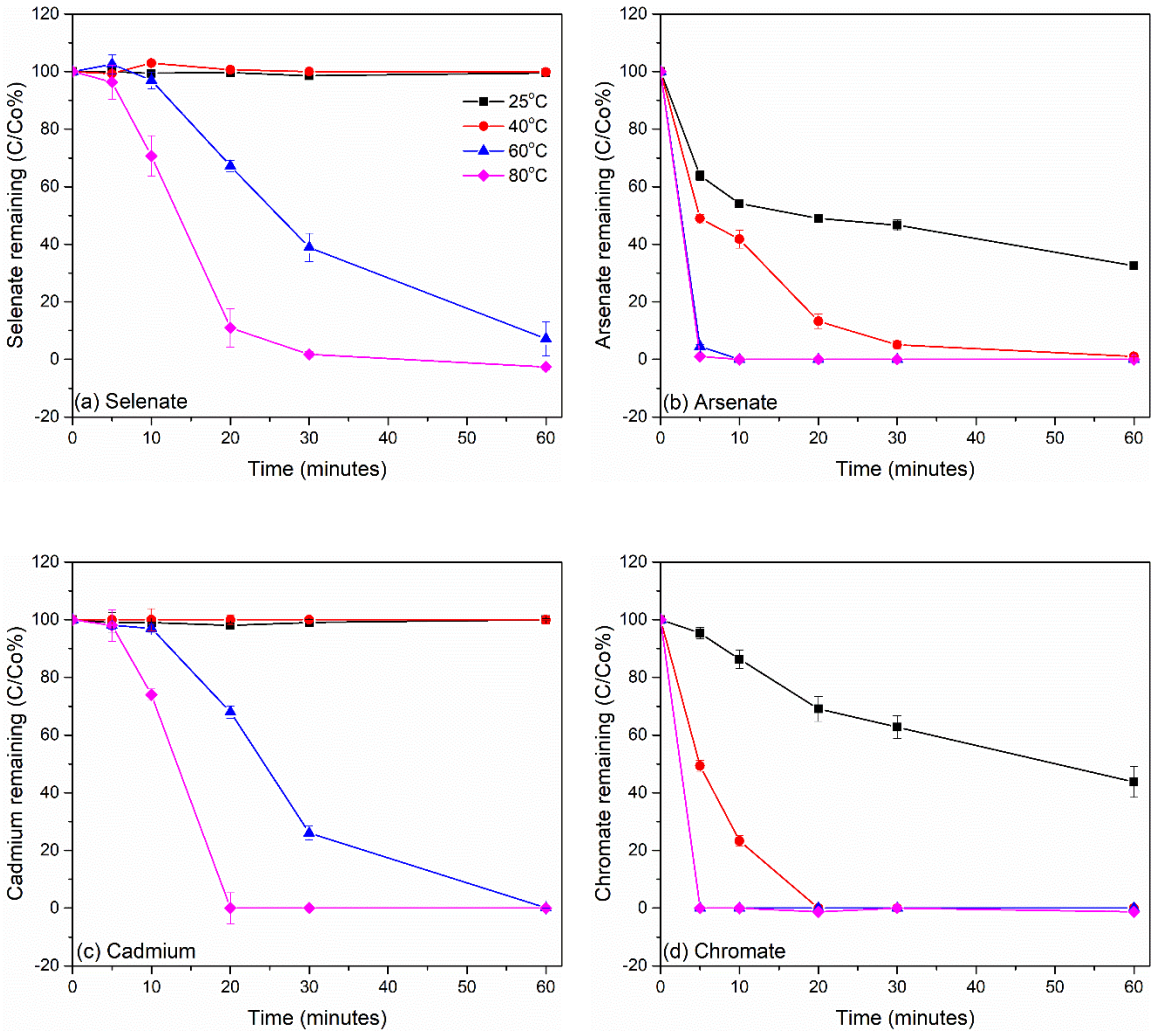

Figure 2.10. Effect of temperature on the removal of (a) selenate, (b) arsenate, (c) cadmium and (d) chromate by 4.17 g/L ZVI in metal brine at 25°C, 40°C, 60°C and 80°C at pH 5.9.

Note that arsenate and chromate (both at 1 mg/L) were rapidly removed within the first 5 minutes even the corrosion of ZVI had not occurred yet as the color of the mixture remained grey which was the color of raw ZVI. The XRD pattern of the ZVI sample after 5 minutes (shown in Figure 2.13 in Section 2.4.3.2) also indicated that green rust had not formed yet. Therefore, removal of the low concentration of arsenate and chromate was likely due to rapid surface adsorption without the help of green rust. On the other hand, the removal of selenate (25 mg/L) and cadmium (5 mg/L) relied on the corrosion of ZVI. The

lag period from 0 to 5 minutes in Figure 10c and 10d indicated that negligible amounts of selenate and cadmium were removed without ZVI corrosion. After 5 minutes, the color of the mixture gradually turned into dark green and the rapid removal of selenate and cadmium started to occur simultaneously.

Reduction of selenate by GR under low salinity and ambient temperature has been well reported in the literature and mentioned in Section 2.4.1. Cadmium (Cd^{2+}) ion removal by nZVI has also been studied previously,[73-74] but the formation of GR was not mentioned or observed. Although removal of cadmium by GR is not well reported in the literature, O'Loughlin et al. studied the reduction of several transition metal cations, including Ag^{I}, Au^{III}, Cu^{II}, and Hg^{II} by GR, and showed that all these metal cations could be reduced to their zero-valent state.[75] Therefore, the cadmium removal observed in this study (Figure 10) was likely due to the reduction by GR.

2.4.2.2 Competition and inhibitory effect between heavy metals

The existence of arsenate (1 mg/L) and chromate (1 mg/L) seemed to have negligible impact on the removal of selenate, as the selenate removal rate (Figure 2.10d) was comparable to that in selenate-only brine (Figure 2.6 and Figure 2.9b). However, when the concentration of arsenate and chromate was increased to 10 mg/L each, significant impact on the removal of selenate (25 mg/L) and cadmium (5 mg/L) was observed. As shown in Figure 2.11a, when 10 mg/L arsenate and 10 mg/L chromate were added together in the metal brine, the removal of selenate and cadmium was both completely hindered, while the color of the mixture remained grey for 60 minutes even though the removal of arsenate and chromate occurred. To evaluate the inhibitory effect of selenate and chromate, respectively,

10 mg/L arsenate and 10 mg/L chromate were added separately in the brine to be with selenate (25 mg/L) and cadmium (5 mg/L). When 10 mg/L chromate was added (Figure 2.11b), the selenate and cadmium removal was still completely inhibited. However, chromate itself was still successfully removed, indicating that the formation of this passive layer is the main mechanism for chromate removal and it is a highly favorable process. Muller et al. reported the successful chromate removal by fluidized ZVI with a Sauter diameter of 3.4 mm which is 3 folds larger than the size of the ZVI particles applied in our study [179]. When 10 mg/L arsenate was added (Figure 2.11c), the selenate and cadmium removal was slower compared to that in the normal metal brine, but still achieved 100% removal at 60 minutes. These results indicated that a high concentration of chromate will completely hinder the reactivity of ZVI on selenate and cadmium removal. Overall, 10 mg/L of chromate completely inhibited the reactivity of ZVI, which is in agreement with previous reports that the corrosion of ZVI could be inhibited by the formation of a passive layer composed of iron-chromium (oxy)hydroxides.[24, 180-181] A high concentration of arsenate slowed down the removal rate of selenate by ZVI due to competition for the reactive sides but did not inhibit the removal.

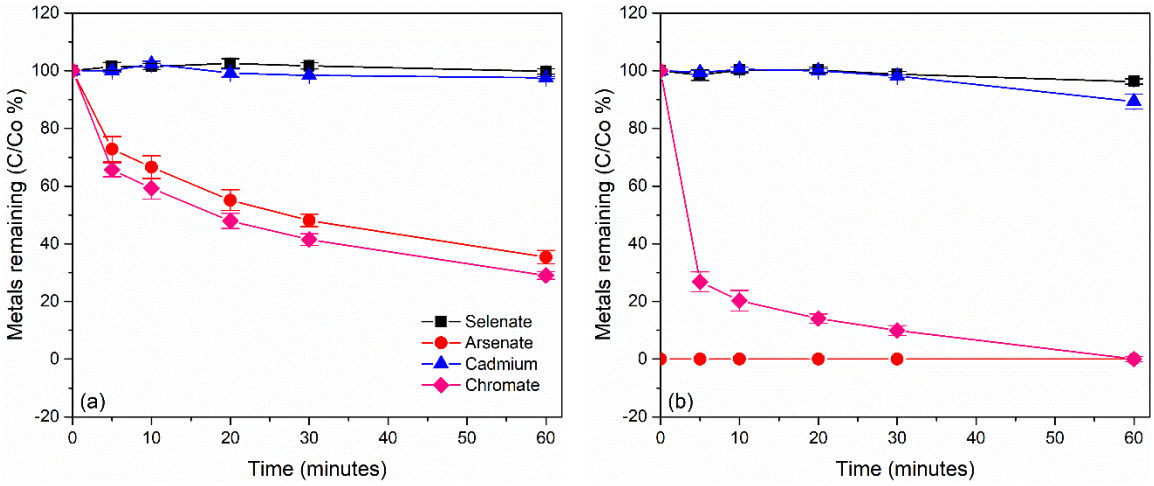

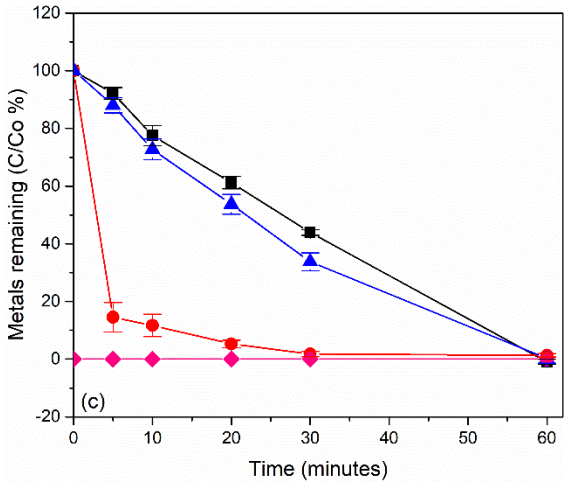

Figure 2.11. Heavy metal removal by 4.17 g/L ZVI at 80°C in simulated metal brine at pH 5.9: (a) 25 mg/L selenate, 5 mg/L cadmium, 10 mg/L arsenate and 10 mg/L chromate; (b) 25 mg/L selenate, 5 mg/L cadmium, 10 mg/L chromate and no arsenate; (c) 25 mg/L selenate, 5 mg/L cadmium, 10 mg/L arsenate and no chromate.

2.4.3 Treatment efficiency of ZVI in selenate-only brine

2.4.3.1 Longevity of ZVI in selenate-only and metal brines

To evaluate the longevity of ZVI, its performance on selenate removal at 80°C was tested in selenate-only brine for 5 hours, along with the monitoring of total iron released into the solution (Figure 2.12a). ZVI (4.17 g/L) performed well even after 5 hours, and selenate was completely removed within each cycle. Note that the somewhat uneven initial selenate concentration measured at the beginning of each cycle indicated the removal of selenate by ZVI was rapid and occurred as soon as selenate was spiked into the suspension. Within 5 hours, the reactivity of ZVI still remained and the iron concentration released into the solution was also detected, which was an indication that Fe(0) was still being oxidized with a decreasing amount but not depleted.

When the ZVI dosage was reduced to 1.67 g/L and the test was extended to 6 hours (Figure 2.12b), the reactivity of ZVI towards selenate removal was lost after 4 hours, and dissolved iron was no longer detected, indicating that Fe(0) was mostly consumed after 4 hours. The similar test with 1.67 g/L ZVI was also conducted in the metal brine for 6 cycles (Figure 2.12c). The removal of selenate was not affected by the existence of other heavy metals. In each cycle, cadmium (5 mg/L), arsenate (1 mg/L), and chromate (1 mg/L) were spiked, along with selenate (25 mg/L), into the mixture but they were quickly removed by the corroded ZVI (GR). Although aliquots of sample were taken right after the spiking, only remaining selenate was detectable in the solution, indicating the removal of Cd(+II), As(+V) and Cr(+VI) was quite rapid and effective. After 4 hours, the reactivity of ZVI for selenate removal was lost, and most of the Fe(0) was consumed as the iron concentration in the solution was no longer detectable.

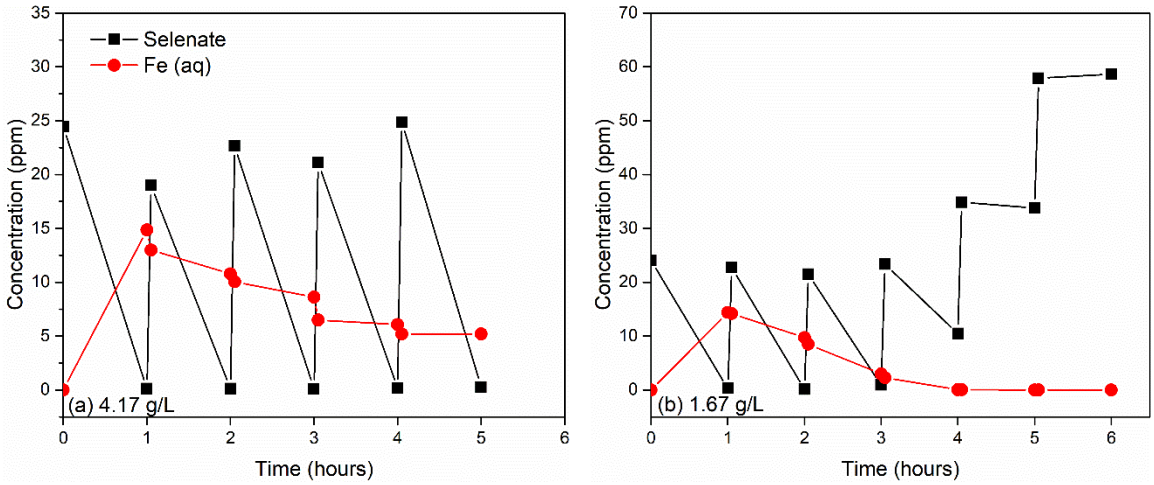

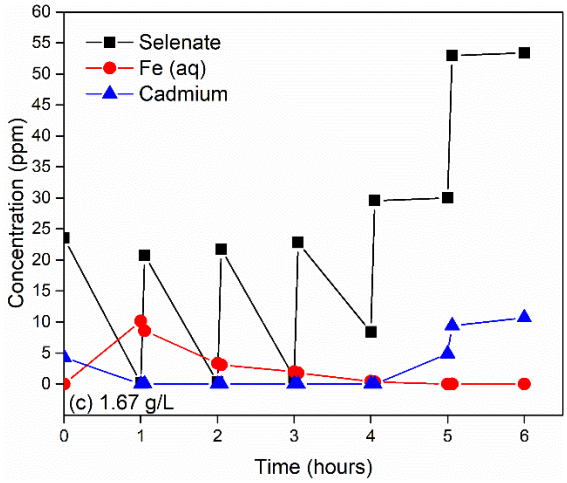

Figure 2.12. Selenate removal and total iron release at 80°C by (a) 4.17 g/L; and (b) 1.67 g/L of ZVI in selenate-only brine at pH 5.9. (c) Selenate and cadmium removal and total iron release at 80°C by 1.67 g/L ZVI in metal brine at pH 5.9. Reacted ZVI (green rust) remained in the mixture was used repeatedly in each cycle to treat the freshly added heavy metals for longevity test.

2.4.3.2 XRD of reacted ZVI samples

The reacted ZVI samples taken at 5, 60 and 360 minutes from the longevity test (Figure 2.12c) were filtered and vacuum dried for XRD analysis, and compared with the raw ZVI. The XRD patterns (Figure 2.13) suggested that, during the first 5 minutes of reaction, ZVI was slowly depassivated because only Fe(0) peak was shown. The passive layer around the raw ZVI was amorphous, thus not detectable by XRD. The XRD pattern of the sample taken at 60 minutes clearly showed the presence of GR (as mentioned in section 2.4.1.1) and the remaining Fe(0). After 360 minutes, Fe(0) was depleted and magnetite was formed. GR still existed, but it was no longer reactive for selenate removal (Figure 2.12c). The reacted ZVI became black as the color of magnetite, as detected by XRD.

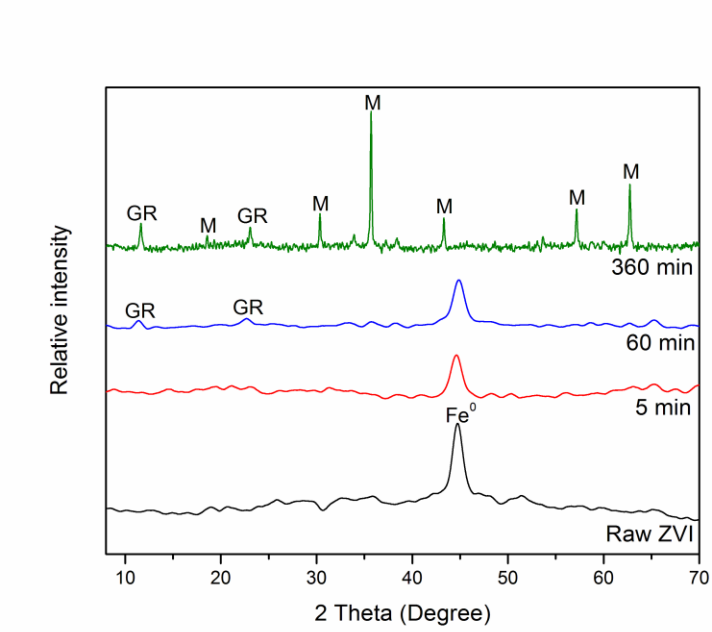

Figure 2.13. XRD patterns of ZVI samples during the longevity test. Fe^0 = raw ZVI (PDF# 00-006-0696); GR = green rust (PDF# 00-040-0127); M = magnetite (PDF# 01-080-6402)

As Figure 2.12c shows, although the removal of selenate was no longer observed after 4 hours, the amount of selenate increased was equal to the amount added, indicating previously removed selenate did not release back into the aqueous phase. The formation of magnetite didn't result in more selenium in the aqueous phase either. Therefore, the removed selenate was likely reduced to elemental selenium in the interlayers of GR, as observed in other studies.[35, 44]

2.4.4 Treatment efficiency of ZVI in real brine

2.4.4.1 Heavy metal removal in real FGD brine

While the major characteristics of the real FGD brine were similar to those of the simulated brine (Table 2.1), some differences existed. The removal of heavy metals by 4.17

g/L ZVI was conducted in the real FGD brine at 80°C, as a comparison to that in the simulated brines (Figure 2.14). Note that the real FGD brine contained little arsenic and a lower concentration (90 μg/L) of chromium. It was found that chromium was completely removed upon the addition of ZVI before the first sampling point at 5 minutes; thus, the results of As or Cr are not shown.

The removal rates of selenium and cadmium were both slower in the real brine compared to those in the simulated brine (Figure 2.14), primarily due to different brine matrices. Although chromate was shown to inhibit the corrosion of ZVI (Figure 2.11), its concentration in the real brine was not high enough to cause the inhibitory effect observed. Meanwhile, there were considerable concentration differences for some major anions (e.g. nitrate and sulfate) and metal cations (e.g. Ca^{2+} and Mg^{2+}) in the real brine *vs.* in simulated brine. It is known that nitrate and sulfate could compete with heavy metal oxyanions for ZVI adsorption and reduction [19, 38, 182]. Metal cations such as Mg^{2+} could also affect the corrosion of ZVI surfaces [183]. Therefore, the effects of oxyanions and metal cations on selenate removal were studied to help explain the hindered reactivity in the real brine.

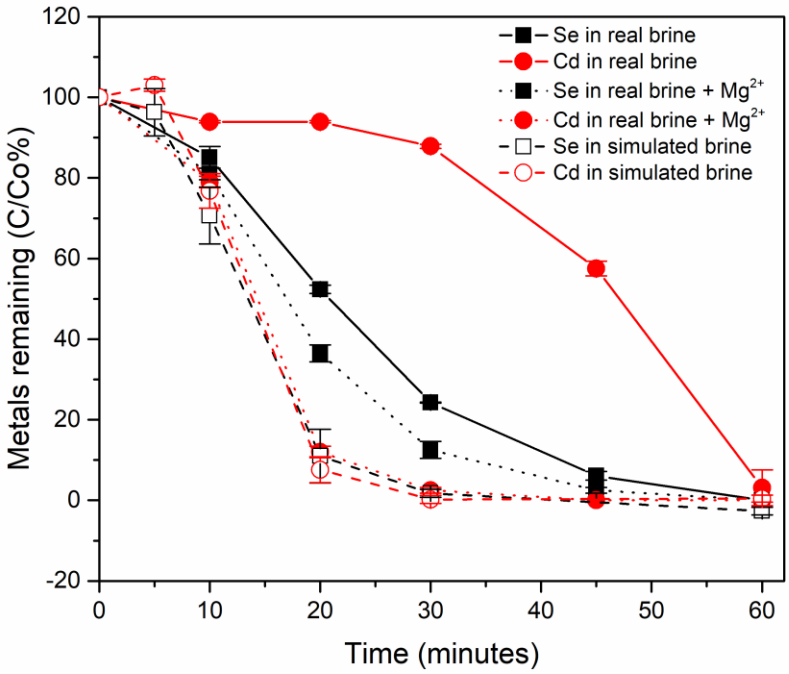

Figure 2.14. Selemium and cadmium removal in real FGD brine with and without the addition of Mg^{2+} compared to that in simulated brine using 4.17 g/L ZVI at 80°C.

2.4.4.2 Effect of nitrate and sulfate

The effects of nitrate and sulfate on the removal of selenate by 4.17 g/L ZVI was tested at 80°C in simulated selenate-only (25 mg/L) brine. Both nitrate and sulfate had only a slight effect on the removal rate of selenate (Figure 2.15). Therefore, nitrate and sulfate were unlikely the cause for the slower reaction in the real brine.

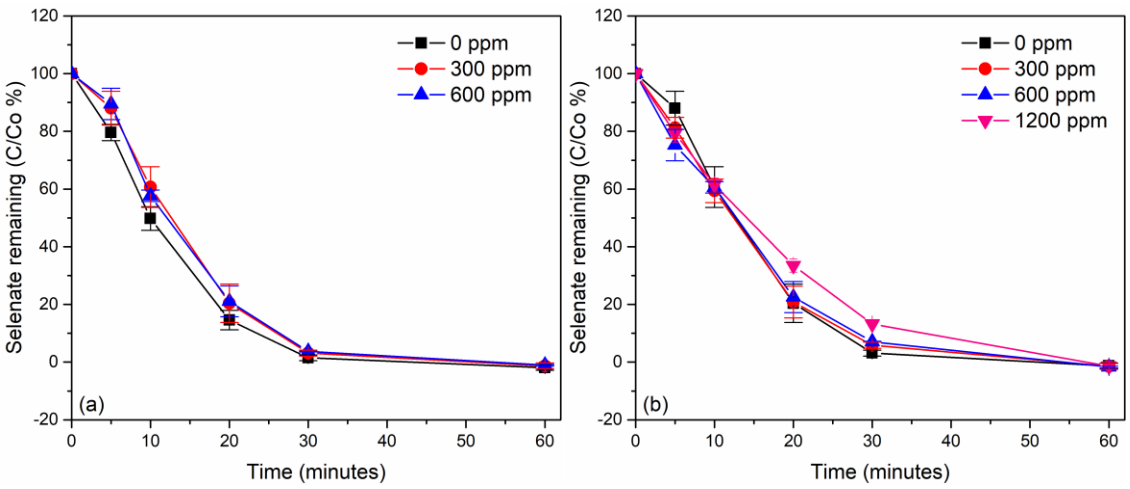

Figure 2.15. Effect of (a) nitrate and (b) sulfate on selenate removal in simulated selenate-only (25 mg/L) brine selenate using 4.17 g/L ZVI at 80°C.

2.4.4.3 Effect of Mg^{2+} on the depassivation of aged ZVI

One important factor which could account for the slower removal rate of heavy metals in the real brine was the lower Mg^{2+} concentration compared to that in the simulated brine (Table 1). Liu et al. studied the depassivation of aged ZVI by divalent cations and showed that Mg^{2+}, along with other cations, could destroy the passive layer of aged ZVI by complexing with the passive iron oxide coating on the ZVI surfaces. This complexation enhanced the dissolution of the hydrated surface, therefore enhancing ZVI's reactivity [183]. Among the effective divalent cations recognized in that study,[183] Mg^{2+} is one of the major metal cations which is naturally present in the FGD brine.

To assess whether Mg^{2+} played an important role in the simulated brines in this study, selenate removal was tested in DI water matrix with a pH of 5.5 at 80°C. The results showed no removal of selenate, likely due to the lack of Mg^{2+} in the DI water system. Further on, the recipe of the simulated FGD brine was adjusted to study the importance of

Mg^{2+}. As Table 2.1 shows, the most dominant metal cation in the simulated brine was Ca^{2+} (57,580 mg/L), and Mg^{2+} and Na^{+} were at 9,340 mg/L and 990 mg/L, respectively. As Figure 2.16 shows, replacing Mg^{2+} and Na^{+} by Ca^{2+} (indicated as "Ca^{2+}-only brine", total Mg = 0 mg/L) in the simulated brine significantly lowered the removal rate of selenate. On the other hand, replacing Ca^{2+} and Na^{+} by Mg^{2+} ("Mg^{2+}-only brine", total Mg = 44,320 mg/L) or replacing Ca^{2+} with Na^{+} ("Na^{+} and Mg^{2+} brine", total Mg = 9,340 mg/L), led to a similar reaction rate of selenate removal as that in the unadjusted simulated brine. Results in Figure 2.16 confirmed that Mg^{2+} accounted significantly for the reactivity of ZVI, but further increasing Mg^{2+} concentration did not further increase the reactivity.

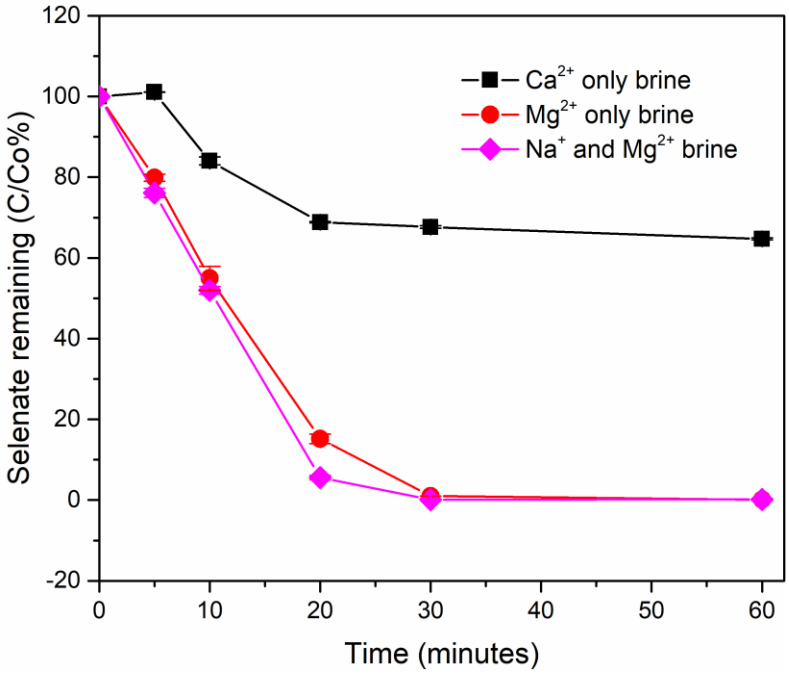

Figure 2.16. Effect of Mg^{2+} on selenate removal by ZVI (4.17 g/L) in adjusted simulated brine at 80°C. [Mg(+II)] = 0, 44,320, and 9,340 mg/L in "Ca^{2+}-only brine", "Mg^{2+}-only brine", and "Na^{+} and Ca^{2+} brine", respectively.

The effect of Mg^{2+} was further tested in the real FGD brine at 80°C using 4.17 g/L ZVI. $MgCl_2$ salt was added into the real brine to match the concentration (9,340 mg/L) of Mg^{2+} in simulated FGD brine. By adding Mg^{2+} into the real brine (Figure 2.14), the removal rate of both selenate and cadmium was increased significantly. This result further demonstrated that for real FGD brines with a low concentration of Mg^{2+}, Mg^{2+} could be amended to enhance the reactivity of aged ZVI.

2.5 CONCLUSIONS

The investigation of the removal of heavy metals by aged ZVI in concentrated FGD brines have led to several important new findings in this study. High temperature and Mg^{2+} are the dominant factors that will enhance ZVI's reactivity for the removal of selenate, arsenate, cadmium, and chromate in brine matrices. At 80°C, other factors such as pH, TDS, nitrate and sulfate become negligible, in contrast to their well-known interference with ZVI's reactivity under ambient temperature conditions. Meanwhile, the existence of Mg^{2+} in the brine is also important due to its ability to destruct the passive layer around the aged ZVI particles. Low concentrations of arsenate and chromate can be rapidly adsorbed by ZVI. Once the ZVI is corroded, the formation of GR leads to the removal of selenate and cadmium. Although GR is not stable in oxic condition, the high temperature lowers the concentration of dissolved oxygen in the brine, thus improving the stability of GR. The longevity of ZVI depends on how fast the Fe(0) is depleted and the stability of GR. The Mg^{2+} concentration in the tested real brine was lower than that in the simulated brine, and this could be a key factor which caused the slower selenium removal rate in the real brine compared to that in the simulated brine.

Based on the results of this study, aged, micron-sized ZVI is an effective material for treating hot FGD brine. Although the high temperature reaction condition makes this process energy intensive, the brine generated through thermal evaporation provides the high temperature condition. Hence, the ZVI treatment should be considered post evaporation of FGD wastewater. Magnetite as the final product could be easily removed magnetically to minimize the harms of heavy metals to the environment.

CHAPTER 3. SOLIDIFICATION/STABILIZATION OF FLUE GAS DESULFURIZATION BRINE AND COAL FLY ASH FOR HEAVY METALS AND CHLORIDE IMMOBILIZATION: EFFECTS OF S/S CONDITIONS AND ZERO-VALENT-IRON PRETREATMENT

3.1 ABSTRACT

Effective management of the flue-gas-desulfurization (FGD) wastewater and coal combustion residues (CCRs) are major challenges in the coal-fired power industry. The zero liquid discharge (ZLD) method through combining concentrated FGD brines and CCRs in solidification and stabilization (S/S) is promising because it has the potential of treating both wastes in the same process without the discharge of wastewater. This study evaluated the performance of such a ZLD method for the immobilization of heavy metals (Se, As, Cd and Cr) and chloride in FGD wastewater and/or CCRs. The effects of different coal fly ash (bituminous and sub-bituminous), activating agent (PC and lime) and pretreatment of brines by zero valent iron (ZVI) on the S/S process were evaluated. Short-term and long-term leaching tests were conducted to evaluate performance of the S/S solids in pollutant retainment. The pre-treatment of FGD brine by ZVI enhanced the retainment of heavy metals when BCFA ash was used, but not when SCFA was used since it already performed quite well without ZVI pretreatment. Quantitative X-ray diffraction (XRD) and scanning electron microscopy (SEM) analyses strongly indicated the formation of Friedel's salt is critical in the retainment of heavy metals and chloride. SCFA contains higher lime

and reactive aluminate content than BCFA, thus S/S solids made with SCFA contains higher amount of Friedel's salt. With the same type of CFA, using lime as the activating agent provides more alkalinity that PC, thus further enhance the formation of Friedel's salt.

3.2 INTRODUCTION

The United States coal-fired power industry faces increasing demands to improve solid waste and wastewater disposal practices.[4] Over 130 Mt of coal ash (or referred to as coal combustion residuals (CCRs)) are produced annually in the U.S., and more than half are disposed in landfills or surface impoundments.[184] The disposal of coal ash poses environmental risks due to elevated levels of heavy metals in these wastes and the potential of the heavy metals to leach over time. The Tennessee Valley Authority (TVA) Kingston Fossil Plant coal fly ash (CFA) slurry spill in December 2008 is the largest coal-ash spill accident in the U.S. history. The failure of a dike released about 4.1 million cubic meters of CFA slurry, which eventually spilled into the Emory River.[185] The extended spill covered and damaged 300 acres of surrounding land,[186] exposing severe environmental risk to the nearby residence and biota. TVA conducted a six-years-long recovery project which costed $1.18 billion dollars and 6.7 million man hours.[185] In 2015, the U.S. Environmental Protection Agency (USEPA) released the CCR rule regarding the disposal of CCRs from electric utilities,[187] which sets stringent requirements and timeline for the coal-fired power plants to safely transport and dispose CCRs.

Furthermore, the flue gas desulfurization (FGD) scrubbers at coal-fired power plants purge wastewaters contain significant concentrations of heavy metals (e.g. Se, As, Cr, Cd and Hg) and large amounts of salts (e.g. Cl^-, Ca^{2+}, Mg^{2+}, Na^+ and SO_4^{2-}),[1] which need

proper treatment prior to any discharge into receiving water bodies. In 2009, a typical coal-fired power plant could generate on average 2.1 million gallons of FGD slurry blowdown per day.[6] The solids in the slurry will be separated and the remaining wastewater will be either recycled back to the scrubber or transferred for treatment. In 2014, an estimated total of 210 million cubic meters of FGD wastewater was produced.[5] To reduce the amount of toxic metals and other pollutants discharged from the power plants, the USEPA released the Steam Electric Power Effluent Limitation Guidelines (ELG) in 2015, which sets stringent limits on As, Hg, Se and other pollutants' release to the environment from FGD wastewater.[6] However, due to the technical difficulty and financial burden to comply with this regulation, implementation of the ELG has been postponed for another two years.

As the coal-fired power plants are in urgent needs of more effective treatment and disposal strategies for the two major wastes of CFA and FGD wastewater generated on-site, interest in zero liquid discharge (ZLD) for wastewater treatment has been growing in recent years. The ZLD approach is attractive because it helps the power plants meet the stringent wastewater discharge limits, maximize water recycling at the plants, and potentially generate useful solid products. While ZLD eliminates FGD wastewater discharge, it will likely increase pollutant strength in the solid residuals from the wastewater, rendering these challenging solids in need of more effective stabilization technology before disposal or putting in alternative use. For that, we have developed a promising ZLD method by co-disposing FGD brine with CFA and Portland cement (PC) in a solidification/stabilization (S/S) process.[18] We have demonstrated that this co-disposal ZLD approach is effective in immobilizing As(V), Cd(II), Hg(II) and Se(IV) in the produced solidified/stabilized solids; however, oxidized forms of heavy metals, such as

selenate (Se(VI)) and chromate (Cr(VI), are challenging to immobilize without addition of an reductant when bituminous coal fly ash (BCFA) was applied.[18]

On the basis of the promise of the above ZLD approach, in this study we were motivated to couple the S/S process with a stronger reductant, zero valent iron (ZVI) pre-treatment, as well as explore the impact of S/S conditions for improving heavy metals and chloride immobilization. ZVI has been shown by many studies to be able to remove selenate, chromate and other metals from wastewater.[13, 24, 35, 73, 182, 188] However, one of the drawbacks of ZVI technology is that the ZVI surface becomes passivated with iron oxide layers when in contact with wastewater.[15-17] This passive layer can decrease the reactivity of ZVI toward target contaminants by creating a barrier that limits the flow of electrons from ZVI under the iron oxides to the target contaminants.[15-17] Therefore, this passive layer must be destructed for ZVI to work. Our recent study has demonstrated that low-cost, aged and micron-sized ZVI (1-3 μm) with passive layers could still achieve significant heavy metal removal in FGD wastewater brines at elevated temperature.[189] Therefore, the same ZVI was utilized in this work to pretreat the FGD brine before mixing with CFA for the S/S process.

Due to its cementitious properties, CFA has successfully replaced a portion of PC in many S/S processes that treat waste streams with heavy metal contamination.[18, 81, 85, 92, 107, 130-131] While CFA also contain heavy metals of concern, the resulted S/S mixtures were shown to be effective in immobilizing the target heavy metals in many cases.[18, 85, 91-92, 106-107] The properties of CFA are highly influenced by the type of fuel (coal) and the combustion conditions.[108] In 2017, 774.6 million tons of coal was produced in the U.S., and approximately 45.6% of the coal produces BCFA and 45.4% produces SCFA, and

about 92.8% of the total coal use was for energy production.[109] The most significant difference between these two CFAs is the higher CaO content in SCFA. SCFA with CaO contents >20% can be classified as cementitious materials.[110] Once mixed with water, the resulting slurry will be cured over time through pozzolanic reactions to generate the S/S solids.

The properties of CFA will influence the performance of the S/S process for heavy metal immobilization. Our previous[18] study demonstrated that S/S solids using SCFA resulted in better retainment of Se(VI) than using BCFA due to higher formation of Friedel's salt, which is denoted as AFm phase and belongs to the family of layered double hydroxides (LDHs). Friedel's salt is capable of binding heavy metal oxyanions [111-113] and chlorides.[114-116] The previous results that S/S solids using BCFA generated a negligible amount of Friedel's salt, which could be due to the lack of reactive aluminate in BCFA.[18] Meanwhile, the previous study also used PC as the activating agent with BCFA in the S/S process, which probably provided limited alkalinity for dissolving the glassy phases in BCFA. Alternatively, S/S processes using stronger activating agents such as hydrated lime or quick lime (i.e. $Ca(OH)_2$ and CaO) can provide more alkalinity for the pozzolanic reaction to proceed, which may facilitate the S/S in Friedel's salt formation and leach less heavy metals and chloride.[82, 107, 117-120]

Overall, this study is aimed to further optimize the ZLD approach in the S/S of co-disposed FGD brine and CFA. Both lime and PC as activating agents were evaluated for the S/S process with BCFA and SCFA, respectively, and compared for the performance in the retainment of heavy metals and chloride by short-term and long-term leaching tests. Simulated and real FGD brine with or without the pre-treatment by ZVI were used in the

S/S process. The minerology, especially Friedel's salt, of the S/S solids formed under the different conditions was carefully examined to provide insight for the contaminant retainment mechanism.

3.3 EXPERIMENTAL SECTION

3.3.1 Chemicals and materials

ZVI spherical particles with a labeled size of 1-3 micron in diameter was purchased from Fisher Scientific and its characterization is presented in section 2.3 in chapter 2. BCFA and SCFA were obtained from coal-fired power plants in the southeastern United States. PC was obtained from Home Depot (Cartersville, Georgia). Compositions of CFAs and PC were previously reported by our group.[18] Calcium hydroxide (hydrated lime) at 95+% purity was purchased from Acros Organics. Chemicals for making the simulated FDG brine is described in section 2.3 in chapter 2. The simulated FGD brine was synthesized by dissolving appropriate metal salts in deionized (DI) water, which was generated from a Millipore nanopure water purification system. This simulated brine with heavy metals added is named "metal brine" (MB). Without the heavy metals, the brine is named "metal-free brine" (MFB). Real FGD wastewater was collected following the solid separation of the FGD blowout from a coal-fired power plant in the Southeast of U.S. and used to generate the real FGD brine in this study. The generation of real FGD brine (RB) is described in section 2.3 in chapter 2. The compositions of the simulated and real brines, respectively, are shown in Table 2.1. Overall, the MB and RB had comparable characteristics (Table S1): pH (5.9 vs. 6.5), total dissolved solids (TDS) (126,000 vs. 133,000 mg/L), and chloride (80,000 vs. 77,800 mg/L). MB had higher heavy metal

concentrations than RB for the purpose of easier evaluation of removal efficiency: Se (25 vs. 3.1 ppm), As (1.0 pm vs. non-detectable), Cd (5.0 vs. 0.8 ppm) and Cr (1.0 vs. 0.09 ppm).

3.3.2 Pretreatment of brine by ZVI

The pretreatment of FGD brines by ZVI for heavy metal removal was previously studied[189] and the optimized reaction condition was applied in this study. Briefly, 60 mL of simulated or real brine was placed in a 100-mL borosilicate glass bottle and preheated in a heating bath to 80°C. ZVI powder (0.25 g) was added into this reactor to allow the reaction to proceed for one hour. Throughout the reaction, the temperature was maintained at 80°C and the reaction suspension was stirred by a magnetic stir bar (1.5" × 0.312") at 550 rpm. After one hour, the reactor was removed from the heating bath and allowed to cool down (unstirred) to the room temperature (25 °C). The reacted ZVI was remixed and the suspension was taken for the S/S process without filtering out the reacted ZVI.

3.3.3 Solidification and stabilization

S/S solid samples were prepared in duplicate using the recipes shown in Table 3.1. The weight percentage of each ingredient (i.e., brine, CFA and activating agent) followed the optimized condition in the previous study.[18] CFA and Portland cement/lime were first added into a stainless steel mixer, then simulated brine or real brine (treated or non-treated by ZVI) was poured into the mixer, generating a slurry which was mixed for 20 minutes.

The resulting paste was poured into a plastic mold and placed in a humid environment for curing for exactly 28 days before the leaching tests.

Table 3.1. Four recipes for the S/S process

Recipe	Coal Fly Ash	Activating Agent	Simulated or Real Brine
1	BCFA (90 g)	Portland cement (15 g)	45 g
2	BCFA (90 g)	Lime (15 g)	45 g
3	SCFA (90 g)	Portland cement (15 g)	45 g
4	SCFA (90 g)	Lime (15 g)	45 g

3.3.4 Leaching tests

Three different leaching tests were conducted to evaluate the performance of various S/S solids for heavy metal and/or chloride immobilization. All the glassware used in the experiments were rinsed with 5% nitric acid and then DI water, and dried before use.

U.S. EPA 1311[170]: For the USEPA 1311 leaching test (i.e. Toxicity Characteristic Leaching Procedure, TCLP), each S/S solid block was crushed by a hammer into small pieces which were then sifted by a 0.95 cm sifter. Fifty grams of the sifted solids were added into 1.0 L of extraction fluid in a plastic bottle. The extraction fluid was prepared by diluting 5.9 mL of acetic acid into 1.0 L of DI water. The mixture was then rotated at 30 rpm for 18 h under room temperature. After settling down, each sample was vacuum filtered through 0.45 μm acid-washed glass fiber filters. The filtered extraction fluid was acidified by nitric acid (5 mL of nitric acid into 95 mL of filtered extraction fluid) and the sample was stored at 4-5 °C before analysis.

Modified U.S. EPA 1313 [171]: The USEPA 1313 test is similar to the USEPA 1311 test except that the final leachate pH is controlled at a target value and nitric acid is used. The procedure and apparatus applied in this modified leaching test were the same as those of the standard USEPA 1313 method except using a different concentration of acetic acid instead of nitric acid in the extraction fluid. The goal of this modified leaching test was to target a similar final leachate pH (around 7) among all the S/S solids without changing other conditions. To determine the amount of acetic acid needed to add to each of the S/S solid to reach the final pH of 7 in the leachate after rotation, pre-titration was conducted for each type of solid on a smaller scale (5.0 g of crushed and sieved solids and 0.1 L of extraction fluid).

U.S. EPA 1315 [172]: The cured S/S solid monoliths generated in this study were applied in the long-term leaching test similar to the USPEA 1315 method. Each monolith was tied up by a plastic string which was fixed under the cap of a 500-mL plastic bottle. The length of the string allowed the solid to hang in the middle of the solution in the bottle. It took 480 mL of DI water to fill the bottle, and the final liquid volume (cm^3) to solid surface area (cm^2) ratio was around 9:1. At each sampling time specified in the USPEA 1315 method, the mass of the solid (with the cap and string whose mass was pre-measured) and the pH of the leachate were measured. The leachate was then poured into a container, acidified with nitric acid and stored at 4-5 °C for further measurements. Fresh DI water was added again into the bottle and the same procedure was applied in the next sampling time. The leaching tested lasted for a total of 63 days.

3.3.5 Analytical methods

The pH was measured by an Orion Star^{TM} A111 bench-top pH meter. The concentrations of heavy metals were detected by a Perkin Elmer 8000 inductively coupled plasma – optical emission spectroscopy (ICP-OES) (Waltham, MA). The detection limit for was around ppb for Se, 5 ppb for As, 0.2 ppb for Cd and 0.1 ppb for Cr. The washing solution used on the ICP-OES was 5% trace-metal-grade nitric acid. The chloride concentration was measure by a Dionex ion chromatography (IC) system (Sunnyvale, CA) with a detection limit around 100 ppb. The morphology of powdered S/S solids was obtained on a Zeiss Ultra60 field emission scanning electron microscopy (FE-SEM) (Carl Zeiss, Germany) operated at 5 kV. The crystal phases of the powdered S/S solids were analyzed using a PANalytical X'Pert PRO Alpha-1 X-ray diffractometer (XRD) (Almelo, Netherlands) at 45 kV and 40 mA, with the Cu *K*α radiation (λ = 1.542 Å) and a scanning rate of 0.033º per 100 seconds over a 2θ range between 4-70º. The S/S solids powder was generated by crushing the solids and sifting through a sieve with a mesh of 90 microns. For quantitative XRD, rutile was used as the internal standard (5% by weight) and the Rietveld method was applied to obtain the weight percentage of Friedel's salt, ettringite, and amorphous phase. XRD and FE-SEM analyses of S/S solids were done at the Institute for Electronics and Nanotechnology Materials Characterization Facility at Georgia Tech.

3.4 RESULTS AND DISCUSSION

3.4.1 Short-term leaching results of S/S solids

3.4.1.1 S/S solids made with simulated metal brine

Four different S/S solids (according to recipes in Table 3.1) were subjected to the USEPA 1311 and modified 1313 leaching tests, respectively, and the measured pH values of the leachate from the samples are shown in Table 3.2. As shown, the leachate from the modified 1313 leaching tests had the pH range at 6.6-8.1, lower than the leachate pH range of 6.6-11.9 from the USEPA 1311 leaching tests.

Table 3.2. The pH of leachate after 18 h of rotation in the USEPA 1311 and modified 1313 leaching tests

Type of S/S solid	1311	Modified 1313
BCFA + cement	6.6-7.3	6.6-7.3
BCFA + lime	9.8-10.2	6.8-7.2
SCFA + cement	9.7-10.1	7.1-8.1
SCFA + lime	11.5-11.9	6.9-7.5

The retainment of heavy metals (Se, As, Cd and Cr), evaluated by both leaching tests, were compared among the different S/S solid samples as shown in Figure 3.1. The retainment was calculated based on equation 1, where $M_{leachate}$ was the mass of metal in the leachate, M_{MB} was the mass of metal introduced from simulated metal brine (MB), and M_{MFB} was the mass of metal in the leachate of S/S solids made with metal-free brine (MFB). The M_{MFB} value represents how much heavy metals (existed in CFA and activating agents, not from brine) could be leached out. The level of heavy metals that could be leached from the CFA/PC or CFA/lime without the contribution from the brine were evaluated by generating S/S solids with MFB using the same recipes in Table 1 and subjecting these solids to the leaching tests. The amounts of Se, As, Cd, and Cr that could be leached from the S/S solids made with MFB in the 1311 and modified 1313 leaching

tests are shown in Table 3.3. In general, the amounts of background heavy metals were quite low compared to those introduced by MB (0.375 mg for Se, 0.015mg for As and 0.075 mg Cd, respectively). However, a significant amount (104 ppm)[18] of Cr existed in the PC utilized in this study.

$$Retainment\ \% = (1 - \frac{M_{leachate}}{M_{MB\ added} + M_{MFB\ leached}}) \times 100\% \quad \text{(eq.1)}$$

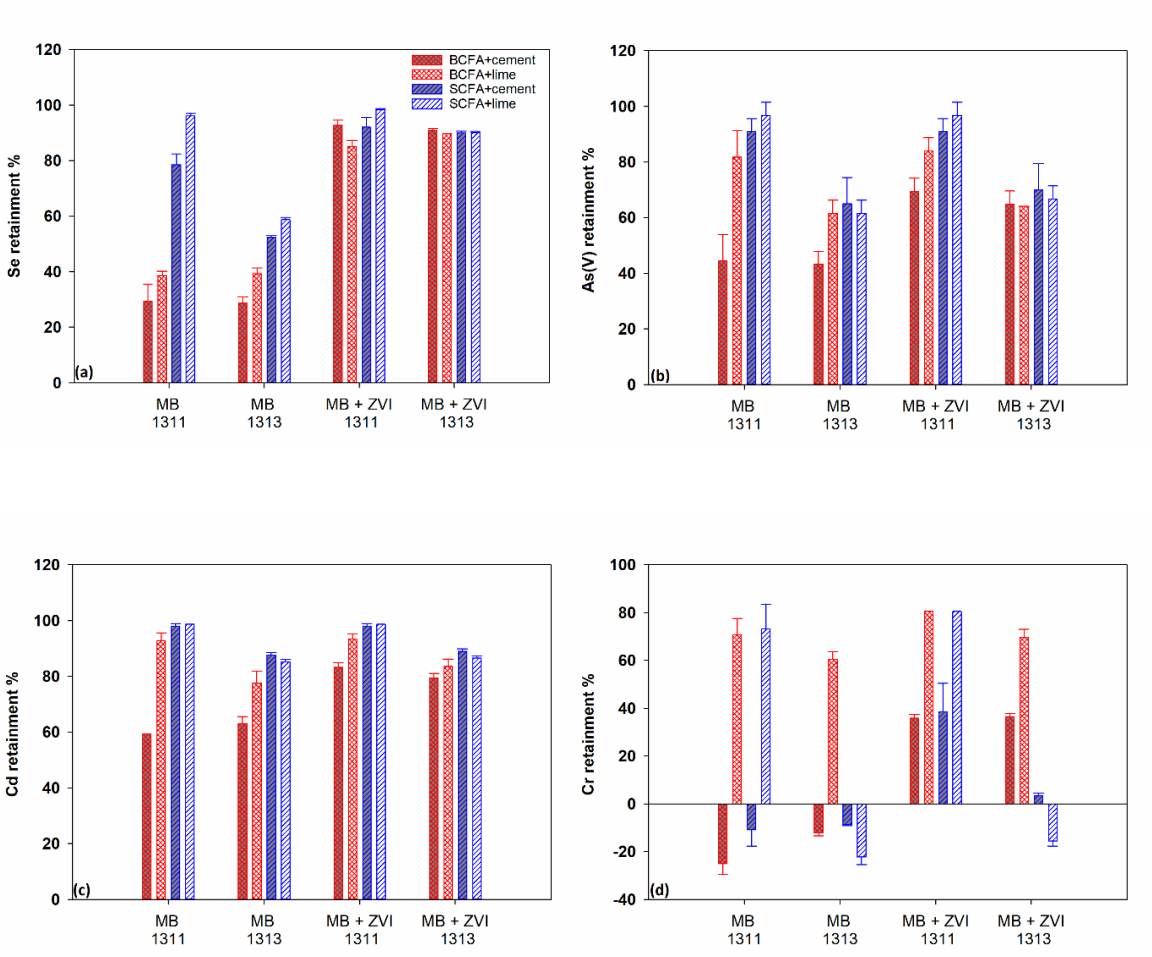

Figure 3.1. Heavy metal retainment (in %) of different S/S solids evaluated by two leaching tests (USEPA 1311 and modified 1313 methods). "MB" represents simulated metal brine without ZVI treatment, "MB+ZVI" represents simulated metal brine treated with ZVI which was mixed into the S/S process. (a) Selenium; (b) Arsenic; (c) Cadmium and (d) Chromium.

Table 3.3. Mass of heavy metals (in mg) released by 50.0 g of S/S samples made with metal-free brine in 1.0 L of leachate in the USEPA 1311 and modified 1313 leaching tests. (S/S solids made according to Table 3.1 recipes)

Type of S/S solid	Se		As		Cd		Cr	
	1311	1313	1311	1313	1311	1313	1311	1313
BCFA + PC	0.023	0.025	0.003	0.004	0.008	0.007	0.031*	0.043*
BCFA + lime	0.024	0.031	0.007	0.005	0.002	0.007	0.005	0.006
SCFA + PC	0.027	0.028	0.002	0.005	0.001	0.001	0.026*	0.107*#
SCFA + lime	0.003#	0.031	0.001	0.005#	0.001	0.003#	0.006	0.053#

* Cr level in the leachate was mainly introduced from PC;
# Higher amounts of acid added enhanced the leaching.

Figure 3.1a shows the retainment of selenium by different S/S solids. It should be noted that at least 65% and 50% of Se immobilized was Se(VI) for BCFA and SCFA S/S solids respectively, as introduced from MB (25 ppm Se(VI)), while the oxidation states of Se in CFA (7 ppm in BCFA and 14 ppm in SCFA)[18] and activating agents were less clear and not determined in this study. Results of the 1311 leaching test showed that the S/S solids made with BCFA retained only 30-40% of selenium, while S/S solids made with SCFA retained 80-96% of selenium. The Se retainment was improved by a modest degree when lime was the activating agent instead of PC for both cases of CFAs. The use of lime instead of PC in the S/S clearly increased the solids' leachate pH in the 1311 leaching test (Table 3.2). The final pH of the leachate is likely to influence the metal leaching potential. Indeed, as Table 3.2 shows, after the 1311 leaching test, the S/S solid made with SCFA and lime had the highest final leachate pH at 11.5-11.9 and also the highest selenium retainment (96%). However, this S/S solid's leachate pH was dropped to 6.9-7.5 in the modified 1313 leaching test (due to the higher amount of acid added before the leaching

test), which led to decrease of selenium retainment to 60% (Figure 3.1a). For the S/S solids made with BCFA, the selenium retainment did not differ much in both 1311 and 1313 leaching tests. This result could be attributed to the similar leachate pHs (around 7) in three of the four leaching tests.

Arsenic (Figure 3.1b) and cadmium (Figure 3.1c) had much lower concentrations in the leachate (slightly above or near the detection limit) than selenium due to their lower concentrations in MB. Nevertheless, retainment of As and Cd mostly follow the same trend as Se in that SCFA and lime gave better retainmant than BCFA and PC. However, chromium retainment (Figure 3.1d) showed a different trend. S/S solids with PC added leached a much greater amount of chromium than those with lime added, even higher than the amount of chromium introduced by the brine (0.015 mg compared to the mass of Cr in Table 3.3) and thus leading to an overall negative % retainment. Due to the high concentration (104 ppm)[18] of Cr in PC, PC is the dominant source of Cr in the leachate. Therefore, S/S solids with PC added leached more Cr than those with lime added. Meanwhile, the S/S solid made with SCFA and lime also leached a significant higher amount of Cr in the modified 1313 leaching test compared to that in the 1311 leaching test (Figure 3.1d). The most likely reason to cause this was acid addition in the 1313 test. For the final leachate pH to drop from 11.7 to around 7 in the 1313 test, the amount of acetic acid added before the leaching test was increased by 2.6 times compared to that in 1311 to neutralize the higher alkalinity contributed from SCFA and lime. This higher amount of acid likely enhanced the leaching of Cr from the SCFA (64 ppm Cr in SCFA)[18]. On the other hand, the S/S solids with BCFA and lime required only a slightly higher amount of

acid in 1313 test compared to that in 1311 test, so the Cr leaching from the ash (141 ppm Cr in BCFA)[18] was not enhanced significantly.

From the results in Figure 3.1, it can be concluded that S/S solids made with SCFA perform better than BCFA in terms of heavy metal retainment. Overall, SCFA with lime has the best performance among the four types of S/S solids. The S/S solid made with BCFA and PC has the worst retainment for the heavy metals, which requires other improvements on this process to reduce metal leaching potential.

3.4.1.2 S/S solids made with real brine

The leaching results of heavy metals from the S/S solids made with real brine following the four recipes (Table 3.1) are shown in Figure 3.2. It should be noted that the concentration of heavy metals in the leachate are shown because retainment % could not be calculated by eq. 1 due to the lack of a metal-free version of RB. Again, S/S solids with SCFA released less heavy metals than those with BCFA based on both 1311 and 1313 leaching tests. Lowering the leachate pH (modified 1313) also resulted in more leaching of heavy metals, especially for S/S solids with SCFA, as previously discussed. The concentrations of these four heavy metals in RB were much lower than those in MB, and thus the heavy metals detected in the leachate were from RB as well as CFA and the activating agents (e.g., the mass of Se in the leachate of S/S solid made with BCFA and PC is 170% of the mass of Se introduced from RB). Notice that the S/S solid made with SCFA and lime achieved the best performance by leaching less than 10 µg/L of all four heavy metals combined in the 1311 test. The S/S solid made with BCFA and PC had the worst performance by leaching the most amount of heavy metals; even so, the amount of heavy

metals leached were still significantly below the maximum concentration of contaminants for toxicity characteristics regulated by USEPA[170].

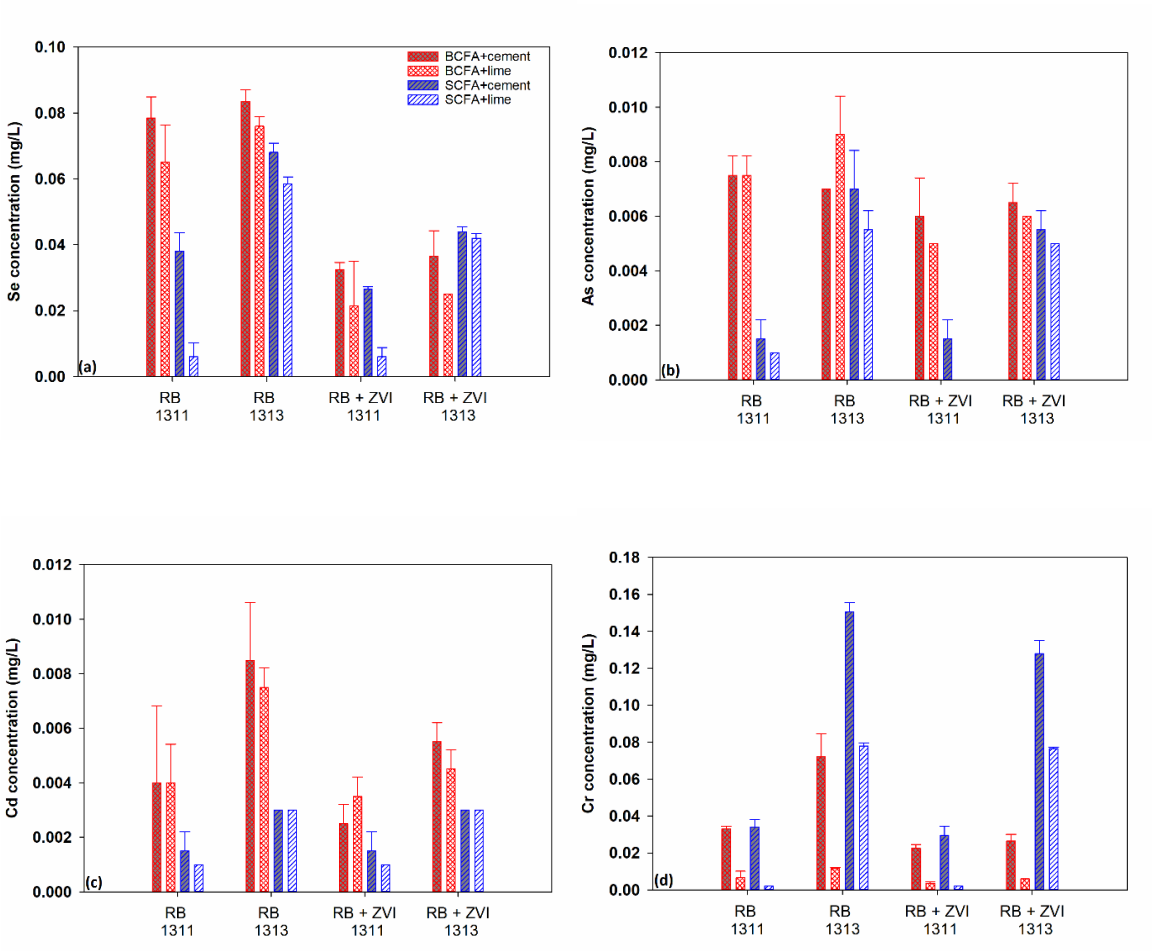

Figure 3.2. Heavy metal concentrations in the leachate from different S/S solids (made with real brine) and leaching tests. "RB" represents real brine without ZVI treatment, "RB+ZVI" represents real brine treated with ZVI which was mixed into the S/S process. (a) Selenium; (b) Arsenic; (c) Cadmium and (d) Chromium.

3.4.1.3 Impact of ZVI pretreatment of brines

The MB and RB were pretreated by ZVI and the treated brines were used to generate S/S solids according to the four recipes in Table 1, followed by the 1311 and modified 1313 leaching tests of the solids. Results of this set of S/S solids in retaining heavy metals

are also shown in Figure 3.1 and Figure 3.2 for easier comparison with those without ZVI pre-treatment of brines. Based on the 1311 results, pre-treatment of MB by ZVI enhanced the retainment of heavy metals for the BCFA S/S solids but not much for SCFA S/S solids, primarily because the SCFA S/S solids already performed quite well without ZVI pretreatment. According to our previous study[189], the ZVI treatment of MB and RB could completely remove Se(VI), As(V), Cd(II) and Cr(VI) from the liquid brine due to reduction, precipitation and/or adsorption of heavy metals to ZVI and iron precipitate particles. Therefore, the ZVI-pretreated brines likely contributed only very trace amounts of heavy metals in the aqueous phase in the S/S process. However, since the reacted ZVI was not filtered from the pre-treated brines in this study, it was possible that the reduced heavy metals bound on ZVI and iron precipitates could be released into the leachate if the reacted ZVI and/or iron precipitates were corroded by acids in the leaching tests.

As shown in Figure 3.1a, ZVI pretreatment greatly enhanced the retainment of Se by BCFA S/S solids from 30-40% to 85-95%, likely due to the effective removal of Se(VI) by ZVI in MB. Regarding the impact of lower leachate pH, Figure 1a shows that ZVI pre-treatment of brine could help maintain the high retainment of Se in the S/S solids even the leachate pH was lowered significantly in the 1313 leaching test.

The retainment of As (Figure 3.1b) and Cd (Figure 3.1c) was also improved by ZVI-pretreatment of MB, but the impact was less pronounced compared to Se because the concentrations of As(V) (1 ppm) and Cd(II) (5 ppm) in the metal brine were much lower than that of Se(VI) (25 ppm). Moreover, the level of As and Cd detected in the leachate of S/S solids made with the pretreated brine was very close to that from the S/S solids made

with MFB, indicating that the leaching of As and Cd was probably more related to CFA and activating agents, not the pretreated brine.

The retainment of Cr (Figure 3.1d) by S/S solids with PC addition was also greatly enhanced, not only by the ZVI-pretreatment of brine, but also the introduction of reacted ZVI into the S/S solids. For example, for the S/S solid made with BCFA and PC, the Cr retainment in 1311 leaching test was increased by almost 60% by ZVI, but the complete removal of Cr(VI) (1 ppm) in the brine could at most account for 30% of increase in retainment. Therefore, the additional retainment of Cr (from PC) was likely due to the reacted ZVI introduced into the S/S mixture, indicating that the reacted ZVI was still reactive for Cr removal during mixing in the S/S process. In analogy, such contribution of reacted ZVI in the S/S mixture for enhanced retainment likely also occurred for the other heavy metals. Our previous study[189] indicated that when the ZVI was applied to treat the MB at 80 °C for one hour, green rust (GR) was generated which could remove heavy metals including selenate, arsenate, cadmium and chromate. As long as GR was stable and Fe^0 was not depleted, the Se(VI) in brine could be completely removed in less than one hour while Cd(II), As(V) and Cr(VI) could be completely removed within one minute. The majority of the GR formed remained stable even during the one hour when the reaction mixture of ZVI and brine was cooled down to the room temperature. Thus, mixing this reacted ZVI (with GR formation) with CFA and activating agent in the S/S process provided GR that could facilitate the immobilization of heavy metals in the S/S slurry.

Figure 3.2 shows that ZVI pretreatment of RB also enhanced the retainment of heavy metals in the S/S solids, leading to lower concentrations of Se, As, Cd and Cr in the leachate compared to those without ZVI pretreatment of RB. Note that the improvement brought

about by ZVI pretreatment of brine was not as obvious as it appears in Figure 3.1 in the case of MB; this was partly due to the much lower concentrations of heavy metals in RB than in MB (Table 3.1) and thus the difference was not as easy to be seen.

3.4.2 Long-term leaching results of S/S solids

Although short-term leaching tests provide a fast evaluation of the S/S solids for heavy metal immobilization, the 1311 and 1313 tests involved crushing the solids and rotating the sample during the test which is not realistic considering the actual landfills' conditions. Therefore, the long-term leaching test (the USEPA 1315 method) was utilized to evaluate the leaching potential of heavy metals and chloride using the monolith of the S/S solid and refreshing the extraction fluid over the time to better simulate the landfills' conditions. The physical properties of the monoliths are shown in Table 3.4. During the 1315 leaching test, it was found that the change of mass of S/S solid blocks was almost negligible over the 9 weeks of leaching test (Table 3.4). As shown in Figure 3.3a, during the 9-week span, the pH of leachate from the four types of S/S solids gradually increased from 10.0–10.5 and peaked to 11.5–12.0 at around the fourth week, and then decreased slightly afterwards to 11.0–11.5, likely due to the consumption of alkalinity from refreshing the extraction fluid (DI water). The leachate of SCFA S/S solids had higher pH values than those of BCFA S/S solids due to the higher lime content in the SCFA. For the same CFA, lime addition also yielded higher leachate pH than PC addition.

Table 3.4. Physical properties of S/S monoliths tested in USEPA 1315 leaching test

Type of S/S solid	Mass (g)	Volume (cm^3)	Surface area (cm^2)	Density (g/cm^3)

BCFA + cement	50.0-50.3	27.7	54.1	1.81-1.82
BCFA + lime	49.8-50.0	30.5	56.7	1.63-1.64
SCFA + cement	49.8-50.2	26.3	52.8	1.89-1.91
SCFA + lime	49.7-49.8	27.7	54.1	1.79-1.80

The leaching of chloride and heavy metals was monitored during the long-term leaching test. Figure 3.3b shows the cumulative chloride release (mg/m^2) over the 9 weeks. Overall, the BCFA S/S solids leached more chloride than SCFA S/S solids. Within the same type of CFA, samples with lime addition retained more chloride than those with PC addition. Note that the significant leaching of chloride was mainly due to its high concentration (80,000 ppm) from the simulated MB. While part of the chloride could be bound within certain mineral phases formed in the S/S solids (see discussion in the next section), most of the chloride likely remained loosely bound on the surfaces and/or inside of the S/S solids, due to the high abundance of chloride. Once exposed into the DI water, the chloride adsorbed on the solid surfaces was washed off rapidly, as represented by the initial high chloride release at 2 hours (0.083 day in Figure 3.3b). As the leaching test proceeded with longer time, the chloride leaching gradually tapered off (shown in log scale), indicating the concentration difference of chloride between the S/S solid and the extraction fluid (DI water) became smaller. Overall, the S/S solid made with BCFA and PC had the most chloride leaching, while the S/S solid made with SCFA and lime had the lowest chloride leaching, with about 50% versus 15% of total chloride from MB leached after 63 days. For the same type of CFA, S/S solids with PC addition leached more chloride than S/S solids with lime addition.

In terms of heavy metal leaching, the concentrations of heavy metals found in the 1315 leachate of the S/S solids were always quite low and sometimes near the detection limits throughout the leaching test. The results of Se and Cr are shown in Figure 3.3c and 3.3d. Arsenic and cadmium concentrations in the leachate were below the detection limits and thus they were well immobilized in the S/S solids with negligible leaching potential. In general, the leaching of Se showed a similar trend as the leaching of chloride among the four types of S/S solids. S/S solids made with BCFA leached more selenium than those with SCFA. Lime addition was better than PC addition for Se immobilization. For chromium leaching (Figure 3.3d), S/S samples with PC added leached considerably more chromium, due to the chromium existed in the PC as discussed previously. In contrast, S/S samples with lime added (either SCFA or BCFA) leached only trace amounts of chromium, suggesting that chromium from the brine and either type of ash could be well immobilized in this S/S process.

Notice that the leaching curves of Se and Cr did not plateau at the longer leaching time like chloride did, but kept increasing. This behavior suggested that the leaching of Se and Cr was not diffusion-controlled, but was more likely related to the dissolution or exchange reaction of mineral phases in the S/S solids which could retain these heavy metals (see more discussion in the next section). Even with measurable leached concentrations, the amounts of Se and Cr leached at the end of 63 days were still quite low. For example, the amount of Se leached was 5-10% of the total Se in MB for the four S/S solids after 9 weeks. Therefore, the heavy metals from the brine were greatly immobilized by the S/S process, especially for the samples made with SCFA.

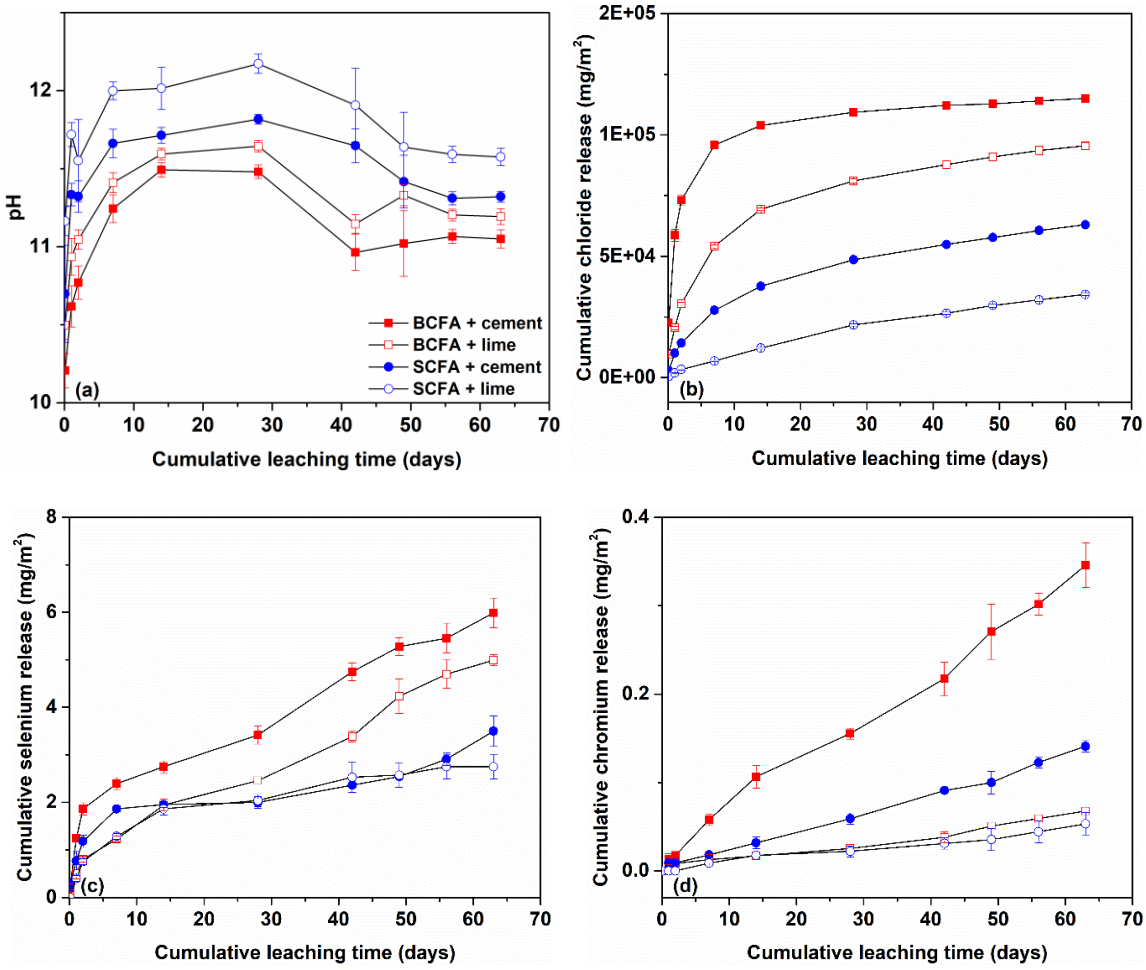

Figure 3.3. Results of the USEPA 1315 leaching test of S/S solids made from simulated MB with 4 different recipes: (a) Change of pH of leachate over 9 weeks, and Cumulative mass release of: (b) chloride, (c) selenium and (d) chromium over time.

3.4.3 Mineralogy of the S/S Solids

The S/S solids made from simulated MB using the four different recipes in Table 3.1 were evaluated for mineralogy by XRD prior to leaching tests. As shown in Figure 3.4, several phases in the S/S solids were confirmed by the XRD analysis, including ettringite (Et), Friedel's salt (FS), quartz (Q), gypsum (G), mullite (M), periclase (P) and calcite (C). Notably, both ettringite (an AFt phase, or triphase) and Friedel's salt (an AFm phase, or monophase) were present in all the samples, but the presence of Friedel's salt was not very

significant in the S/S solid made with BCFA and PC compared to the other S/S solids. Meanwhile, the S/S solid with BCFA and PC exhibited the worst heavy metal and chloride immobilization as discussed in the previous sections.

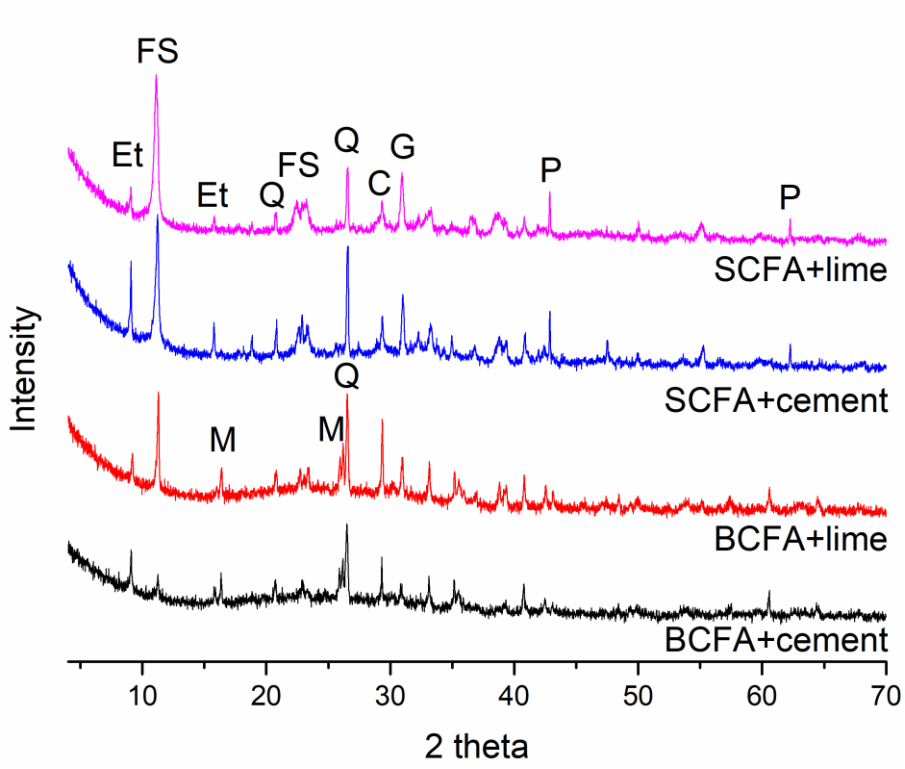

Figure 3.4. XRD spectra of four different S/S solids made with simulated metal brine.

Both monophase ($Ca_2(Al,Fe)(OH)_6)\cdot X\cdot xH_2O$) and ettringite ($Ca_6Al_2(OH)_{12}(SO_4)_3\cdot 26H_2O$) are important phases for heavy metal immobilization.[81] Comparatively, monophase has the higher affinity to adsorb heavy metal oxygen anions such as selenate compared to ettringite.[113] Different monophases are denoted by AFm-X, where X is an anion of CO_3^{2-}, Cl^-, OH^-, or SO_4^{2-}. AFm-Cl is known as Friedel's salt.[125] Ettringite is denoted by AFt-SO_4.[156] The AFm phase structure consists of positively charged $Ca_2[Al(OH)_6]^+$ layers, producing a net charge imbalance.[125, 128] Anions (X) occupy the area between the layers of $Ca_2[Al(OH)_6]^+$ to balance the mineral's charge.[125, 128] The

exchange of anions in the interlayers with external anions is typically highly favored.[125, 128] Because chloride is the dominant anion in the FGD brine in terms of concentration (i.e. 80,000 ppm in MB this study), the dominating AFm phase to be formed during the S/S process is expected to be Friedel's salt. Ettringite has a column-like structure with inter-channels containing anions and water molecules. Ettringite can also remove oxyanions through anion exchange.[117, 149, 157-158]

Regarding Se^{VI} immobilization, previously Baur and Johnson had studied the sorption of Se^{VI} to AFm-SO_4 and AFt-SO_4 through synthesis of the minerals and contact them with Se^{VI} in aqueous solution.[113] There was weak sorption to AFt-SO_4 (Rd = 0.03), but strong sorption of Se^{VI} to AFm-SO_4 (Rd = 2.06), indicating that solid rich in AFm-SO_4 would significantly immobilize Se^{VI}.[113] Through XRD analysis, the authors determined that Se^{VI} sorption increased the $Ca_2[Al(OH)_6]^+$ layer spacing due to SeO_4^{2-} replacing for SO_4^{2-} as the primary mechanism of Se^{VI} immobilization.[113] Another study by Wu *et al.* demonstrated that AFm-Cl effectively and rapidly removed Se^{VI} from aqueous solutions through surface adsorption and SeO_4^{2-} exchanging for Cl^- in the interlayers.[126] In general, AFm phases have shown significant affinity for immobilizing oxyanions, such as Se^{VI}, As^V and Cr^{VI}, through anion exchange.[125-128]

Besides metal removal, AFm-Cl formation in S/S has been proposed to bind Cl^- in high salt waste.[129-131] Lampris *et al*. attempted to S/S municipal solid waste incineration (MSWI) fly ash with Cl^- content of 130,000−220,000 ppm using PC with the aim to immobilize Cl^- through AFm-Cl formation.[130] In 72-day tank leaching tests, the authors observed Cl^- releases at 40-50% even with PC addition up to 50%.[130] In contrast, AFt phases have the ability to bind SO_4^{2-}, but not Cl^-.[131]

To assess the importance of Friedel's salt and ettringite in the S/S solids for immobilization of heavy metals and chloride, quantitative XRD using the Rietveld method was applied to the S/S samples to determine the weight percentage of these two minerals, as shown in Table 3.5. Based on the results, samples with lime addition had much higher Friedel's salt formation and less amorphous phase compared to the samples with PC addition using the same type of CFA. S/S samples with SCFA obviously had higher Friedel's salt formation and less amorphous phase compared to the S/S samples with BCFA. Lime addition and the lime content in the SCFA provided adequate alkalinity to enhance the speed of pozzolanic reaction. Reactive aluminate phase in the SCFA also provided Al for the formation of AFm phases.

Table 3.5. Weight percentage of Friedel's salt, ettringite and amorphous phase in the S/S solids before leaching test

Type of S/S solid	Friedel's Salt%	Ettringite%	Amorphous%
BCFA + cement	4.9%	5.8%	64.9%
BCFA + lime	15.0%	1.1%	57.5%
SCFA + cement	27.9%	7.0%	43.6%
SCFA + lime	40.4%	4.0%	29.2%

Combining this result (Table 3.5) and the long-term leaching result shown in Figure 3.3, one can see that the retainment of chloride and selenium are closely corelated to the formation of Friedel's salt. Samples with more Friedel's salt formation retained more chloride. By plotting the % of Friedel's salt in the solids vs. the cumulative chloride leaching (Figure 3.5a), a linear relationship with a R^2 value of 0.989 was obtained.

Therefore, the formation of Friedel's salt is likely to be the primary chloride binding mechanism. By plotting the % of Friedel's salt in the solids vs. the cumulative Se leaching (Figure 3.5b), a linear relationship with a R^2 value of 0.979 was obtained. This result strongly suggested that the formation of Friedel's salt was also likely to be the primary selenate immobilization mechanism.

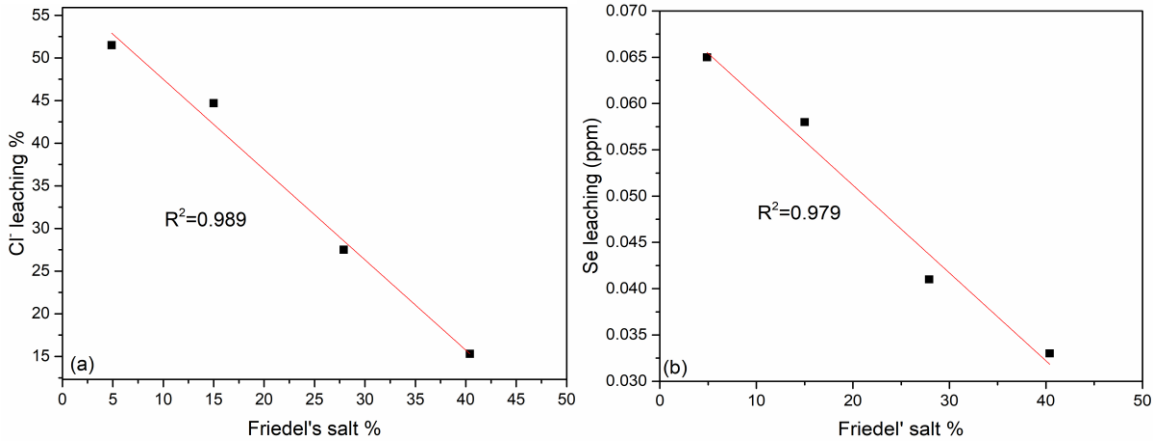

Figure 3.5. Relationship of Friedel's salt weight percentage in the S/S solids vs. the total leaching of (a) chloride and (b) selenium from the EPA 1315 leaching test. (*Note:* In Figure S2a, the cumulative chloride leaching percentage was calculated based on the total mass of chloride leached over 63 days and the total mass of chloride introduced from the simulated metal brine. The chloride from CFA and activating agent were ignored due to the significant amount of chloride in the simulated metal brine (80,000 ppm)).

Figure 3.6 shows the XRD spectra of the S/S solid made from RB with SCFA and lime before and after the 1311 and modified1313 leaching tests, respectively. It is clearly seen that, after the 1311 leaching test when the final pH of the leachate was 11.7, the peaks of ettringite were no longer present. After the modified 1313 leaching tests when the final pH was around 7.7, the peaks of both ettringite and Friedel's salt were no longer present. The pH domain for the stability of various AFm and AFt phase have been reported.[150-154] In general, both phases are less stable when the pH is less than 11. After the 1311 leaching

test, both ettringite and Friedel's salt dissolute to a certain extend. Ettringite has a much smaller weight percentage than Friedel's salt, so its peak disappeared while a significant amount of Friedel's salt still remained. After 1313 leaching test, both peaks disappeared because they were both destructed due to dissolution at pH 7.7. The disappearance of these peaks after leaching combined with the result of more Se leaching after the modified 1313 leaching test strongly suggested that the Friedel's salt formed in the S/S solids accounted the most for the Se retainment. During the long-term leaching test, as the pH dropped over time (Figure 3.3a), the stability of Friedel's salt could be affected which could result in selenium and chromium leaching in the later stage.

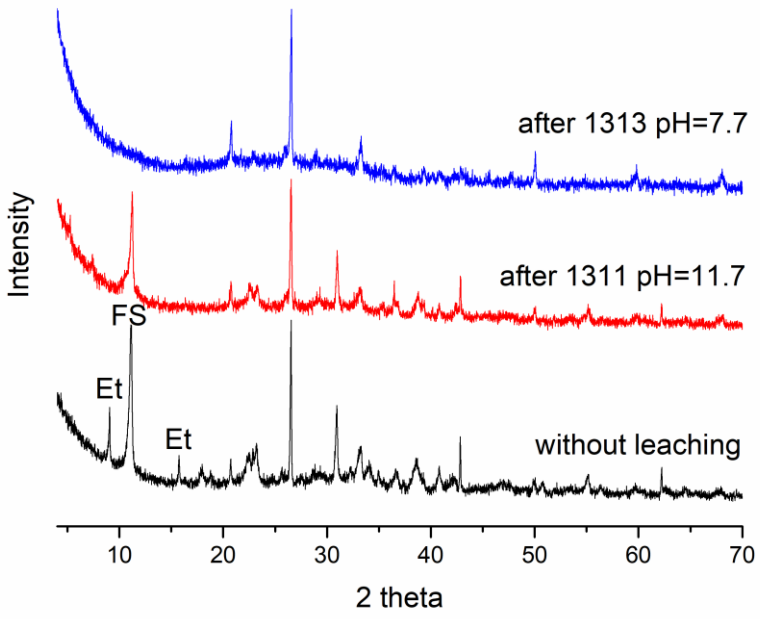

Figure 3.6. XRD spectra of S/S solids made from SCFA and lime with real brine before and after leaching tests.

The S/S solids made from the SCFA and lime with RB before and after the modified 1313 leaching tests were analyzed using FE-SEM. Figure 7a shows the S/S solid before leaching tests. It can be seen that there were some needle shaped structures which resemble the shape of ettringite, and some hexagonal flakes which resemble the shape of Friedel's salt. However, these particular shapes were not seen in the S/S solid after the leaching test, as shown in Figure 7b. These results were in good agreement with the results from XRD analysis.

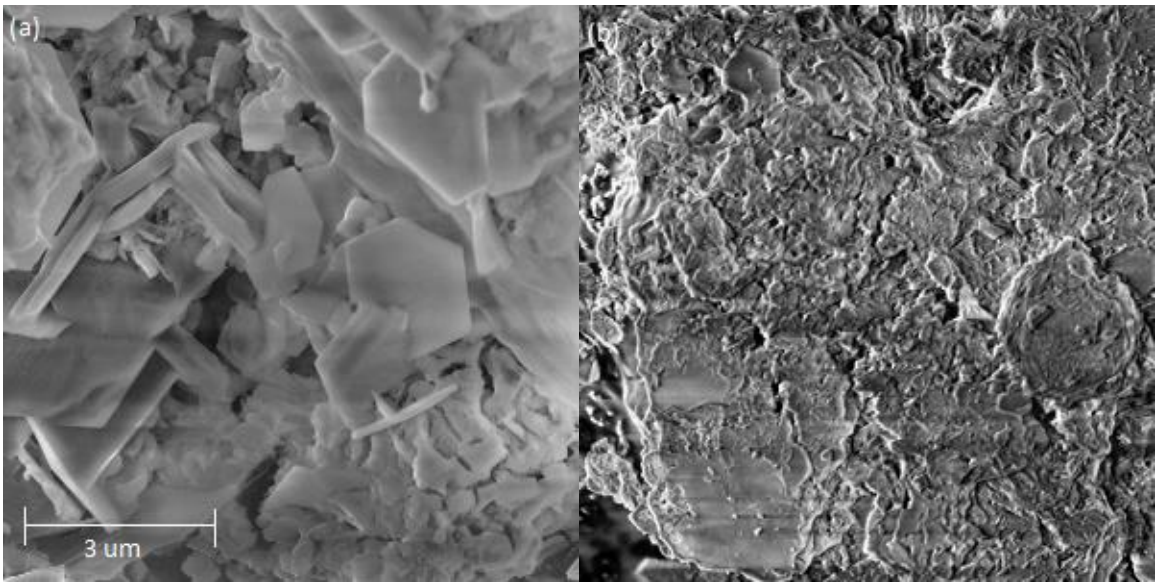

Figure 3.7. SEM image of S/S solid made of SCFA and lime with RB before (a) and after (b) modified 1313 leaching test (same scale applies on both images).

3.5 CONCLUSIONS

Results of this study show that the co-disposal of FGD brine with CFA via a S/S process is a promising ZLD method. The S/S solids using SCFA performed better in terms of heavy metal (Se(VI), As(V), Cd(II) and Cr(VI)) and chloride immobilization than the

S/S solids using BCFA. Furthermore, SCFA with lime had the best performance compared to using PC as the activating agent. Considering the lower performance of BCFA in S/S for heavy metal immobilization, pre-treatment of brine by ZVI prior to the S/S process could significantly enhance the retainment of heavy metals. The formation of Friedel's salt in the S/S solids played a major role in the retainment of heavy metals and chloride. However, Friedel's salt was stable at high alkaline pH (≥11), leading to potential concerns of heavy metal leaching in the real landfills when more acidic conditions are encountered. Based on the results from this work, the performance of this ZLD method dealing with BCFA could be further enhanced by three approaches: (1) combining the S/S process with a reduction process (e.g. pre-treatment of brine by ZVI); (2) increasing the formation of Friedel's salt (or AFm phase) by optimizing the mixing recipe; and (3) adjusting the mixing recipe to decrease the permeability of the bulk S/S solid, which could affect the stability of the AFm phases inside the solid.

CHAPTER 4. MINERALOGY OPTIMIZATION FOR METAL AND CHLORIDE IMMOBILIZATION IN CO-DISPOSED FLUE GAS DESULFURIZATION BRINES AND BITUMINOUS COAL FLY ASH

4.1 ABSTRACT

Increasing treatment regulations for coal combustion residues and wastewater generated at coal-fired power plants resulted in the implementation of zero liquid discharge (ZLD) treatment options. A novel ZLD treatment method which couples the concentrated flue gas desulfurization (FGD) brine with a solidification/stabilization (S/S) process using coal fly ash and Portland cement was developed and further optimized. Previous work demonstrated that S/S process with bituminous coal fly ash (BCFA) required further optimization and identified that Friedel's salt was the key mineral for the immobilization of Se(+VI) and chloride. This study further optimized the mineralogy of the S/S solids in co-disposed FGD brines and BCFA for metal and chloride immobilization. S/S solids made by various mixing recipes and conditions were subject to long-term leaching test and quantitative X-ray diffraction (QXRD) analysis. Addition of reactive aluminate and adequate amounts of lime could enhance the formation of Friedel's salt, which is capable of binding halides and heavy metal oxyanions. S/S samples made with 10% lime, 2.5% sodium aluminate, 30-35% of FGD brine and 52.5-57.5% of BCFA (by mass) could retain the majority of halides (>50%), selenate (>90%), arsenate (>99%) and chromate (>99%) from the brine after 9 weeks of leaching tests. Addition of gypsum could enhance the formation of ettringite, which is capable of binding borate. However, higher ettringite

formation did not enhance the immobilization of halides and selenate. The hydraulic conductivity of the S/S solids could be another important factor for contaminant leaching because it could affect the stability of Friedel's salt under leaching condition. Meanwhile, it could also govern the immobilization of halides because the halide concentration from the brine exceeded the binding capacity of Friedel's salt.

4.2 INTRODUCTION

The United States coal-fired power industry faces increasing demands to improve solid waste and wastewater disposal practices.[4] Over 130 Mt of coal ash are produced annually in the U.S. and more than half are disposed in landfills or surface impoundments.[184] The disposal of coal ash poses environmental risks due to elevated levels of heavy metals in these wastes and potential to leach. The ashes may become more contaminated as the recently implemented Mercury and Air Toxics Standards (MATS) for flue gas emissions control is expected to transfer more mercury and other metal pollutants to fly ash. Furthermore, incidents of coal ash pond spills, such as at the Tennessee Valley Authority's Kingston station in 2008 and Duke Energy's power plants near the Dan River in North Caroline in 2014, have prompted the industry to move toward all dry disposal of fly ash.

In addition to coal ash, the flue gas desulfurization (FGD) purge wastewaters at coal-fired power plants contain significant concentrations of heavy metals (e.g. Se, As, Cr, Cd and Hg) and large amounts of salts (e.g. Cl^-, Ca^{2+}, Mg^{2+}, Na^+ and SO_4^{2-}),[1] which will contaminate receiving water bodies if discharged without proper treatment. Recently, the USEPA released (but postponed) Steam Electric Power Effluent Limitation Guidelines

(ELG Rule), which sets stringent limits on As, Hg, Se and other pollutants' release to the environment from FGD wastewater.[6]

Thus, coal fly ash (CFA) and FGD wastewater are both major wastes generated at coal-fired power plants and in urgent needs for more effective disposal strategies to minimize negative environmental impact. The zero-liquid discharge (ZLD) options for FGD wastewater have gained significant interest because of the elimination of environmental wastewater discharge and water reuse maximization in power plants. For that, we have developed a novel ZLD method by coupling brine concentration with a solidification/stabilization (S/S) process through co-disposing FGD brine with CFA and a pozzolanic agent (e.g. Portland cement (PC) or lime). We have demonstrated the promising success of this ZLD method in retaining heavy metals and producing stabilized S/S solids with low leaching potential.[18, 190-192] Our ZLD approach is highly attractive with several advantages: (1) lower costs with much lower energy demands than the traditional ZLD methods, (2) enhanced immobilization of metals and salts in the generated solids for safer landfill disposal, and (3) simultaneous stabilization and disposal of two major wastes (i.e. FGD brines and CFA) from the coal-fired power plants. In this approach, CFA is beneficially utilized to encapsulate FGD brines and in turn stabilized within the same process, which is highly positive for the industry.

Among the heavy metals, oxyanions in their most oxidized forms, such as Cr^{VI} and Se^{VI}, are typically difficult to immobilize. Se^{VI} is shown by our and other studies to be the most difficult heavy metal to immobilize due to high solubility and lack of sorption to most mineral surfaces.[1, 18, 190-192] Indeed, our previous works demonstrated that S/S using bituminous coal fly ash (BCFA) can achieve good retainment for As^{V}, Cd^{II}, Hg^{II} and Se^{IV};

however, good retainment of Cr^{VI} and Se^{VI} oxyanions requires addition of a reductant such as $FeSO_4$ (FS) or a pretreatment of brine by ZVI.[18, 189] However, it's challenging to further increase the retainment efficiency without a reduction process.[18, 190-192] In contrast, S/S using sub-bituminous coal fly ash (SCFA) can effectively immobilize Se^{VI}, even without a reduction process. It was determined that the enhanced formation of Friedel's salt (AFm-Cl) and its good capacity to uptake SeO_4^{2-} was responsible for the immobilization of Se^{VI} in the SCFA S/S solids.

In addition, Friedel's salt immobilizes chloride and thus reduces chloride leaching from the S/S solids.[189] Reducing the release of chloride from the coal-fired power plant wastes is desired because elevated chloride levels can adversely affect freshwater biota.[193-196] Besides chloride, bromide has also become a concern since it has been widely used for mercury control.[132] By adding bromide salts into the coal combustion unit, bromide will be oxidized to bromine, which will oxidize the elemental mercury into $HgBr_2$ which is a more water-soluble compound and can be easily removed by the FGD system.[132] Mercury that ended up in the FGD wastewater will need to be further treated, whereas bromide is not regulated and commonly discharged into the environment. Therefore, it may be reasonable to expect that the bromide concentration in the downstream waterbodies has the potential to increase over time as more FGD systems and bromide-based mercury control measures are applied across coal-fired power plants to meet the USEPA regulations for Hg control. This elevated bromide concentration has the potential to increase the formation of brominated disinfection byproducts (DBPs), which are of greater health concerns than the chlorinated DBPs,[133-134] at water treatment plants impacted by bromide discharge from upstream coal-fired power plants. Therefore, it is important for upstream coal-fired power

plants to consider bromide control measures if there are water treatment utilities at downstream.[132]

Besides Friedel's salt, ettringite ($Ca_6Al_2(OH)_{12}(SO_4)_3 \cdot 26H_2O$), was also detected in the S/S solids. Although ettringite does not bind chloride[78] and it has a weak affinity to SeO_4^{2-} compared to the AFm phase[113], it has a great affinity to bind borate.[140, 149] Although boron is not currently regulated in ELG or drinking water standards and has shown limited adverse effect on humans, it is still harmful for humans to be exposed to it over a long time.[135] Boron leached from coal combustion residuals (CCRs) is considered one of the major sources of boron in the environment.[135] The behavior of boron during coal combustion is consider as a two-step process: volatilization and heterogeneous condensation. During combustion, most boron compounds are volatilized to the gaseous phase. Some volatilized boron compounds are enriched into the clinker and CFA, while the remaining boron will be completely absorbed by the wet FGD system since most boron compounds are water soluble. [135] Boron is very often associated with the smallest particles in the coal ash, accumulated on the water-soluble fraction of the particle surface, and therefore has a very high leaching rate.[141-143] Therefore, the retainment of borate will also be a desired goal for the S/S process.

While BCFA is less effective than SCFA for Se^{VI} immobilization, unfortunately power plants that burn bituminous coal have more difficult FGD wastewater problems than sub-bituminous coal plants. Because bituminous coal contains higher sulfur content than sub-bituminous coal, bituminous FGD systems generate a larger volume of wastewater with more concentrated salts and heavy metals.[4] Approximately 45.6% of the coal produced in the US is bituminous and 45.4% is sub-bituminous, with 93% of the coal

utilized for energy production.[109] It will not be feasible to utilize SCFA from other sub-bituminous plants for FGD wastewater at a bituminous plant due to significant transportation costs and the fact that SCFA commands a higher beneficial reuse value. Hence, developing an optimum S/S process for FGD brines and BCFA from bituminous coal plants is particularly needed. This research project aimed to address this need, with the goal to optimize the immobilization of heavy metal oxyanions, particularly Se^{VI}, and Cl^- in concentrated FGD brines through S/S with BCFA, by enhancing the formation of desired phases in the S/S solids. As the AFm phase plays a crucial role in the immobilization of Se^{VI} and Cl^-, it is important to review the possible factors that can influence the minerology of the S/S solids.

In this work, the impact of pH, temperature, and the addition of lime, reactive Al_2O_3, and gypsum on the mineralogy of the BCFA S/S solids were evaluated. Quantitative XRD was conducted to determine the weight % of desired phases which was then used to correlate with the long-term leaching test results.

4.3 EXPERIMENTAL SECTION

4.3.1 Chemicals and Materials

The bituminous CFA (BCFA) used in this study was obtained from a bituminous coal-fired power plant in the southeastern United States. The characterization and metal concentrations of the BCFA and SCFA samples were determined and reported by the previous study.[190] Sodium aluminate ($NaAlO_2$, technical grade), hydrated lime ($Ca(OH)_2$, 98%), quick lime (CaO, 99.5%), and gypsum ($CaSO_4 \cdot 2H_2O$, 98+%) were purchased from Fisher Scientific (Hampton, NH). All chemicals were used as received.

All chemicals used for making the simulated FGD brines were in analytical grade and used as received. Sodium selenate (Na_2SeO_4), sodium arsenate heptahydrate ($Na_2HAsO_4 \cdot 7H_2O$), cadmium chloride ($CdCl_2$), and sodium chromate (Na_2CrO_4), were purchased from VWR (Radnor, PA). Calcium chloride dihydrate ($CaCl_2 \cdot 2H_2O$), sodium chloride (NaCl), magnesium nitrate hexahydrate ($Mg(NO_3)_2 \cdot 6H_2O$), magnesium chloride hexahydrate ($MgCl_2 \cdot 6H_2O$), magnesium sulfate heptahydrate ($MgSO_4 \cdot 7H_2O$), boric acid (H_3BO_3) and sodium bromide (NaBr) were purchased from Fisher Scientific (Hampton, NH). The simulated brines were produced by dissolved the above-mentioned salts in ultrapure deionized (DI) water generated from a Milli-Q nanopure water purification system. The pH of the brine was around 5.9.

To study the removal of bromide and boron, a modified version of the simulated brine (noted as "brine B" in the Results and Discussion section, pH was also around 5.9) was made by spiking in 25 ppm of borate (originally not added), and 8,000 ppm bromide (originally 1,312 ppm). Also, chromate concentration was increased to 25 ppm (originally 1 ppm) because 1 ppm of chromate was completely removed from all the previous samples after S/S. The chromate concentration was increased to a higher level for evaluating the impact of various mixing recipes on chromate removal. The brine B was applied when the effect of hydrated lime versus quick lime was studied. The compositions of the original simulated FGD brine ("brine A") and the modified simulated brine ("brine B") are shown in Table 4.1.

Table 4.1. Characteristics of the simulated FGD brine A and brine B.

Composition	**Concentration**	**Composition**	**Concentration (ppm)**

	(ppm)		
TDS	126,000 (A); 133,700 (B)	**Mg**	9,340 (A and B)
Chloride	80,000 (A and B)	**Se(VI)**	25 (A and B)
Nitrate	300 (A and B)	**As(V)**	1.0 (A and B)
Bromide	1,312 (A); 8,000 (B)	**Cd(II)**	5.0 (A and B)
Ca	57,580 (A and B)	**Cr(VI)**	1.0 (A);25 (B)
Na	990 (A); 2940 (B)	**B(III)**	25 (B only)

4.3.2 Generation of the S/S Solids

Various weight percentages of BCFA, simulated FGD brine A or brine B (30% and 35%), lime or quick lime (5% and 10%), sodium aluminate (0%, 2.5%, and 5%), and gypsum (0%, 2.5%, and 5%) were mixed. The BCFA, simulated brine, and additives were added together to a stainless-steel bench-scale mixer and mixed immediately for approximately 10 min. To test the effect of brine temperature, the brine was heated to 80°C using a hot plate and then poured into the mixer immediately. Part of the resulting mixing slurry was poured into cylindrical plastic containers (48 mm (diameter) × 60 mm), and cured in a humid environment for 14 days before conducting the USEPA 1315 leaching test. Some of the cured S/S solids were stored under vacuum (500 mmHg) and used later for QXRD measurements within 3 days after the curing of the S/S solids. To prepare the QXRD samples, S/S solids were crushed and then sifted through a sieve with a mesh of 90

microns. Rutile was then added as an internal standard (5% by weight) and the QXRD was done on the same day.

4.3.3 Long-term Leaching Test

The cured S/S solid monolith was applied in the USEPA 1315 leaching test. The solid block had a mass of 50 g with a total surface area of 54 cm^2. The solid block was tied up by a plastic string which was fixed under the cap of a 500-mL plastic bottle. The length of the string allowed the solid to hang in the middle of the bottle. It took 480 mL of DI water to fill the bottle, and the final liquid to solid surface area ratio was around 9:1. At each sampling time specified in the method, the mass of the solid and the pH and conductivity of the leachate were measured. The leachate was then poured into a container, acidified with nitric acid and stored in refrigeration for further measurements. Fresh DI water was added again into the bottle and the same procedure was applied in the next sampling time.

4.3.4 Hydraulic Conductivity Test

Selected samples were cured separately for the hydraulic conductivity test. The mixing recipe for these samples are shown in result section 4.4.6. The preparation of these samples was same as described in 4.3.2. After curing, the samples were sent to a commercial lab who applied the American Society for Testing and Materials (ASTM) method d5084.

4.3.5 Analytical Methods

The pH was measured by an Orion Star^{TM} A111 bench-top pH meter. The concentrations of heavy metals were detected by a Perkin Elmer ICP-OES 8000 instrument (Waltham, MA). The washing solution used for ICP was 5% trace-metal-grade nitric acid. The concentrations of halides were measure using a Dionex ion chromatography with conductivity measurement (Sunnyvale, CA). The minerology of the S/S solids was analyzed by quantitative XRD (QXRD) using the Rietveld method to obtain the weight percentages of Friedel's salt and ettringite, respectively.

4.4 RESULTS AND DISCUSSION

Based on many tests in our previous study, the optimal mixing ratio for solidification and stabilization is approximately 30% of brine, 60% of BCFA and 10% of activating agent by mass. In this study, addition of extra additives or change of the amount of activating agent were conducted to systematically evaluate the impacts on the S/S solid mineralogy. Thus, the change of the weight percentage of the additives or lime was compensated by the weight percentage of BCFA, while the weight percentage of brine remained unchanged. The S/S solids with 30% of brine were tested first and the recipes utilized are shown in Table 1. This set of samples were designed to study the effect of each additive (sodium aluminate or gypsum) on the minerology of the final S/S solids with either 10% or 5% of lime. Sodium aluminate is a good source of active aluminum for the formation of Friedel's salt, while gypsum provides sulfate for the formation of ettringite.

Table 4.2. Mixing recipes for S/S solids with 30% of brine. SA = sodium aluminate; G = gypsum

Sample #	Brine A	BCFA	Lime	Additives

1	30%	60%	10.0%	Not added
2	30%	57.5%	10.0%	2.5% SA
3	30%	57.5%	10.0%	2.5% G
4	30%	55.0%	10.0%	2.5% SA and 2.5% G
5	30%	62.5%	5.0%	2.5% SA
6	30%	62.5%	5.0%	2.5% G
7	30%	60.0%	5.0%	2.5% SA and 2.5% G

One issue noticed within this group of samples was that, when sodium aluminate was added at 2.5% weight (Samples #2, 4, 5, and 7 in Table 4.2), the S/S mixtures became too dry and the monoliths produced after curing had significant holes and cracks. Therefore, it was deemed necessary to increase the brine weight percentage (to 35%) to compensate for the water demand by aluminate additive, and the modified recipes are shown in Table 4.3. Furthermore, the new recipes were also employed in additional tests using a modified simulated brine ("Brine B" in Table 4.1), hot brine (80 °C) or quick lime for comparison, as shown in Table 4.2. The results from the quantitative XRD (QXRD) analysis for each S/S solid sample are also included in Table 4.3.

Table 4.3. Mixing recipes of S/S solids and their corresponding QXRD results. SA = sodium aluminate; G = gypsum FS = Friedel's salt, and Et = ettringite

Sample #	Brine	BCFA	Lime/ Quick lime	Additives	FS%	Et%
1	30%	60.0%	10.0% lime	Not added	15.0	1.1
2	35%	55.0%	10.0% lime	Not added	12.4	0.9
3	35%	52.5%	10.0% lime	2.5% SA	22.7	0.6
4	35%	52.5%	10.0% lime	2.5% G	10.1	12.9

5	35%	50.0%	10.0% lime	2.5% SA and 2.5% G	23	10.6
6	35%	57.5%	5.0% lime	2.5% SA	6.0	4.2
7	35%	57.5%	5.0% lime	2.5% G	0.5	3.7
8	35%	55.0%	5.0% lime	2.5% SA and 2.5% G	8.4	11.1
9	hot 30%	60.0%	10.0% lime	Not added	14	1.1
10	hot 35%	52.5%	10.0% lime	2.5% SA	22.5	1.2
11	hot 35%	50.0%	10.0% lime	2.5% SA and 2.5% G	23.7	10.8
12	Brine B 30%	60.0%	10.0% quick lime	Not added	13	1.3
13	Brine B 35%	52.5%	10.0% quick lime	2.5% SA	25	1.2
14	Brine B 35%	50.0%	10.0% quick lime	2.5% SA and 2.5% G	25.9	10.2
15	Brine B 30%	60.0%	10.0% lime	Not added	13.7	1.3
16	Brine B 35%	52.5%	10.0% lime	2.5% SA	20.8	1.3
17	Brine B 35%	50.0%	10.0% lime	2.5% SA and 2.5% G	24.2	9.7

Most experiments used Brine A, except those used Brine B. Hot brine: 80 °C.

The 17 samples shown in Table 4.3 were subjected to the USEPA Method 1315 long-term leaching test and the results are shown in Figures 4.1 – 4.6, which will be discussed along with the QXRD results in the sections below. Note that for heavy metals' leaching, only selenate could be detected in the leachate. Other heavy metals (i.e., arsenate, chromate, and cadmium) were close to complete removal with concentrations in the leachate either non-detectable or close to the analytical instrument (ICP and IC) detection limits, so their data are not reported. The excellent retainment of these heavy metals could be related to both monophase and ettringite. Zhang and Reardon studied the uptake of B,

Cr, Mo and Se by ettringite and OH^--substituted hydrocalumite (AFm-OH).[149] They found that the anion uptake rate by monophase is higher than ettringite. Ettringite shows an anion preference in the order of $B(OH)_4^- > SeO_4^{2-} > CrO_4^{2-} > MoO_4^{2-}$, while hydrocalumite shows an opposite trend. McCarthy also reported that, through the synthesis of borate- and selenate-substituted ettringite, >95% of the borate and selenate could be removed from the hydration solution.[156] Klemm and Bhatty reported that when arsenate, chromate and selenate are in the hydration solution, arsenate shows a greater affinity to form ettringite than selenate and chromate, while the latter oxyanions incorporate into ettringite at equal molar ratio. However, when sulfate is present, it dominates other oxyanions for the formation of ettringite. Sulfate could also replace oxyanions in the substituted ettringite.[157] Albino reported the formation Cd^{2+}- and Cr^{3+}-substituted ettringite during the synthesis experiments to incorporate various divalent and trivalent metals into ettringite.[158] In terms of mineral formation, the effect of each additive will be discussed separately, along with the leaching test results in the sections below.

4.4.1 Effect of Lime Addition

QXRD*:* The hydration of BCFA is a process of pozzolanic reaction. For this reaction to proceed, adequate alkalinity is required to dissolve the glassy silicate and aluminate phases in the mixture. As shown in Table 4.3, for the mixture with 10% lime added (Sample #2), there was about 15% of Friedel's salt formed in the S/S solids. By adding 2.5% of aluminate (Sample #3), the Friedel's salt content was increased to nearly 23%. When lowering the lime addition to 5% and keeping the aluminate at 2.5% (Sample #6), there was only 6% of Friedel's salt formation likely due to the lack of alkalinity. To further

investigate the impact of lime on Friedel's salt formation with or without aluminate, additional samples were made for QXRD analysis and the results are shown in Table 4.4.

In Table 4.4, without the addition of sodium aluminate, increasing lime addition from 10% to 15% did not increase the amount of Friedel's salt formed, likely due to the limitation of available aluminate in the ash (Samples #1-3). By adding 2.5% of aluminate, further increase of lime addition slightly increased the Friedel's salt formation from 23% to 27% (Samples #4-6). Therefore, in terms of Friedel's salt formation, adequate lime is required for the reaction to proceed, but extra lime is not beneficial for Friedel's salt formation when the aluminate source is limited.

Table 4.4. Mixing recipes of S/S solids with different amounts of lime and their corresponding QXRD results. (SA = sodium aluminate; FS = Friedel's salt)

Sample#	Brine A	BCFA	Lime	Additive	FS%	Et%
1	30%	60.0%	10.0%	Not added	15.0	1.1
2	30%	57.5%	12.5%	Not added	12.2	3.8
3	30%	55.0%	15.0%	Not added	12.6	1.0
4	35%	52.5%	10.0%	2.5% SA	22.7	0.6
5	35%	50.0 %	12.5%	2.5% SA	22.8	0.9
6	35%	47.5%	15.0%	2.5% SA	26.8	1.4

Leaching tests: In term of chloride leaching, 20%-40% (in weight % compared to the original amount of chloride in the brine) of chloride was leached from the S/S solid samples with in which 10% lime was added (Samples #3-5 in Table 4.3), but 30%-70% of chloride was leached from S/S samples with 5% of lime addition (Samples #6-8) in Table 4.3), after 63 days of leaching as shown in Figure 4.1a. In terms of selenium leaching,

selenium concentrations in the leachate from the S/S solid samples with 10% of lime addition (Samples #3-5 in Table 4.3) were close to the detection limit. On the other hand, the S/S solid samples with 5% of lime addition (Samples # 6-8 in Table 4.3) leached about 2-7% of selenate (calculated based on the amount of selenate introduced from the brine) after 63 days as shown in Figure 4.1b. Combining the leaching test and the QXRD results, we can conclude that S/S solids with 10% lime addition generated more Friedel's salt, and immobilized more chloride and selenate than S/S samples with only 5% of lime addition. The extra alkalinity from the greater amount of lime added not only facilitated Friedel's salt formation but could also help maintain the high pH of the leachate and thus prevented the dissolution of Friedel's salt.

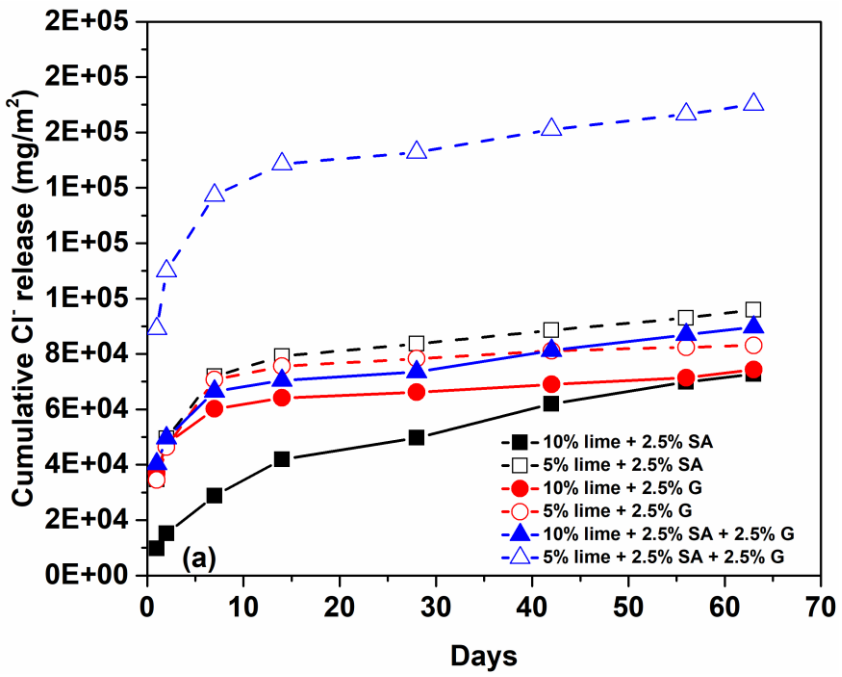

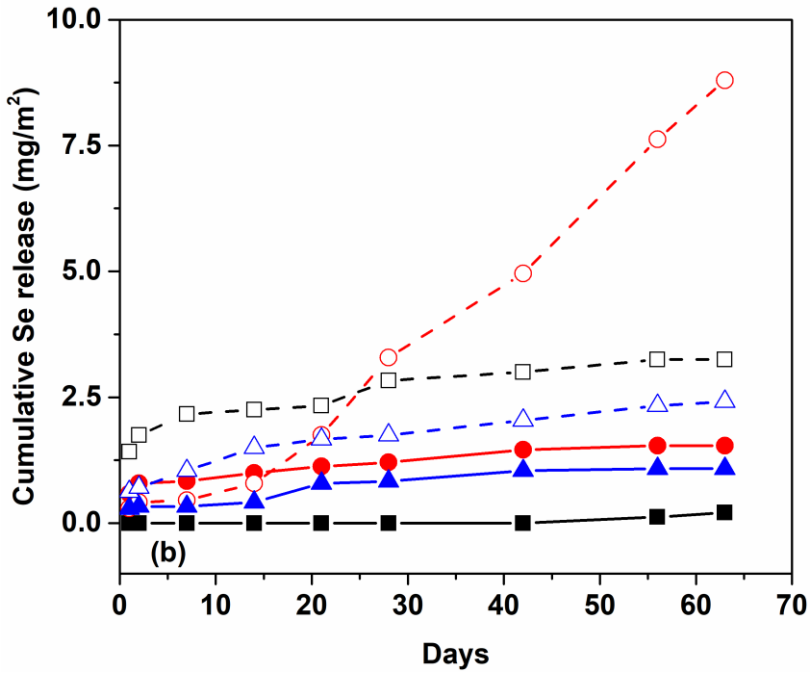

Figure 4.1. Effects of lime addition combined with aluminate (SA) and/or gypsum (G) addition on (a) cumulative chloride leaching and (b) cumulative Se leaching from S/S solids with 35% of brine.

4.4.2 Effect of Aluminate Addition

QXRD: Aluminate addition provides the source of Al which is part of the layered double hydroxide (LDH) in AFm phases. As shown in Table 4.5, by increasing the amount of aluminate added into the S/S mixture while keeping 10% of lime, Friedel's salt increased from 15% to 32% (Samples #1-4). Therefore, with adequate lime addition, more aluminate addition will increase the Friedel's salt formation.

Table 4.5. Mixing recipes of S/S solids with different amount of aluminate and their corresponding QXRD results. (FS = Friedel's salt; Et = ettringite.)

Sample #	Brine A	BCFA	Lime	Additive	FS%	Et%
1	30%	60.0%	10.0%	Not added	15.0	1.1
2	35%	53.75%	10.0%	1.25% SA	18.9	1.8

3	35%	52.5%	10.0%	2.5% SA	22.0	0.6
4	35%	50.0%	10.0%	5.0% SA	32.6	0.1

Note that, although aluminate addition enhances the formation of Friedel's salt, it causes the S/S mixture to become drier and solidify more quickly than without aluminate addition. S/S samples without aluminate addition stayed as slurry or paste during the mixing and could be poured into the mold readily for curing. Preliminary tests showed that samples with 5% of aluminate addition solidified quickly during the mixing and thus a satisfactory monolith solid could not be obtained for the leaching tests later. S/S samples with 2.5% of aluminate addition also dried more quickly than other samples without aluminate addition; however, by increasing the FGD brine percentage from 30% to 35%, the mixture could stay as a paste during the mixing and be transferred into the mold. Therefore, one potential issue with aluminate addition is that it may increase the porosity of the S/S solid due to the faster drying rate, thereby affecting the leaching potential.

Leaching tests: In terms of chloride leaching, Figure 4.2a shows the cumulative chloride leaching of Samples # 2, 3 and 5 in Table 4.3. The S/S solid with aluminate addition (Sample #3, Table 4.3) retained more chloride than the sample without aluminate addition (Sample #2, Table 4.2). However, this difference was more significant at the early stage of the leaching test. Long-term wise, the difference in chloride leaching potentials became smaller which might be due to difference in permeability of these two solids which would require further additional study. When both aluminate and gypsum were added (Sample #4, Table 4.3), there was more chloride leached out than that from the sample with only aluminate addition (i.e. Sample #3). This increase of chloride leaching related to

gypsum addition was more pronounced when only 5% of lime was added in the S/S mixture (Sample #8 in Table 4.3 and data shown in Figure 4.1a). One significant factor causing this unusual higher leaching of chloride for Sample #8 could be the high hydraulic conductivity of the sample (shown later in Table 4.7). Another possibility could be due to the damage of the monolith (especially on the surface) when the S/S solids were made. It was difficult to remove the cured samples from the plastic molds without a certain degree of damage because of the low strength of the solid (likely caused by inadequate alkalinity with only 5% of lime). In terms of selenate leaching, S/S solids with aluminate addition leached less selenate compared to that without aluminate addition, as shown in Figure 4.2b. Similarly, when both aluminate and gypsum were added, there was more selenium leached out compared to the sample with only aluminate added. This increase of selenium leaching could be due to the competition between sulfate and selenate when gypsum was introduced.

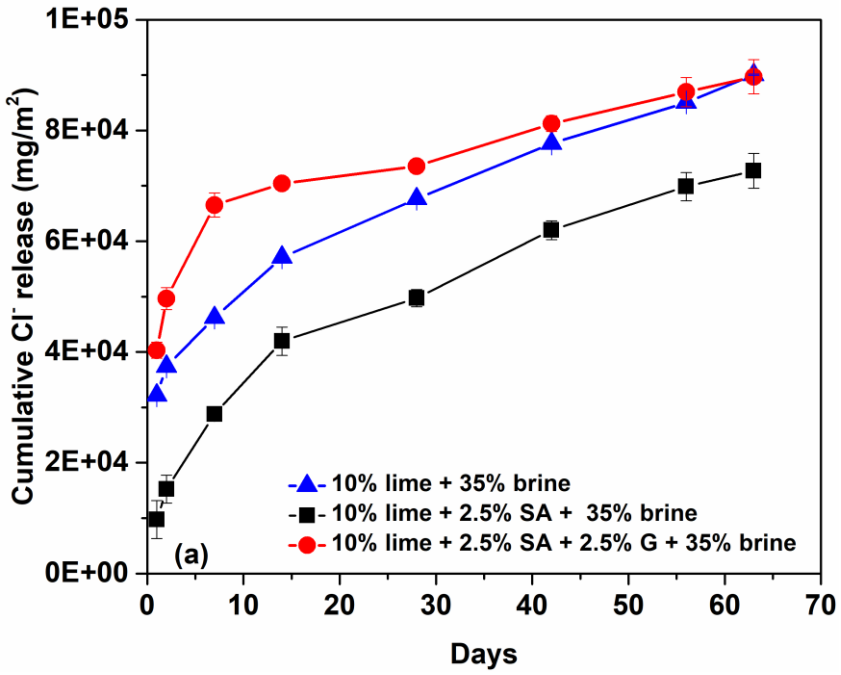

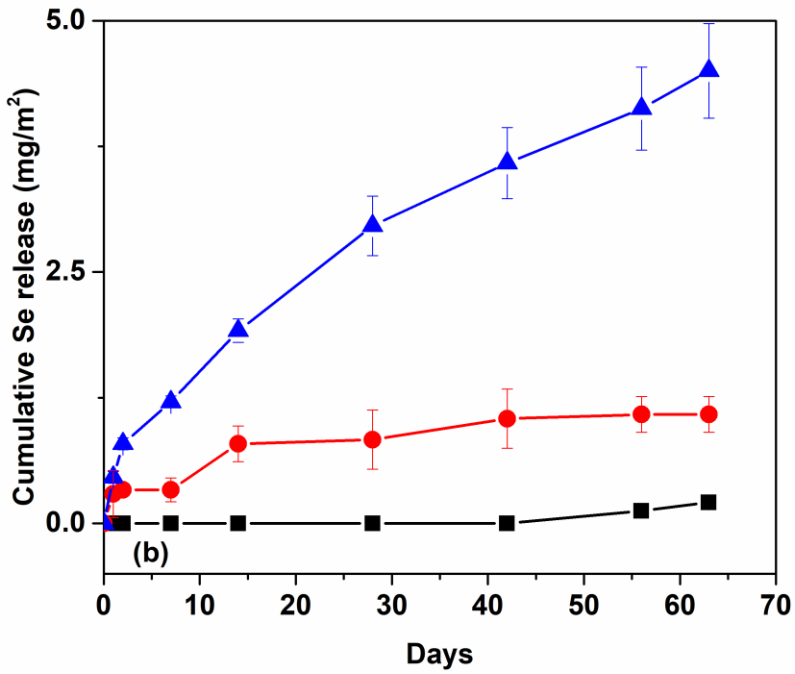

Figure 4.2. Effects of aluminate addition on (a) cumulative chloride and (b) cumulative selenium leaching from S/S solids.

4.4.3 Effect of Gypsum Addition

QXRD: Gypsum provides sulfate into the system and enhances the formation of ettringite. For example, as shown in Table 4.3, Sample #2 with 10% lime addition but without gypsum only formed 1% of ettringite. By adding 2.5% of gypsum (Sample #4), the ettringite was increased to 13%. To further investigate the effect of gypsum on ettringite formation, S/S mixtures with 0.5-5.0% of gypsum addition were made and their QXRD results are shown in Table 4.6. Meanwhile, as mentioned in the introduction, ettringite has a strong affinity with borate. Therefore, to evaluate the impact of adding gypsum, brine B was utilized in this set of study.

Table 4.6. Mixing recipes of S/S solids with different amounts of gypsum and their corresponding ettringite weight percentage in the S/S solids.

Sample #	Brine B	BCFA	Lime	Gypsum	Ettringite%
1	30%	60.0%	10.0%	Not added	1.1
2	30%	59. 5%	10.0%	0.5%	1.5
3	30%	59.0%	10.0%	1.0%	4.7
4	30%	58.5%	10.0%	1.5%	6.2
5	30%	58.0%	10.0%	2.0%	7.7
6	30%	55.0%	10.0%	5.0%	16.2

As seen in Table 4.6, higher gypsum addition resulted in higher formation of ettringite. Plotting Ettringite weight % vs. gypsum added generated a linear relationship with a $R^2 = 0.98$.

Leaching tests: Ettringite formation had no significant effect on chloride leaching since it doesn't bind chloride (data not shown). For the S/S samples in Table 4.6, the results of boron and selenium leaching are shown in Figure 4.3. In terms of boron leaching, Figure 4.3a shows that S/S solids made with a higher dosage of gypsum, which generated more ettringite, leached less amount of boron. However, this trend was not observed in selenium leaching (Figure 4.3b) since ettringite has much weaker affinity with selenate, as mentioned in the introduction.

Cox et al. reported the leaching of boron (as borate or boric acid) from bottom ash and fly ash.[144] The boron content in CFA was found as high as 1,900 ppm and more than 50% was leachable into the water. Jankowski at al. studied the mobility of As, B, Mo and Se from selected Australian fly ashes.[140] Long-term (144 h) batch leaching tests were performed using two acidic and two alkaline CFAs and leaching solution with initial pH of 4, 7, and 10. The results suggested that boron has the highest relative mobility of all four

elements, and the decrease of B, As and Se in the leaching solution in contact with alkaline CFA could be attributed to the formation of ettringite. At high pH values, boron can co-precipitate with $CaCO_3$.[145-146] There are also several studies that reported the formation of borate substituted ettringite.[147-149]

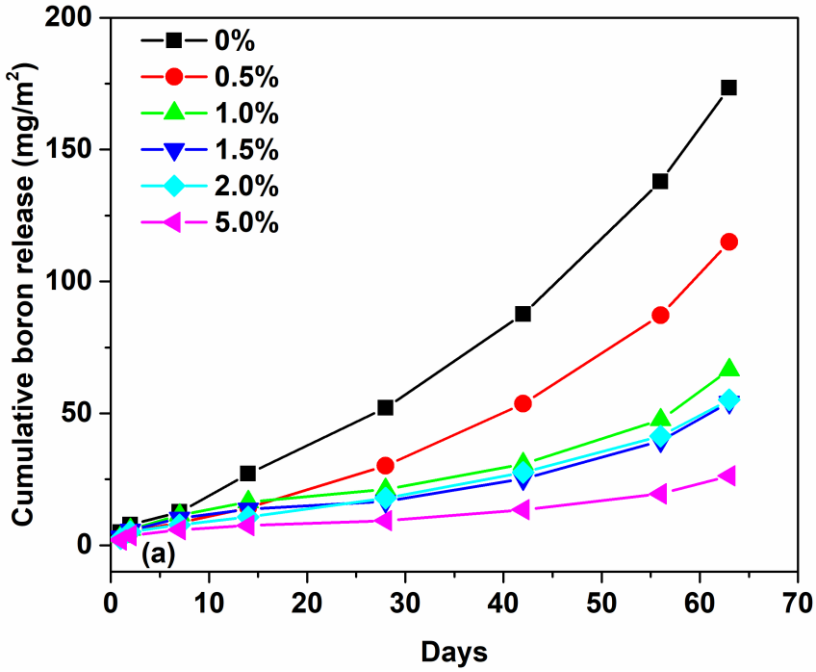

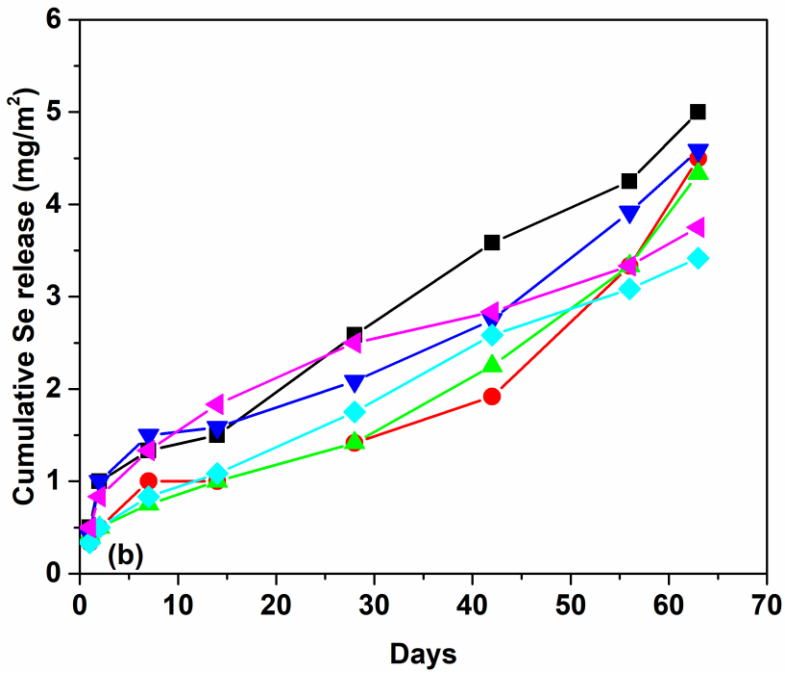

Figure 4.3. Effects of gypsum dosage (0%-5.0%) on the cumulative leaching of (a) boron and (b) selenium from S/S solids.

4.4.4 Effect of Brine Temperature

QXRD: S/S samples with hot FGD brine heated to 80 °C was also made to compare with samples with room temperature FGD brine using the same S/S mixing recipes. Although previous literatures suggested that the temperature could play an important role on the stability of both monophase and ettringite [150-151, 155], the temperature during our mixing process was not controlled, thus the hot brine cooled down fast once in contact with the mixer. Therefore, raising the temperature of brine did not result in significant difference in terms of minerals formation and their percentages (see comparisons between Samples #1 vs. #9, #3 vs. #10, and #5 vs. #11 in Table 4.3).

Leaching tests: Although the addition of hot brine vs. room temperature brine didn't change the mineralogy of the S/S solids. The samples with hot brine and aluminate addition

leached more chloride during the first 2 days than the corresponding samples with room temperature brine, as shown in Figure 4.4. After 2 days, the amount of chloride released from both samples were similar. Therefore, the different was only to due the amount of chloride during initial surface wash-off. The hot brine sped up the drying of the mixture when aluminate was added, thus leaving more cracks on the solid surface, which could enhance the surface wash-off. Without the addition of aluminate, adding the hot brine didn't speed up the drying, so no significant difference was observed. Selenium leaching was not comparable among these set of S/S solids because the selenium concentration in the leachate was always close to the analytical detection limit, indicating very low selenium leaching potential.

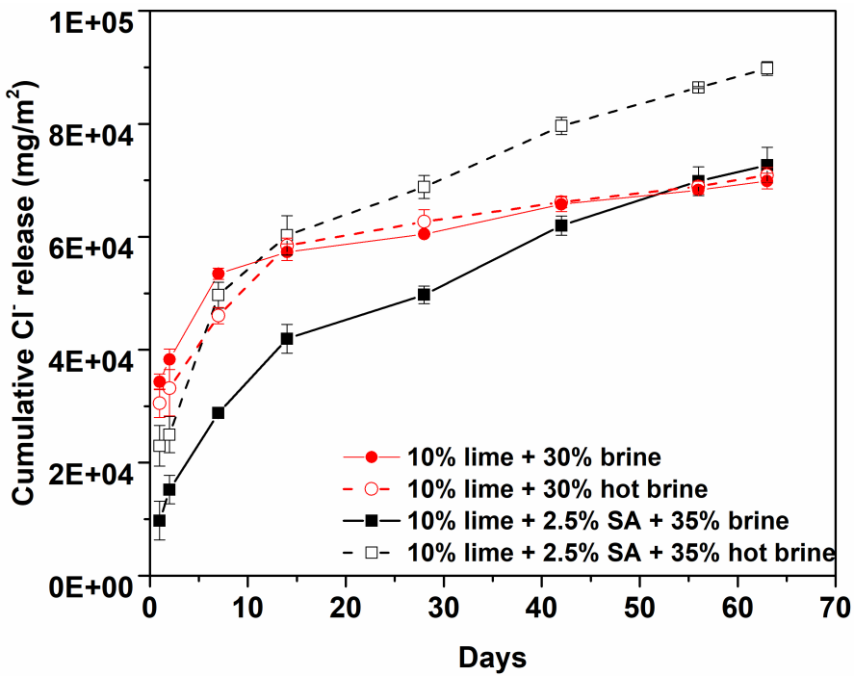

Figure 8. Effect of hot brine with or without aluminate addition on cumulative chloride leaching.

4.4.5 Lime (Hydrated) vs. Quick Lime (Unhydrated)

The use of hydrated lime versus unhydrated quick lime as the activating agent in the S/S was also conducted for comparison. These set of S/S samples were conducted using the modified brine (brine B) as shown by Samples #12-17 in Table 4.3. These set of samples used 30% or 35% of brine, and with or without the sodium aluminate and/or gypsum additives.

QXRD: As shown in Table 4.3, addition of quick lime only slightly increased the formation of Friedel's salt compared to that in the same recipe (i.e. Samples #13 vs. #16, and Samples #14 vs. #17). However, S/S mixture made with quick lime dried faster compared to that made with hydrated lime due to the higher water demand of quick lime. The faster drying rate may affect the permeability of the S/S solids which requires further study.

Leaching Tests: In terms of chloride leaching, S/S samples with hydrated lime addition leached less chloride than the S/S samples with quick lime addition using the same recipe, as shown in Figure 4.5. However, this difference was only seen at the early stage of the leaching test. In the later stage, the difference was no longer significant (Figure 4.5a). Therefore, lime or quick lime does not impact the performance of the S/S for immobilization of chloride in the long term. In terms of bromide leaching (Figure 4.5b), no obvious trend was observed among different samples. The overall leaching percentage of bromide was between 30%-40% after 63 days, which was at the similar level of chloride leaching. The samples without addition of additives (black line with square labels in Figure 4.5) appear to leach less chloride and bromide because those samples had less amount of brine added. In terms of overall retainment percentage, all the samples leached similar level of chloride (~30%), and bromide (30-40%) without clear trend.

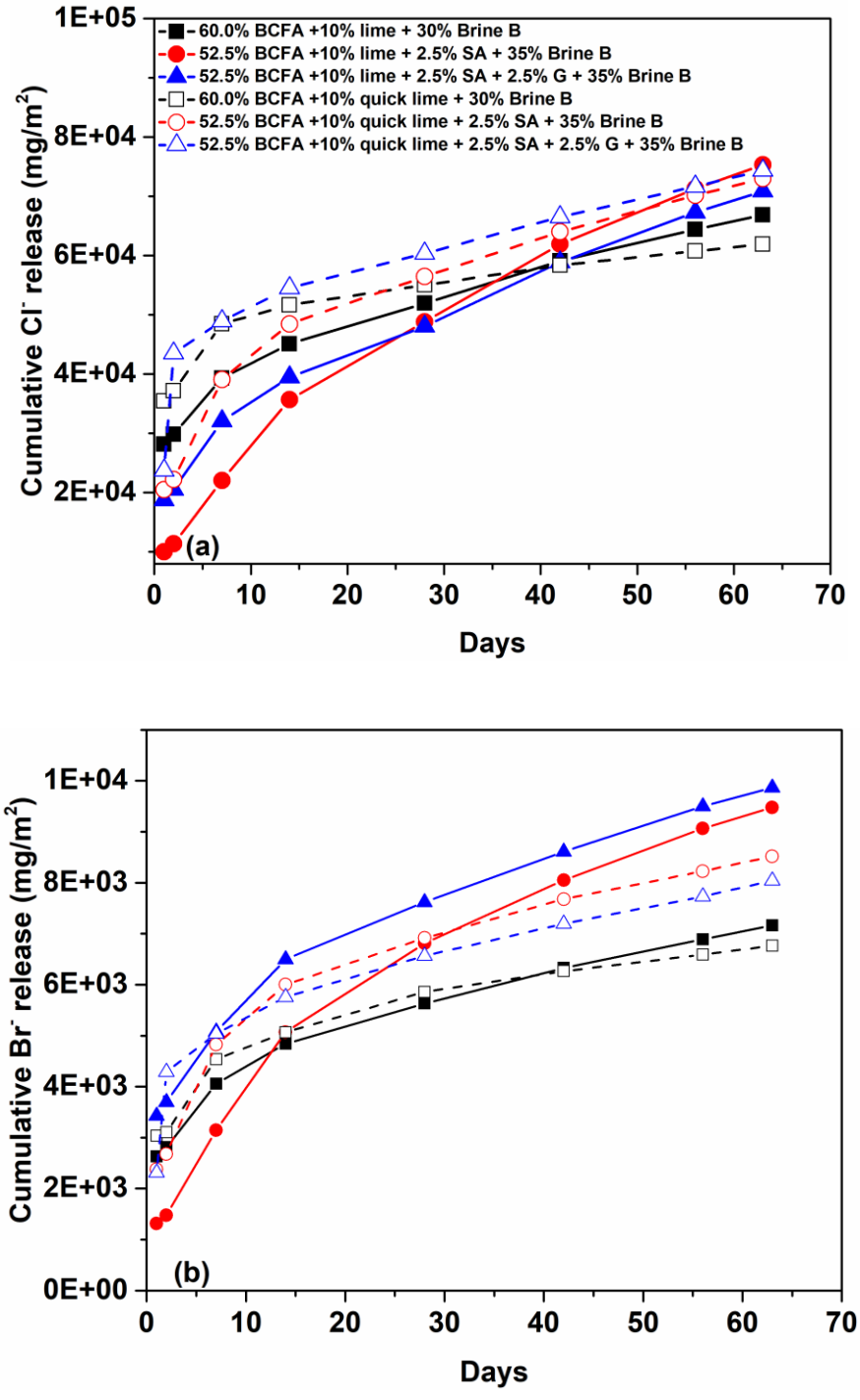

Figure 4.5. Effects of lime or quick lime on cumulative leaching of (a) chloride and (b) bromide from S/S solids with brine B.

Chromate leaching was not detected even using the brine B which contained a higher concentration (25 ppm) of chromate, indicating that the S/S method is excellent for chromium immobilization. Boron and selenium results are shown in Figure 4.6. It was found again that ettringite formation improved the immobilization of boron (Figure 4.6a) but not for selenium (Figure 4.6b), which agrees with the results in the section discussing the effect of gypsum. Therefore, the addition of gypsum is not as important as aluminate and lime for chloride and selenate immobilization but is important for boron. Additionally, S/S samples with quick lime performed slightly better than their corresponding samples with hydrated lime addition. Although quick lime didn't enhance the formation of ettringite compared to hydrated lime, it provided more alkalinity to the reaction since its addition was 10% by weight and quick lime has a lower molecular weight. This extra alkalinity could enhance the stability of ettringite during the long-term leaching test. Figure 4.6b shows the cumulative leaching of selenium. Consistent with the previous results, aluminate addition decreased the selenium leaching. Samples with quick lime also performed slightly better than their corresponding samples with hydrated lime addition.

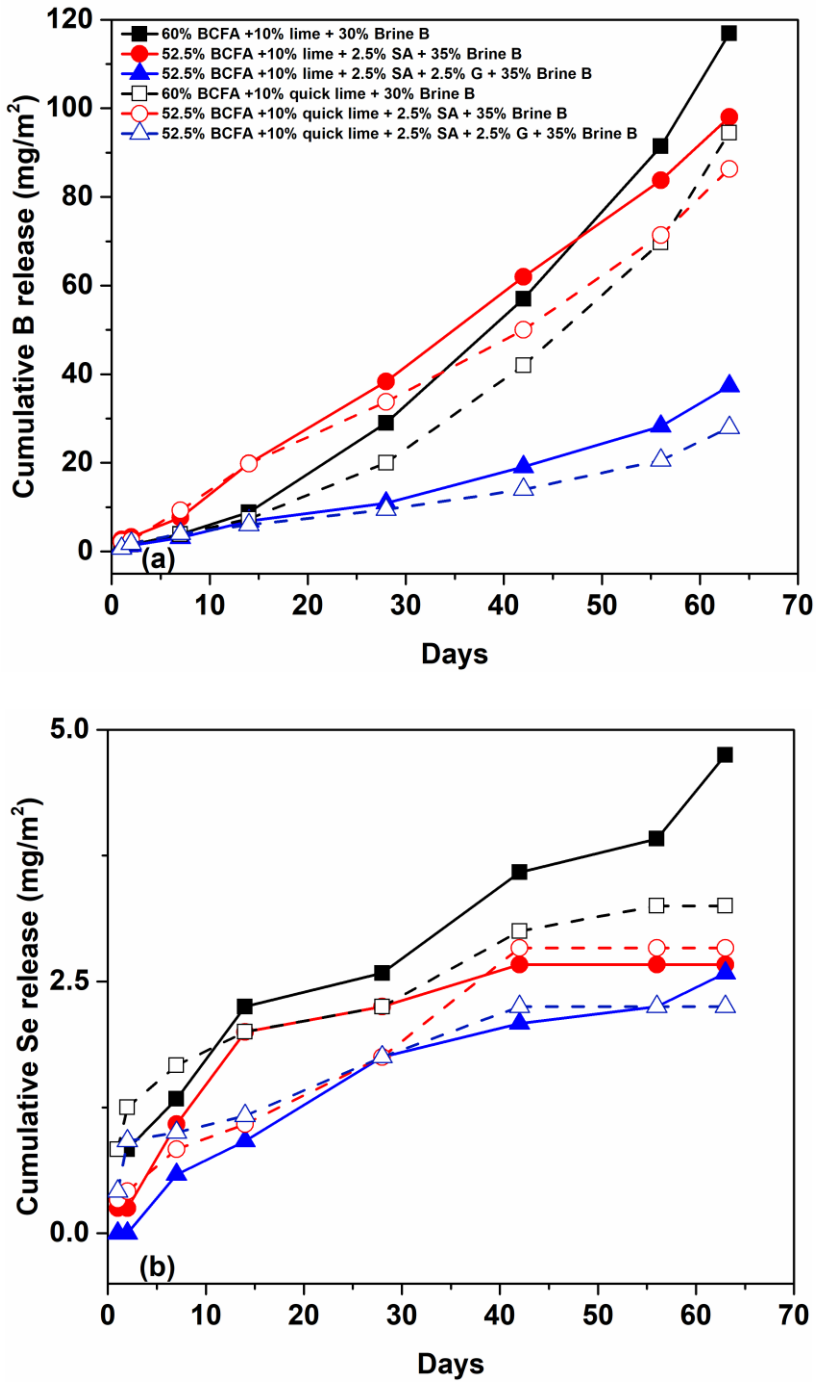

Figure 4.6. Effects of lime or quick lime on (a) cumulative boron leaching and (b) cumulative Se leaching from S/S solids with brine B.

4.4.6 Hydraulic Conductivity

The mixing receipt of the samples whose hydraulic conductivity (K in cm/s) was measured are shown in Table 4.7, along with the K values and FS% of these samples.

Table 4.7. Mixing recipes of S/S solids and their corresponding QXRD and K results. SA = sodium aluminate; G = gypsum FS = Friedel's salt, and K = hydraulic conductivity.

Sample #	Brine	BCFA	Lime	Additives	FS%	K ($\times 10^{-8}$cm/s)
1	35%	52.5%	10.0%	2.5% SA	22.7	3.6
2	35%	57.5%	5.0%	2.5% SA	6	58.9
3	35%	52.5%	10.0%	2.5% G	10.1	7.48
4	35%	57.5%	5.0%	2.5% G	0.5	1.87
5	35%	50.0%	10.0%	2.5% SA and 2.5% G	23	26.1
6	35%	55.0%	5.0%	2.5% SA and 2.5% G	8.4	61.4
7	30%	60.0%	10.0%	Not added	15	11.9
8	hot 30%	60.0%	10.0%	Not added	14	0.26
9	hot 35%	52.5%	10.0%	2.5% SA	22.5	0.63
10	hot 35%	50.0%	10.0%	2.5% SA and 2.5% G	23.7	9.9
11	35%	55.0%	10.0%	Not added	12.4	0.98
12	40%	50.0%	10.0%	Not added	6.4	75.6
13	30%	60.0%	10.0%	Not added	14.5	13.3
14	30%	59.5%	10.0%	0.5% G	14.4	6.2
15	30%	59.0%	10.0%	1.0% G	14.2	4.5
16	30%	58.5%	10.0%	1..5% G	10.4	15.2
17	30%	58.0%	10.0%	2.0% G	9.9	17.7
18	30%	55.0%	10.0%	5.0% G	6.3	23.3

The chloride leaching data of these samples were evaluated by correlating the amount of chloride release during the first week, during week 1-9, and the entire 9 weeks with both K value and FS%. Figure 4.7 shows the leaching of chloride affected by both K and FS%.

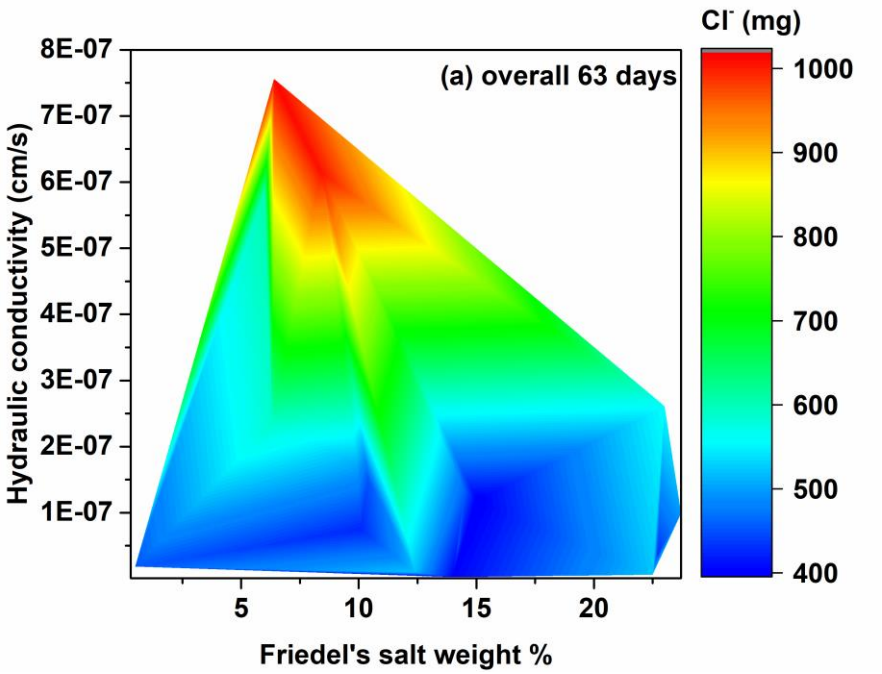

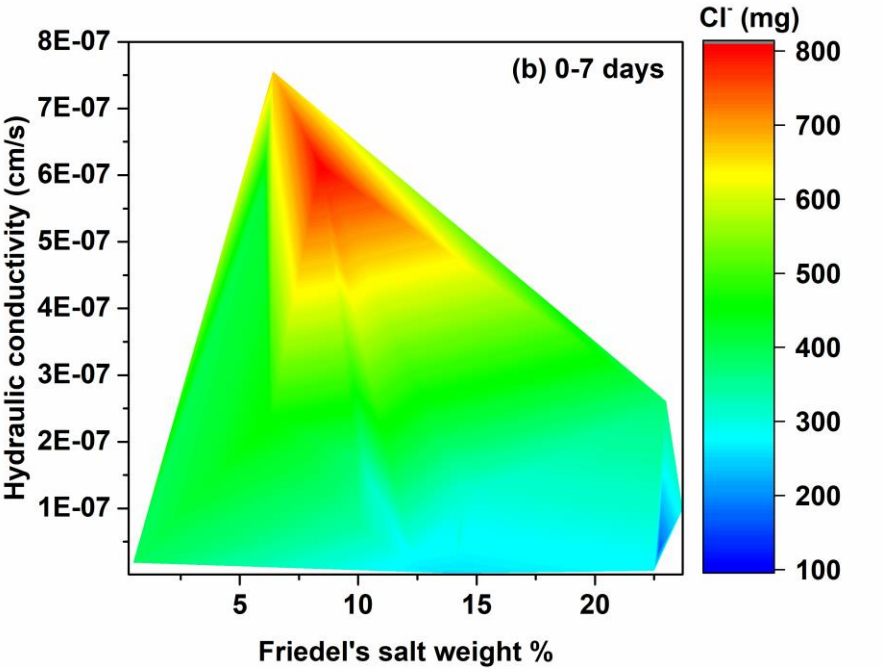

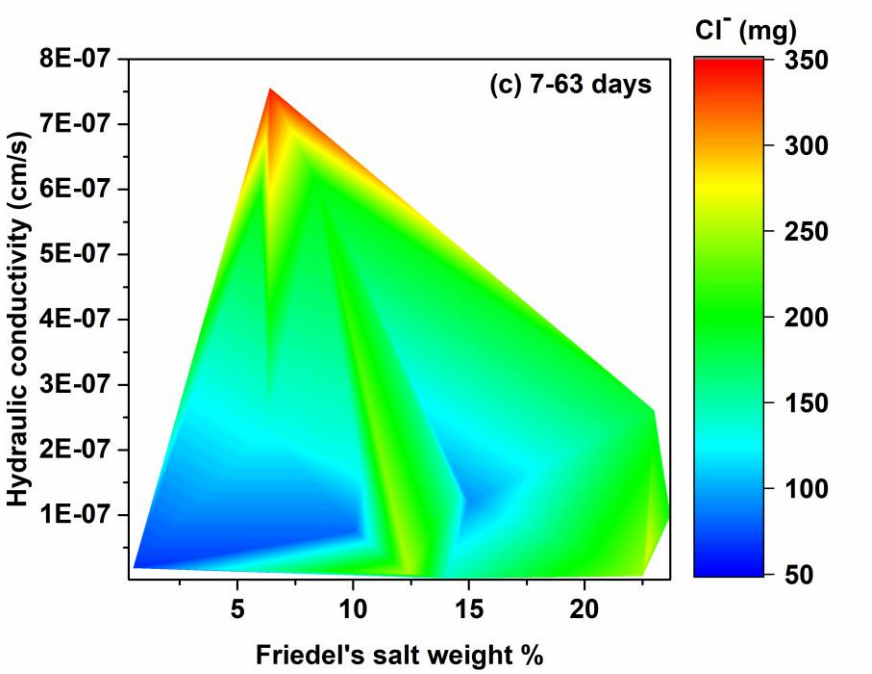

Figure 4.7. Effects of K and FS% on chloride leaching during (a) overall 63 days, (b) 0-7 days, and (c) 7-63 days.

Overall, both low K value and high FS% are important for chloride retainment. On general, the chloride leached out during the first 7 days accounted for most of the chloride leached during the overall process. In the first 7 days, the unbounded chloride retained on the surface and near surface will be released into DI water rapidly. The amount of unbounded chloride would be less when higher amount of FS was formed. Therefore, in Figure 4.7b, the general trend is higher FS% released less amount of chloride. After 7 days, the unbonded chloride originally existed near the surface was already leached out, so the diffusion of unbounded chloride from the inside the S/S solids would contribute to the chloride leaching. The diffusion rate could be related to the hydraulic conductivity of the S/S solids. Therefore, the solids with relatively high conductivity should release more unbounded chloride from the inner solid over long-term. Another possible chloride leaching mechanism the was the dissolution of FS. During the nature of 1315 leaching test,

DI water (pH 5.5) was replaced frequently over time. Therefore, the alkalinity of the solids would be also consumed over time. Although lime was added into this samples during the mixing, the its alkalinity could be consumed during the curing of the solids. During the long-term leaching test, the measured pH of all the samples in this study remained between 11-12, indicating that the solid alkalinity was being consumed. Mineral phase whose structure contained metal hydroxide (e.g. FS) will partially dissolute to generate hydroxide until the pH of the extraction fluid reached to the point where it was stable (this was also observed in the study in chapter 5).[111-112] Figure 6.7c indicates that during the later stage of long term leaching, samples with similar K value but higher FS% released more chloride, which could be an indication of FS dissolution. However, the lower scale of Figure 6.7c indicates that the amount of chloride leaching from FS dissolution was not as significant compared to the amount of chloride leached out during the first 7 days. Overall, based on the results discussed above, a combination of high FS% and low K would be a desired property for the S/S solids. This work has demonstrated that FS% could be improved by adding reactive aluminate with adequate amount of lime. Future work should focus on lowering the K of the solids.

4.5 CONCLUSIONS

In terms of enhanced formation of Friedel's salt and reduced leaching of contaminants (Se and chloride), aluminate addition along with an adequate amount of lime in the S/S process is crucial for the success of this ZLD method. Gypsum addition enhances the formation of ettringite which does not improve the retainment of chloride and Se significantly but will improve the retainment of boron. The addition of hot brine, extra lime and aluminate could make the S/S slurry drier and harden faster. Therefore, the S/S solids

generated under such conditions may be more porous and thus have higher leaching potential. Although the addition of quick lime provides more alkalinity compared to the addition of hydrated lime (due to lower molecular weight of quick lime under the same mass amount addition), quick lime only slightly increases the percentage formation of Friedel's salt in the S/S solid, and thus has no significant impact on chloride leaching.

This work has clearly demonstrated the importance of minerology of the S/S solids on the retainment of contaminants such as selenium and chloride. However, another important factor that must be considered as well is the permeability of the solids because permeability could govern the stability of the minerals inside the solids and the leaching of those free, unbounded contaminants (e.g. excess chloride). Regarding the influence of permeability, our preliminary results on a selected set samples have indicated that the long-term leaching of chloride may correlate more to the permeability of the solids, and less to the Friedel's salt formation, because most of the chloride in the S/S mixture remains as free chloride ions due to the very high concentration of chloride from the brine. Although the AFm phase is capable of binding chloride, the amount of Friedel's salt formed could only bind a small portion of the total chloride introduced from the brine. Meanwhile, the stability of the AFm phase can also affect the immobilization of the contaminants and should be considered. Once the S/S solids are exposed to the landfill conditions, rainwater and leachate may slowly penetrate the solids and the alkalinity could gradually be consumed or washed off. Preliminary analysis of the S/S solids generated in this study indicated a saturated hydraulic conductivity in the range of 10^{-7} to 10^{-9} cm/s which could be defined as impervious. The long-term leaching tests (USEPA Method 1315) conducted in this study covered the span of 9 weeks. For S/S solids to be disposed of in the landfills for years, a

low permeability as well as the optimized mineralogy are critical for the immobilization of contaminants. Therefore, further research should be conducted on how to reduce the permeability while maintaining the desired mineralogy of the S/S solids.

CHAPTER 5. REMOVAL OF SELENATE AND CHROMATE BY FRIEDEL'S SALT AND IMPACTS OF VARIOUS ANIONS

5.1 ABSTRACT

Friedel's salt ($Ca_4Al_2(OH)_{12}Cl_2(H_2O)_4$) is an AFm-Cl phase that belongs to the family of layered double hydroxides and has the ability of taking up various contaminants through ion exchange. Friedel's salt can play an important role in contaminant immobilization when it is formed in the solidification/stabilization (S/S) process. This study investigated the uptake process of Se(VI) and Cr(VI) by Friedel's salt and the impacts of various anions (i.e., sulfate, carbonate, nitrate and chloride) when they were co-existent with the heavy metal oxyanions. Results from sorption and desorption tests suggested that the uptake of Cr(VI) by Friedel's salt was more favorable than the uptate of Se(VI). Sulfate and carbonate exhibited a stronger hindering effect than nitrate and chloride on the uptake of both heavy metals by Friedel's salt. Evaluation of the long-term stability of Friedel's salt before and after the heavy metal uptake revealed that Friedel's salt and Se(VI)-substituted Friedel's salt could gradually transform into stratlingite, another AFm phase with aluminosilicate inside the interlayers, over three months when Friedel's salt was exposed to reactive silicate and aluminate, whereas Cr(VI)-substituted Friedel's salt remained unchanged. About 53% of absorbed Se(VI) was released when this transformation occurred, and 30% of absorbed Cr(VI) was released when this transformation did not occur. This study not only provided more insights on the effects of various anions on the removal of Se(VI) and Cr(VI) by Friedel's salt, but also revealed the potential transformation from Friedel's salt to stratlingite over time.

5.2 INTRODUCTION

Friedel's salt ($Ca_4Al_2(OH)_{12}Cl_2(H_2O)_4$) is an AFm-Cl phase that belongs to the family of layered double hydroxides (LDH). The AFm-X phase (or referred to as monophase) structure consists of positively charged $Ca_2[Al(OH)_6]^+$ layers, producing a net charge imbalance.[116] Anions (X), such as CO_3^{2-}, Cl^-, OH^-, and SO_4^{2-} occupy the space between the layers of $Ca_2[Al(OH)_6]^+$ to balance the mineral's charge.[116, 125] The exchange of anions in the interlayers with external anions is typically highly favored.[125] Friedel's salt has been shown to successfully remove various heavy metals such as selenate[112], chromate[111, 162], arsenate[163-164], and various anion such as chloride[116, 129-131], nitrate[165] and nitrite[166]. Compared to other adsorbents, Friedel's salt is easy and cheap to synthesize and it has demonstrated a high adsorption capacity for contaminants in various types of aqueous systems.[111-112, 162-164]

In our previous study, Friedel's salt was identified as the key mineral phase for the retainment of heavy metals and chloride in the solidified/stabilized (S/S) solids generated from mixing the flue gas desulfurization (FGD) waste brine, coal fly ash (CFA) and an activating agent (e.g. Portland cement or lime).[18, 190-192] Among the heavy metals of interest, selenate and chromate retainment could be enhanced by increasing the formation of Friedel's salt (Chapters 3 and 4). Previously, Wu et al. has demonstrated the effective removal of selenate by Friedel's salt with an uptake capacity up to 1.37 mmol/g. [112] Dai et al. demonstrated the effective removal of chromate by Friedel's salt with an uptake capacity up to 1.4 mmol/g.[111] However, the effects from various anions that may co-exist in the waste stream on the remove efficiency of heavy metals by Friedel's salt was scarcely considered. To the best of our knowledge, the effect of various anions on the removal of

selenate by Friedel's salt has not been reported to date. Previously, Dai et al. investigated the impact of chloride and bicarbonate (at the same concentration of chromate) on the removal of chromate by Friedel's salt and showed that chloride had no impact, whereas bicarbonate lowered the removal percentage by 10%.[111] Considering the complicated matrix in various types of wastewaters such as those from the wet FGD systems, the impacts of various types of anions on the removal of selenate and chromate by Friedel's salt should be evaluated. For our interest related to the previous studies (Chapters 3 and 4), it is important to understand the effects of common anions in the FGD wastewater such as sulfate, (bi)carbonate, nitrate, and chloride on selenate and chromate removal by Friedel's salt.

While the capacity and rate of Friedel's salt to take up selenate and chromate from different wastewater matrices are of interest, the stability of Friedel's salt and its phase change after the uptake of the contaminants is also an important aspect to be considered in the application of Friedel's salt in waste remediation. Baur and Johnson had reported that SeO_4^{2-}-substituted AFm phase was stable in the cementitious system.[152] Perkins and Palmer reported that during the synthesis of CrO_4^{2-}-substituted ettringite, CrO_4^{2-}-substituted monophase was also formed at pH 12; however, at pH >12.5, monophase was the only form. Perkins and Palmer also reported that the stability domain of monophase could be lowered to pH 11 when there was excess free calcium in the system, which favored the formation of monophase.[153-154] Wu et al. showed that selenate-substituted Friedel's salt was stable in water at a starting pH range of 4 -13 with an equilibrium pH around 11. At a lower starting pH, $Ca(OH)_2$ in the framework of LDH was partially dissolved, while at a higher staring pH, $Al(OH)_3$ in the framework of LDH was partially dissolved. However, under

both cases, less than 3% of the selenate was desorbed, indicating the strong fixation of selenate by Friedel's salt. [112] Similar findings regarding chromate-substituted Friedel's salt were also report by Dai et al. in terms of strong fixation of chromate.[111] The findings from the above mentioned studies indicated that AFm phases are likely more stable at around pH 11-12.

In our previous study (Chapter 4), we detected the transformation from Friedel's salt to stratlingite after the USEPA 1315 long-term leaching test. After being under the long-term leaching conditions for three months, the Friedel's salt in the S/S monolith (which was around 15% by weight in the original S/S solid) disappeared but stratlingite was detected instead. Stratlingite is also an AFm phase, but with aluminosilicate ion, expressed as $[AlSi(OH)_8 \cdot 0.25H_2O]^{-1}$, in the interlayers of the LDHs, and is commonly found in hydrated cement and concrete. Stratlingite is more difficult to synthesize than Friedel's salt and its synthesis could take up to 4-6 weeks.[114, 167] Transformation from stratlingite to Friedel's salt when exposed to chloride solution has been shown in previous research.[114, 168-169] However, to the best of our knowledge, no research has demonstrated the transformation from Friedel's salt to stratlingite, or the heavy metal removal by stratlingite. In the S/S solids from the ZLD method as described in our previous study, coal fly ash could provide silicate and aluminate which are required for the formation of aluminosilicate ion in the stratlingite. This could possibly explain the experimental observation of stratlingite formation upon disappearance of Friedel's salt in the S/S solids. Therefore, we propose that the transformation from Friedel's salt to stratlingite could be possible when Friedel's salt is exposed to metasilicate and aluminate, which are commonly used in the synthesis of stratlingite.

Because research on the removal of selenate and chromate by Friedel's salt was still quite limited, the objective of this study was to compare the uptake of these two heavy metal oxyanions by Friedel's salt, as well as to evaluate the impacts of sulfate, carbonate, nitrate and chloride anions on the removal of these two heavy metals by Friedel's salt. Furthermore, the potential transformation of Friedel's salt, and selenate- or chromate-substituted Friedel's salt to stratlingite, was investigated along with the fate of selenate and chromate in the AFm phases over a long-term process. The results of this study will be useful for related processes using AFm phases for heavy metal removal.

5.3 EXPERIMENTAL SECTION

5.3.1 Chemicals

Sodium aluminate ($Na_2O \cdot Al_2O_3$, technical grade), calcium chloride dihydrate ($CaCl_2 \cdot 2H_2O$), sodium selenate (Na_2SeO_4), potassium dichromate ($K_2Cr_2O_7$), sodium sulfate (Na_2SO_4), sodium bicarbonate ($NaHCO_3$), sodium nitrate ($NaNO_3$), and sodium chloride (NaCl) were purchased from Fisher Scientific (Hampton, NH). Sodium metasilicate nonahydrate ($Na_2SiO_3 \cdot 9H_2O$) and hydrated lime ($Ca(OH)_2$, 98%) were purchased from Sigma-Aldrich (St. Louis, MO). All the stock solutions were produced by dissolving the above-mentioned salts in ultrapure deionized (DI) water generated from a Milli-Q nanopure water purification system.

5.3.2 Friedel's salt (FS) synthesis

FS was synthesized following the method reported previously.[163, 166, 197] Briefly, calcium chloride (0.625 M) was dissolved in 500 mL of DI water and the solution was

heated to 65 ºC. Sodium aluminate (0.3125 M) was dissolved 500 mL of preheated DI water and maintained at 65 ºC before use. Sodium aluminate solution was added into the calcium chloride solution through a burette with a flow rate of about 30 mL per minute. The mixture was stirred at 500 rpm with a magnetic stirrer and remained heated at 65 ºC. After 20 minutes, the precipitate was collected immediately by centrifugation and washed two times with DI water to remove a significant portion of the residual salts. This washing procedure was adopted after preliminary washing experience showed that extensive washing to completely remove the residual salts resulted in partial dissolution of FS, as well as carbonate intrusion into the interlayers of FS. After washing, the precipitate was dried in an oven at 65 ºC for 24 hours and stored in a vacuum chamber before use.

5.3.3 Characterization of synthesized and reacted FS

FS and its reacted samples were characterized using a PANalytical X'Pert PRO Alpha-1 X-ray diffractometer (XRD, Almelo, Netherlands) at 45 kV and 40 mA, with the Cu *K*α radiation (λ = 1.542 Å) and a scanning rate of 0.033° per 100 seconds over a 2θ range between 4-70°. The morphology of the prepared FS was obtained on a Zeiss Ultra60 field emission scanning electron microscopy (FE-SEM, Carl Zeiss, Germany) operated at 5 kV. XRD and FE-SEM analyses were done at the Institute for Electronics and Nanotechnology Materials Characterization Facility at Georgia Tech.

5.3.4 Batch sorption and desorption study

The batch experiments to evaluate the sorption of selenate and chromate by FS with and without the effect of different anions were conducted in duplicates. Initial tests were conducted at different FS-to-metal molar ratio (F/M ratio) and solid-to-liquid ratio (S/L

ratio, mass of FS/solution volume) to evaluate the removal of Se(VI) and Cr(VI) and structures of reacted FS. Based on the results, the F/M ratio of 1.0 and the S/L ratio of 10 g/L were decided to be used in the subsequent experiments. To be specific, FS (0.10 g, MW = 561 g/mol) was added into a 15-mL centrifuge tube containing 10 mL solution of 17.4 mM of selenate or chromate (added as sodium selenate or potassium dichromate) so the F/M ratio was around 1.0 and the S/L ratio was 10 g/L. To evaluate the impacts of various anions, the selected anion, sulfate (1.74 and 17.4 mM), carbonate (1.74 and 17.4 mM), nitrate (3.48 and 34.8 mM) or chloride (28.1 mM and 281 mM), was also added into the solution to study its effect on selenate or chromate removal by FS. Before adding FS, the pH of the solution was adjusted to 10 by adding NaOH. At this pH, dichromate and bicarbonate became chromate and carbonate. The sample tube was clamped on a rotator with a rotating speed of 50 rpm to allow reaction for 24 hours at room temperature. At selected time intervals, the sample was removed from the rotator and the pH was measured. Then, the sample was agitated and immediately 0.5 mL of the mixture was transferred into a 2-mL centrifuge vial and centrifuged at 3000 rpm for 5 minutes. The supernatant was collected and diluted 1000 times for anion and heavy metal measurements.

The desorption test was conducted using the same experimental setup described above. The selenate- and chromate-substituted FS samples, named Se-FS and Cr-FS, were prepared by adding 0.1 g of FS in 10 mL of 17.4 mM selenate or chromate solution with a starting pH of 10. The sample was rotated at 50 rpm for 24 hours at room temperature and then centrifuged to obtain the solid. After drying in an oven, 0.1 g of Se-FS or Cr-FS was added into 10 mL of solution containing sulfate (8.7 and 17.4 mM), carbonate (8.7 and 17.4 mM), nitrate (17.4 and 34.8 mM) or chloride (17.4 and 34.8 mM) at pH 10. The same

sampling procedure as described in the sorption test was applied for anion and heavy metal measurements.

5.3.5 Transformation from FS to stratlingite

The transformation from FS, Se-FS and Cr-FS to stratlingite was tested for a period 3 months. Each of the solids was added into 10 mL of solution containing 4 mM of $Ca(OH)_2$, with or without the addition of metasilicate (17.4 mM) and aluminate (17.4 mM). At the end of 1, 2, and 3 months, the pH and heavy metals in the solution were measured for all samples (Table 5.3). The samples with metasilicate and aluminate were prepared in duplicate for each sampling time (6 for each type of FS). At each sampling time, two samples were sacrificed for XRD analysis. Samples without metasilicate and aluminate were also prepared in duplicate, but not sacrificed at each sampling time.

5.3.6 Analytical methods

The pH was measured by an Orion Star^{TM} A111 bench top pH meter (Waltham, MA). The concentrations of heavy metals were detected by inductively coupled plasmas – optical emission spectroscopy (ICP-OES) 8000 (Perkin Elmer, Waltham, MA). The ICP samples were prepared by diluting the supernatant from each test 1000 times using 5% trace metal grade nitric acid. The chloride, sulfate and nitrate concentrations were measured by ion chromatography (IC) (Dionex, Sunnyvale, CA) by diluting the supernatant 1000 times with DI water.

5.4 RESULTS AND DISCUSSION

5.4.1 Characterization of synthesized FS

The XRD pattern and SEM image of synthesized FS are shown in Figure 5.1. Although the entire synthesis process of FS was conducted at ambient conditions, no significant carbonate intrusion was observed. The characteristic peaks matched well with pure FS (JCPDS# 78-1219). The hexagonal plates of FS with obvious aggregation were also clearly seen in the SEM image.

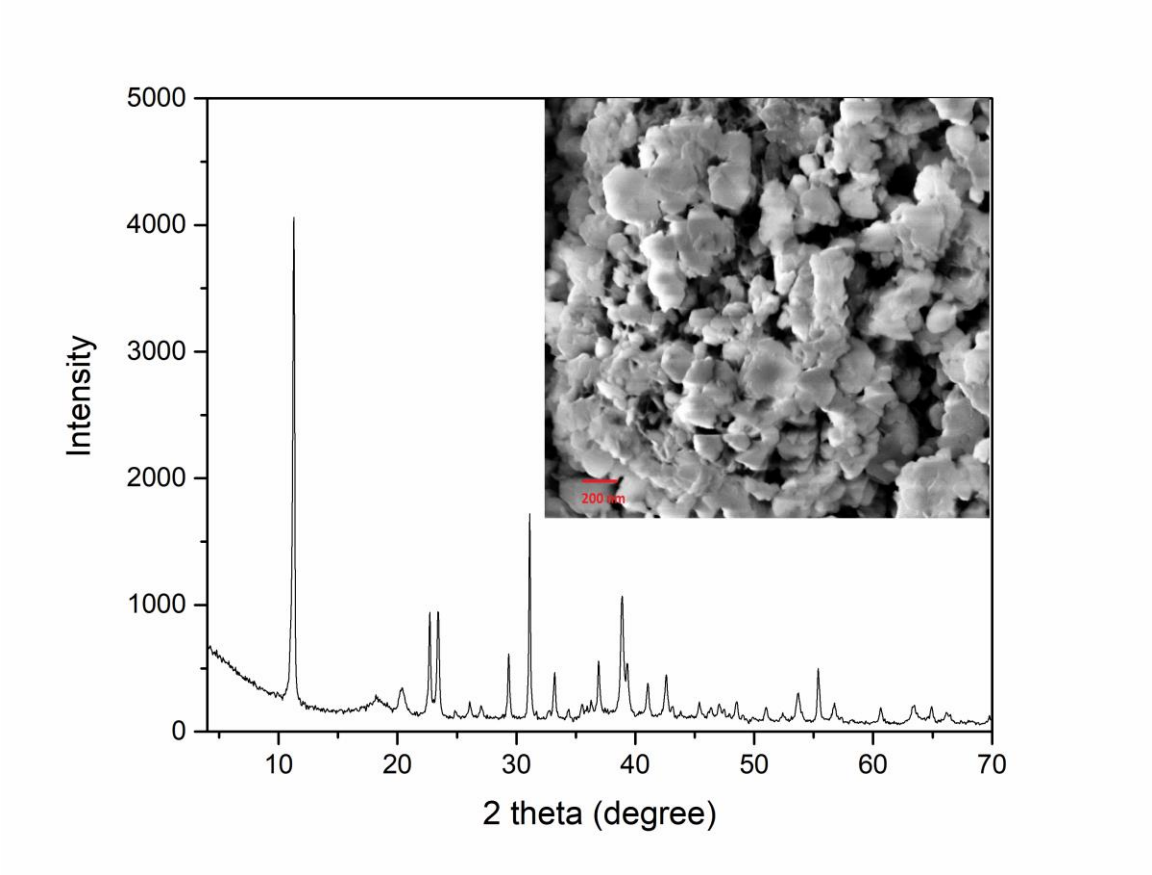

Figure 5.1. XRD and SEM analysis of synthesized FS.

5.4.2 Removal of selenate and chromate by FS

The removal of selenate and chromate by FS was initially tested at the S/L ratio of 50 g/L. The F/M molar ratios were 70 and 46 for Se(VI) and Cr(VI), respectively. At such

high F/M ratios, 71% of total selenate and 91% of total chromate were removed from the solution by FS within 24 hours. The XRD pattern (Figure 5.2a) of the reacted FS indicated that surface adsorption was likely the main removal mechanism because the characteristic peak (003, 11.3º) of Friedel's salt remained unchanged.

Then, similar sorption tests were conducted but at a lower F/M ratio (1.4 and 0.9 for Se(VI) and Cr(VI), respectively) at the S/L ratio of 10 g/L, aiming to observe the anion exchange mechanism. At this low F/M ratio, 69% of total selenate and 67% of total chromate were removed from the solution by FS within 24 hours. The XRD pattern (Figure 5.2a) of the reacted FS indicated that anion exchange occurred for the removal of metal oxyanions because peak shifting was observed. The new peaks are identified as selenate- and chromate-substituted FS (labelled as Se-FS and Cr-FS in Figure 5.2a). For Se-FS, the interlayer distanced increased from 0.78-0.79 nm to 0.96-0.97 nm, resulting in the shift of peak position to a lower 2 theta which was also detected in previous literature.[112] For Cr-FS, the interlayer distance increased to 1.00 nm which also resulted in the peak position shifted to the lower 2 theta, in agreement with the previous reports.[111, 153, 198]

After the sorption test (with low F/M ratios), the reacted FS was removed from the mixture through centrifugation and remixed with 50 mL of DI water with a pH of 10 adjusted by adding NaOH. Within 24 hours, 28% of adsorbed selenate and 14% of adsorbed chromate were desorbed back into the solution, while the XRD peaks of Se-FS and Cr-FS remained (Figure 5.2b), indicating that the heavy metals remained inside the interlayers of Friedel's salt. Notice that once the interlayer of the FS was partially occupied by metal oxyanions, the XRD peaks weakened dramatically and became broader which was due to the structure disorder caused by the anion exchange. Multiple anions, including

heavy metal oxyanion, hydroxide from NaOH, remaining chloride, and carbonate captured from the air all could co-exist inside the interlayers, causing the FS structure to become less crystalline. The peak position also slightly shifted possibly due to less selenate existed in the interlayer and the effect from multiple anions.

Notice that the removal % of both selenate and chromate decreased at the lower F/M ratios compared to those at the higher lower F/S ratio. For selenate, the F/M ratio was 1.4 which was still above 1.0, and so the decrease in Se(VI) removal compared to the removal at the the higher F/S ratio was not very significant. For chromate, the F/M ratio was 0.9 and thus the Cr(VI) removal decreased more significantly than selenate removal. Another possibility for the lower removal at the lower F/M ratios could be due to the slight dissolution of FS when it was exposed to the metal solution. When FS was added into the metal solution, some of it could be dissolved during the initial drop of pH until the pH of the solution was increased to around 11 where FS was stable. When the S/L ratio was 50 g/L (at the high F/M ratio condition), the amount of FS loss due to dissolution was less significant compared to the case when the S/L ratio was 10 g/L (at the low F/M ratio condition). To confirm this explanation, the S/L ratio was decreased to 2 g/L and the F/M ratio was kept same at 1.4 and 0.9 for Se(VI) and Cr(VI), respectively. To the expectation, only 22% of total selenate and 19% of total chromate were removed within 24 hours, compared to 69% of total selenate and 67% of total chromate removal at the S/L ratio of 10 g/L. The pH of the selenate solution was increased from 8.6 to 10.5 while the pH of the chromate solution was increased from 6.6 to 10.3 during those experiments, strongly suggesting that the dissolution of FS partly contributed to the lower removal of heavy metals.

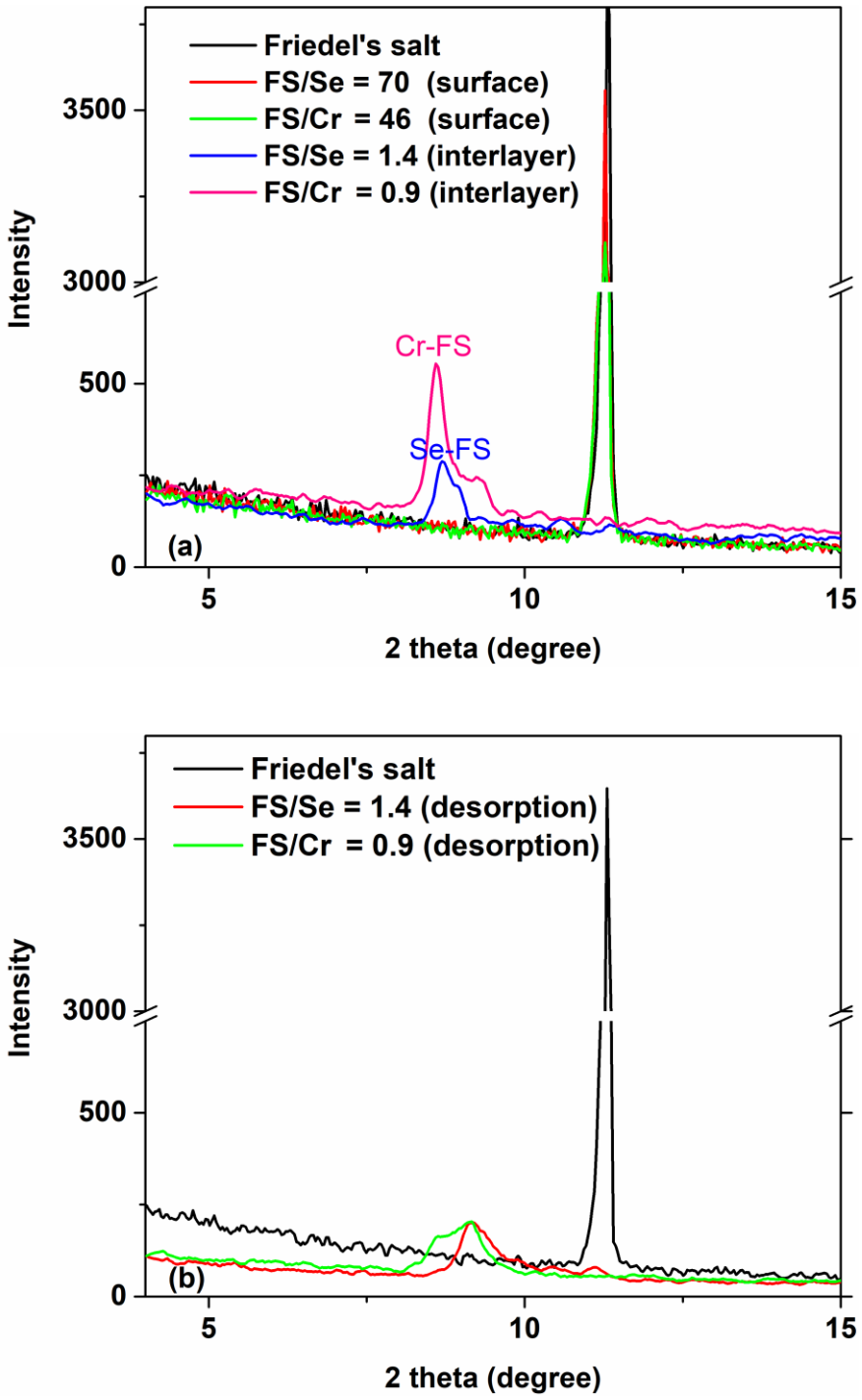

Figure 5.2. XRD patterns of reacted FS: (a) after sorption tests from samples with different FS/Se and FS/Cr ratios, and (b) after desorption tests.

From the results mentioned above, the ideal S/L ratio should be no less than 10 g/L to avoid significant loss of FS due to dissolution. To study the competition between

different anions with selenate and chromate, and the phase transformation of FS, a F/M ratio of 1.0 is approaporate. Considering the total amount of available FS synthesized from the same batch and the number of samples needed to be done, the optimized S/L ratio was determined to be 10 g/L (about 17.4 mM) and applied to all the experiments shown below. Meanwhile, the starting pH of the solution was raised to 10 by adding NaOH to further minimize the dissolution loss of FS.

5.4.3 Competition between Selenate and Chromate

The removal of selenate and chromate by FS with and without the competition from the other metal is shown in Figure 5.3. At the same metal concentration, chromate greatly hindered the removal of selenate (Figure 5.3a), whereas selenate only slightly hindered the removal of chromate (Figure 5.3b). This result indicated that chromate was preferred than selenate by FS when they co-existed in the solution.

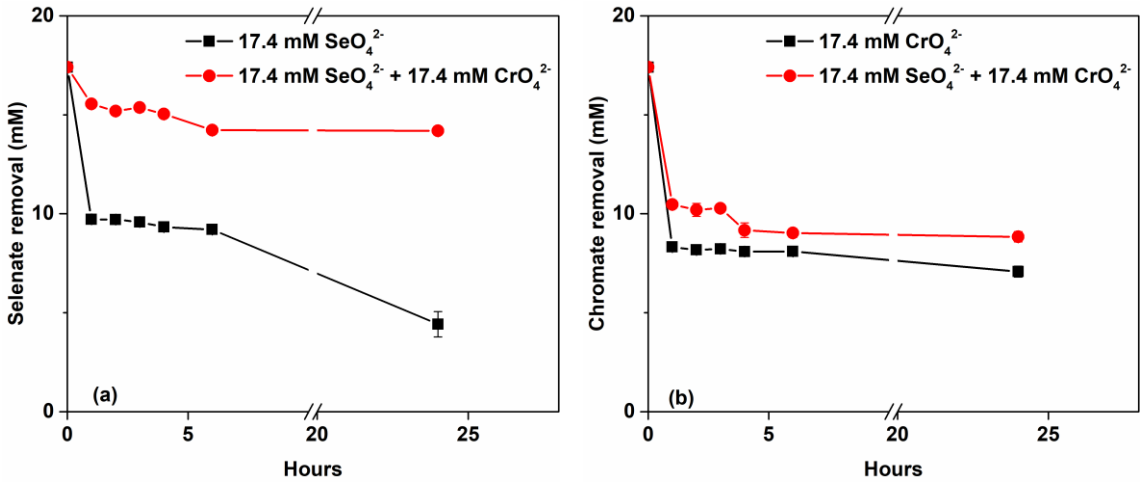

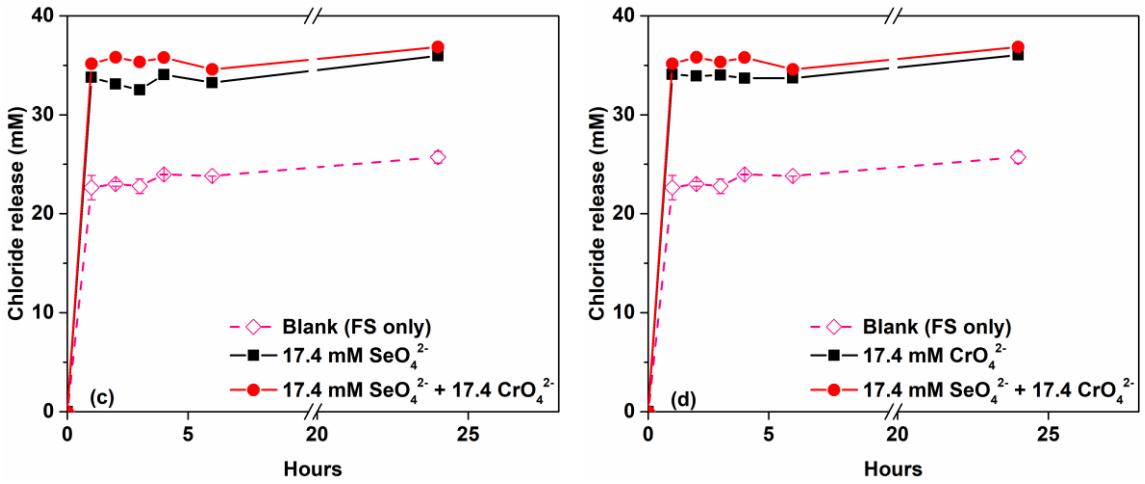

Figure 5.3. Competition between selenate and chromate for their removal by FS. (a) selenate removal affected by chromate; (b) chromate removal affected by selenate; (c) and (d) chloride release with and without the existence of heavy metals.

Figures 5.3c-d also show the chloride release from the FS with and without the presence of heavy metals. For the sample with FS only (Sample #1 in Table 5.1), about 22.6 mM of chloride was released at the very beginning and increased some more to 25.7 mM within 24 hours. The initial rapid release of chloride was likely due to the surface wash-off from the residue chloride on the FS and the partial dissolution of FS since pH of the solution (originally pH = 10) increased to 11.8 within one hour and further increased to 12.0 within 24 hours. For the samples of FS with selenate or chromate (Samples #2 and #3), almost identical change of pH was observed, and the chloride release was increased by 10 to 11 mM. The increase of chloride release was mainly due to the anion exchange of chloride with metal oxyanion since the change of pH in these samples was almost the same as that in the FS only sample, while about 13.0 mM of selenate and 10.3 mM of chromate were removed. Stoichiometrically, each mole of selenate or chromate should replace 2 moles of chloride. However, the increased amount of released chloride was less than the theoretical value based on the removal of heavy metals, indicating that selenate or chromate

was partially removed through anion exchange while the rest was adsorbed on the surfaces of FS without replacing the chloride. The removal pattern of selenate suggested that the removal mechanism involved two stages of process. During the first hour, a rapid removal was observed which indicated the rapid surface adsorption and an initial stage of interlayer anion exchange. Afterwards, the removal rate became much slower which indicated the interlayer anion exchange was still happening but at a slow rate. Previously, in-situ space and time-resolved study suggested that the sorption of anionic dyes on LDH layers started at the edges of the LDH and was followed by diffusion to the basal planes.[199]

In comparison, such a two-step process was not as obvious for the sorption of chromate to FS as in the case of selenate. During the first hour, more chromate was removed (9.1 mM) than selenate (7.7 mM), but the removal rate became much slower after the first hour. Since the XRD pattern showed that chromate-substituted FS was already formed, the chromate could already have been incorporated into the interlayers during the first hour. This result also could explain why chromate was preferred by FS when selenate and chromate co-existed. Between 6 hours and 24 hours of reaction time, more selenate was removed than chromate, indicating the exchange rate of selenate in the later stage is faster than that of chromate. When selenate and chromate co-existed (Sample #4), a total of 11.8 mM of selenate and chromate together was removed which was only slightly higher than the overall removal of selenate or chromate when they were present alone (Samples #2 and #3), indicating the FS had reached the maximum sorption capacity. Also, about 36.9 mM of chloride was released with 24 hours in Sample #4, which was only 0.9 mM higher than the chloride release in the samples with only selenate or chromate.

5.4.4 Effects of different anions on the removal of selenate and chromate by FS

The starting concentration of each reactant is shown in Table 5.1. The F/M ratio for Se(VI) and Cr(VI) was set at 1.0, while the concentrations of different anions were varied to study their effects. FS itself could release more than 25 mM of chloride from the residual chloride left from the FS synthesis and also from some degree of FS dissolution once the mineral was exposed to the solution; thus, the chloride concentrations studied were higher compared to the concentrations of the other anions. Sulfate and carbonate are both negatively 2 charged as selenate and chromated, so the higher end of the concentration of sulfate and carbonate were chosen to be equal FS. Nitrate is negatively 1 charged so its concentration was doubled.

Table 5.1. The starting concentration (mM) of each reactant in all the samples related to the study of the effects of different anions on selenate and chromate removal by FS. Before adding the FS, the solution pH was raised to 10 by adding NaOH.

#	FS	Se(VI)	Cr(VI)	SO_4^{2-}	CO_3^{2-}	NO_3^-	Cl^-
1	17.4						
2	17.4	17.4					
3	17.4		17.4				
4	17.4	17.4	17.4				
5, 6	17.4	17.4		1.74, 17.4			
7, 8	17.4	17.4			1.74, 17.4		
9, 10	17.4	17.4				3.48, 34.8	
11, 12	17.4	17.4					28.1, 281
13, 14	17.4		17.4	1.74, 17.4			

15, 16	17.4	17.4	1.74, 17.4		
17, 18	17.4	17.4		3.48, 34.8	
19, 20	17.4	17.4			28.1, 281

The effects of various anions on selenate removal (Samples #5-12 in Table 5.1) by FS are shown in Figure 5.4a. When 28.1 mM of chloride was added, there was 7.7 mM of selenate remaining in the solution after 24 hours of reaction, compared to only 4.4 mM of selenate remaining in solution without the addition of chloride (Sample #2). When an even higher concentration (281 mM) of chloride was added, the selenate removal was greatly hindered to have 12.1 mM of selenate remaining in the solution not removed. These results showed that a higher chloride concentration could decrease the selenate exchange with chloride in FS.

A low concentration (1.74 mM) of sulfate and carbonate had minimum effects on the selenate removal by FS. However, at a high concentration (17.4 mM, similar to the concentration of selenate), both sulfate and carbonate competed with selenate for FS, as seen by the higher concentration of selenate remaining in the solution, likely by forming sulfate- or carbonate-substituted FS.[200] Figure 5.4c shows the removal of sulfate by FS when it coexisted with selenate. Notice that when the sulfate concentration was equal to the selenate concentration (17.4 mM), more than 90% of sulfate was removed by FS, thus hindering the removal of selenate. Interestingly, nitrate did not hinder the removal of selenate by FS even at the high concentration of 34.8 mM, which was in agreement with the result that only a very small amount of nitrate was removed by FS (Figure 5.4c), indicating anion exchange between nitrate and chloride was not preferred by FS.

The effects of anions on chromate removal (Samples #13-20 in Table 5.1) by FS are shown in Figure 5.4b. Similar to the case for selenate, nitrate and a low concentration of sulfate, carbonate and chloride had minimum effects on chromate removal by FS. A high concentration of sulfate, carbonate and chloride hindered the removal of chromate. The removal rates of sulfate and nitrate (Figure 5.4d) when they coexisted with chromate were also similar to those when they coexisted with selenate (Figure 5.4c). Overall, sulfate and carbonate were stronger competitors than chloride and nitrate for the removal of selenate and chromate by FS. Again, the two-step sorption process by FS was clearly observed for the removal pattern of selenate, but not for that of chromate.

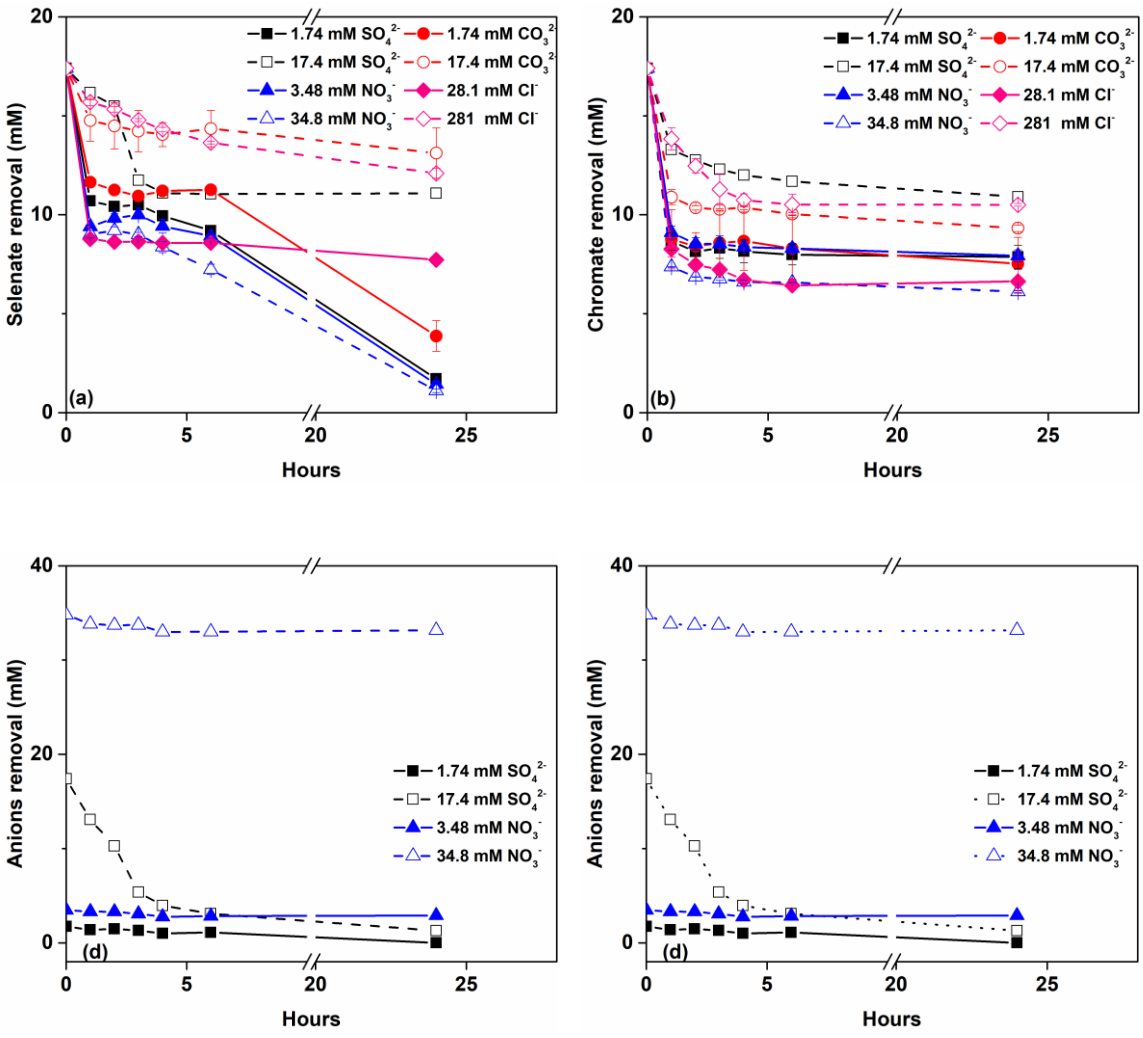

Figure 5.4. Effects of sulfate, carbonate, nitrate and chloride on the removal of (a) selenate and (b) chromate by FS. The removal of sulfate and nitrate by FS when each of them coexisted with (c) selenate and (d) chromate.

The reacted FS samples from the above experiments with a high concentration sulfate, carbonate and nitrate co-existent with selenate (Sample #6, #8 and #10 for selenate) or chromate (Sample #14, #16 and #18) were analyzed for XRD and results are shown in Figure 5.5, along with the XRD results of unreacted FS, Se-FS and Cr-FS. Apparently, both selenate and chromate have intercalated into the interlayer and expanded the interlayer spacing, resulted a lower 2 theta value. Carbonate could also intercalate into the interlayer along with selenate, but it did not further expand the interlayer spacing.[112] Since sulfate was greatly removed by FS and it hindered the removal of selenate, the peak of the FS sample exposed to both selenate and sulfate shifted by a little because the size of sulfate (r = 0.242 nm) is smaller than that of selenate (r = 0.256).[201] Nitrate didn not affect the removal of selenate or chromate, and it did not shift the peak of the metal-substituted FS either.

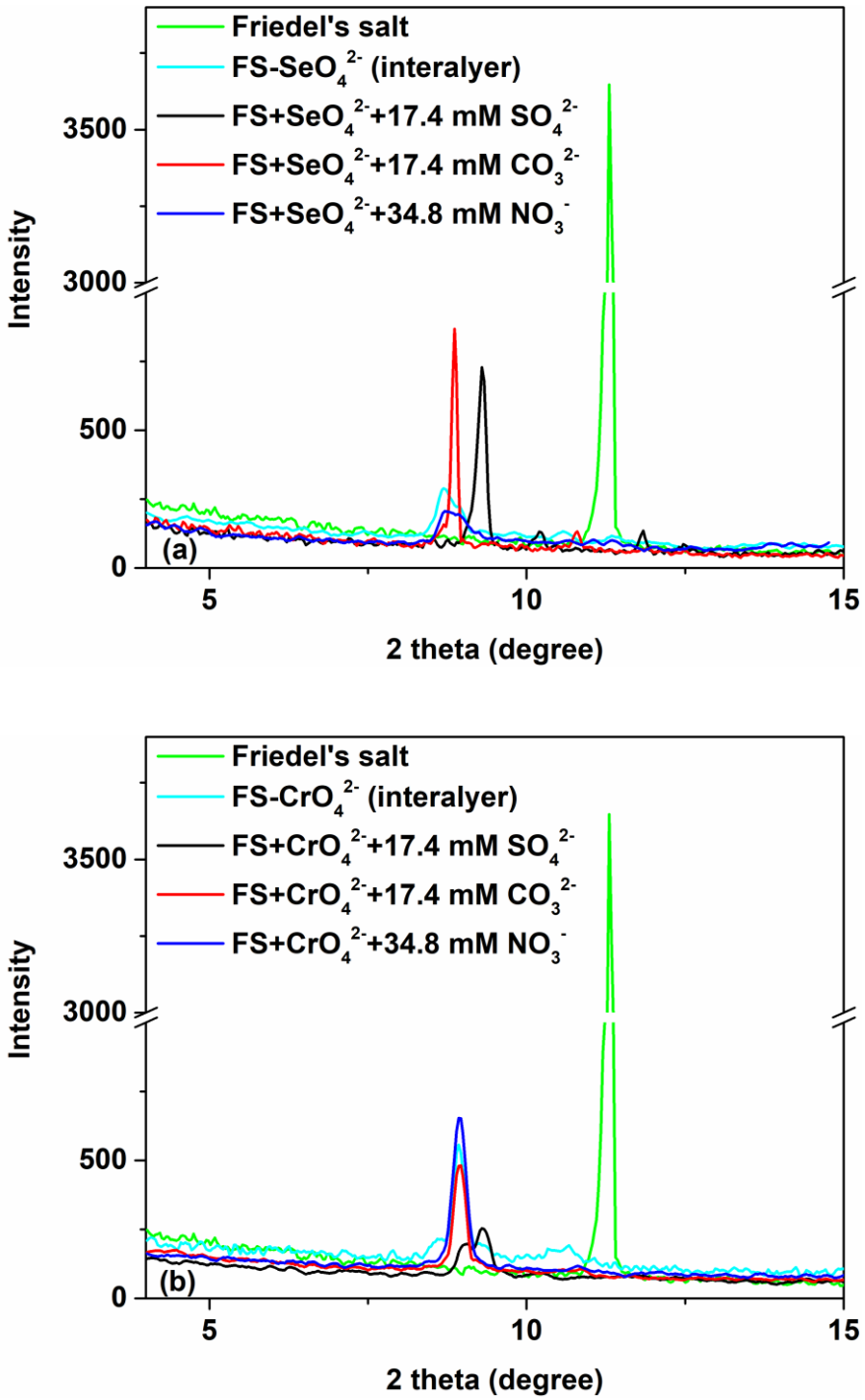

Figure 5.5. XRD patterns of reacted FS samples affected by sulfate, carbonate and nitrate from the sorption tests on (a) selenate and (b) chromate.

5.4.5 Effects of different anions on the desorption of selenate and chromate

Selenate- and chromate-substituted FS, named Se-FS and Cr-FS, were applied for the desorption test. Se-FS and Cr-FS were prepared as Samples #2 and #3 in Table 5.1. In the desorption test, each 0.10 g of Se-FS and Cr-FS could release a maximum concentration of 15.9 mM for selenate and 10.9 mM for chromate if they were all desorbed. Table 5.2 shows the starting concentration of each reactant in all the samples conducted in the desorption test.

Table 5.2. The starting concentration of each reactant in all the samples related to the study on the effects of different anions on the desorption of selenate and chromate from Se-FS and Cr-FS. The starting pH was raised to 10 by adding NaOH.

#	Se-FS * (g/L)	Cr-FS* (g/L)	SO_4^{2-} (mM)	CO_3^{2-} (mM)	NO_3^- (mM)	Cl^- (mM)
1	10					
2		10				
3,4	10		8.7, 17.4			
5,6	10			8.7, 17.4		
7,8	10				17.4, 34.8	
9,10	10					17.4, 34.8
11,12		10	8.7, 17.4			
13,14		10		8.7, 17.4		
15,16		10			17.4, 34.8	
17,18		10				17.4, 34.8

*The molecular weight of Se-FS and Cr-FS should increase slightly after the anion exchange. However, the exact stoichiometry of Se-FS and Cr-FS could not be determined because the anion exchange was not 100%.

The effects of sulfate, carbonate, nitrate and chloride on the desorption of selenate and chromate from Se-FS and Cr-FS are shown in Figure 5.5a-b. The desorption of selenate and chromate from respective Se-FS and Cr-FS without the presence of other anions are

also included for easy comparison. For selenate (Figure 5.6a), nitrate and chloride (17.4-34.8 mM, Samples #7-10 in Table 5.2) had negligible effects. During the first hour, about 16% of adsorbed selenate was rapidly desorbed. Interestingly, after the first hour, the selenate released previously was slowly removed again by the Se-FS. The rapid release of selenate during the first hour was probably mainly from the selenate remained on the surfaces of FS. The continues removal after the first hour indicated that the interlayer anion exchange was still happening, similar to the selenate removal curve shown in Figure 5.3a. Sulfate and carbonate (8.7-17.4 mM) enhanced the release of selenate, similar to their effect on selenate removal discussed above. Figure 5.6c shows the removal of sulfate and nitrate during the selenate desorption process. Notice that a significant amount of sulfate was taken up by Se-FS through anion exchange with selenate. After the first hour, it continued to slowly exchange selenate from the interlayer, as the selenate concentration slowly increased after the first hour. Nitrate concentration almost remained constant since it did not exchange selenate. The results of this test strongly indicated that sulfate is highly preferred by the FS. For the desorption of chromate from Cr-FS (Figure 5.6b), the effects of various anions were similar to those observed for selenate. The flat curve after the first hour indicated the chromate released during the first hour was not taken up by FS, suggesting the interlayer anion exchange had reached equilibrium. The chloride release during the desorption test was also monitored (Figure 5.6e-f). No matter what concentration and what type of anion was tested, the amount of chloride released from each of all the Se-FS experiments was similar to that with the Se-FS only sample (Figure 5.6e). Such a trend was also observed for all the Cr-FS experiments in comparison with the Cr-FS only sample (Figure 5.6f). These results strongly indicated that chloride was released

from the Se-FS and Cr-FS and its release was not affected by the anions, suggesting chloride did not play a role in the desorption of selenate and chromate.

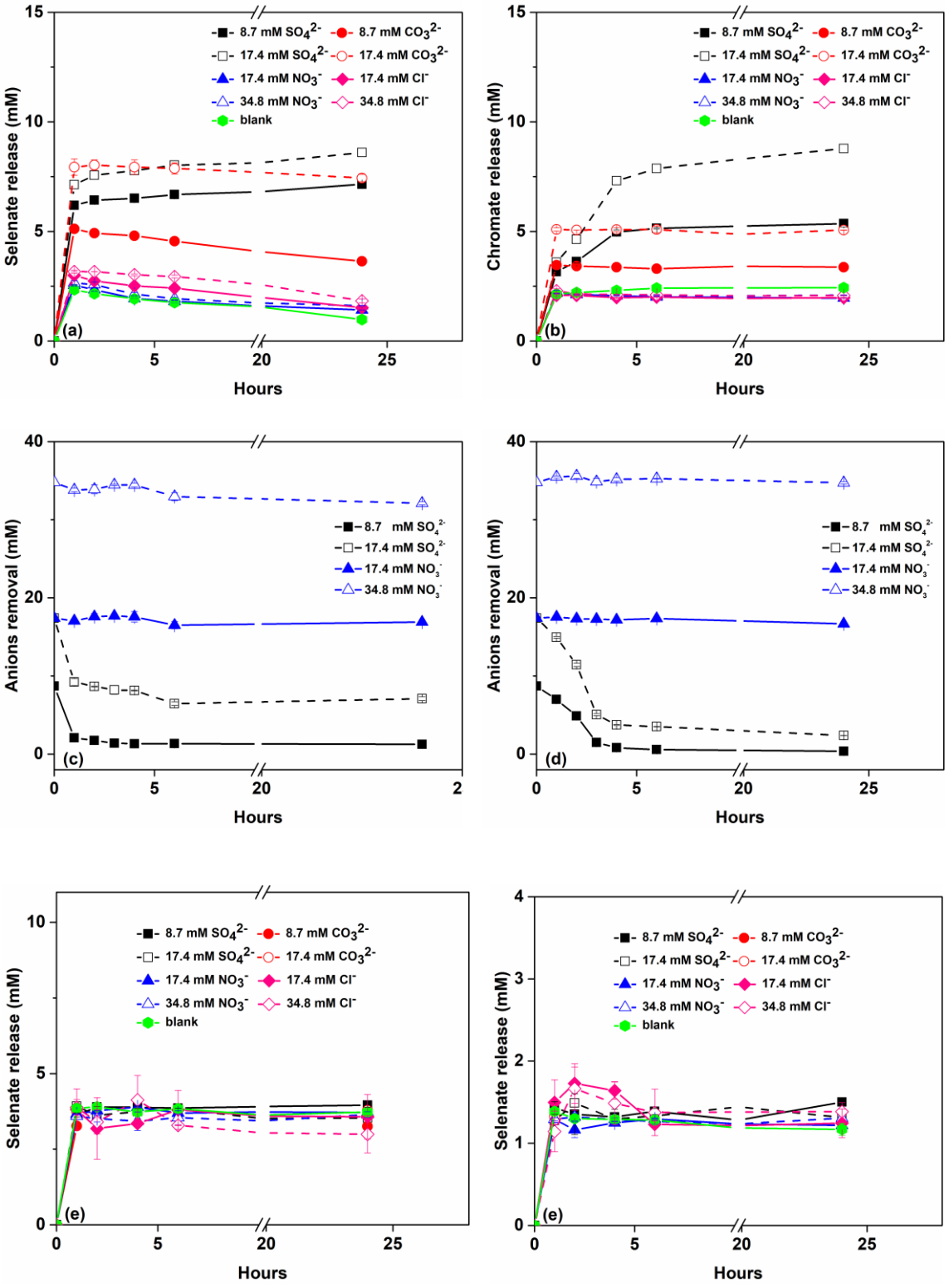

Figure 5.6. Effects of sulfate, carbonate and nitrate on the desorption of (a) selenate and (b) chromate. The removal of sulfate and nitrate during the desorption of (c) selenate and (d) chromate, and the release of chloride during the desorption of (e) selenate and (f) chromate.

5.4.6 Transition from FS to stratlingite

The transformation of FS, Se-FS and Cr-FS to stratlingite was investigated for a period of 3 months. The FS, Se-FS and Cr-FS samples applied in this transformation test were the same as those applied in the sorption and desorption tests discussed above. The starting concentration of each reactant is shown in Table 5.3.

Table 5.3. The starting concentration of each reactant in all the samples related to the study of the transformation from FS to stratlingite.

#	FS (g/10mL)	Se-FS (g/10mL)	Cr-FS (g/10mL)	$Ca(OH)_2$ (mM)	SiO_3^{2-} (mM)	AlO_2^- (mM)
1	0.10			4.0		
2	0.10			4.0	17.4	17.4
3		0.10		4.0		
4		0.10		4.0	17.4	17.4
5			0.10	4.0		
6			0.10	4.0	17.4	17.4

Previous tests on Samples #1 and #2 in Table 5.3 for a period of 30 days resulted in no obvious transformation from FS to stratlingite. Therefore, the reaction time for this test was extended to 3 months. The XRD patterns of FS in Sample #1 and #2 are shown in Figure 5.7. After 3 months, FS remained stable without the exposure to metasilicate and

aluminate. With the addition of metasilicate and aluminate, FS was converted to stratlingite whose characteristic peak was at 6.9º. The aluminosilicate ion, expressed as $[AlSi(OH)_8 \cdot 0.25H_2O]^{-1}$, expanded the interlayer distance from 0.79 nm to 1.26 nm, thus shifting the peak to a lower 2 theta value.

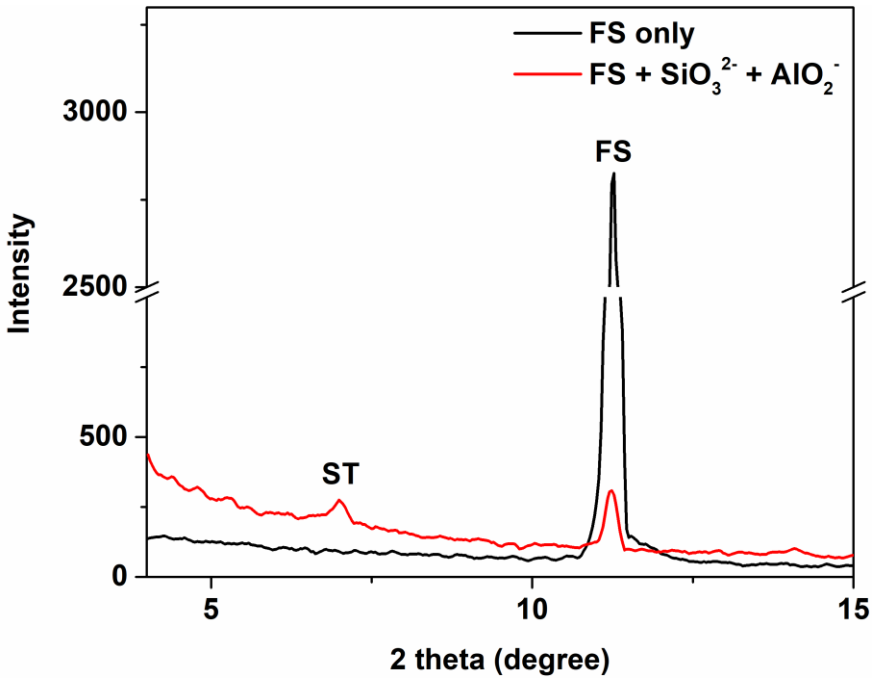

Figure 5.7. Transformation of FS to stratlingite.

Transformation from Se-FS and Cr-FS to stratlingite (Samples #3-6 in Table 5.3) was also tested for a period of 3 months. The selenate and chromate concentrations during the transformation test were monitored at each month. As mentioned earlier, at this experimental condition, the maximum concentration of selenate and chromate could be released by Se-FS and Cr-FS was 15.9 mM and 10.9 mM, respectively, if complete

desorption occurred. Table 5.4 shows the concentration of selenate and chromate released by Se-FS and Cr-FS during the transformation test for Samples #3-6 in Table 5.3.

Table 5.4. Concentrations of selenate and chromate released by Se-FS and Cr-FS during their transformation to stratlingite.

Sample # (Se or Cr)	1 month (mM)	2 months (mM)	3 months (mM)
3 (Se)	5.36 ± 0.10	4.08 ± 0.21	4.18 ± 0.18
4 (Se)	8.55 ± 0.11	8.51 ± 0.09	8.57 ± 0.13
5 (Cr)	2.58 ± 0.09	2.58 ± 0.26	2.51 ± 0.09
6 (Cr)	3.27 ± 0.14	3.11 ± 0.08	3.06 ± 0.06

As shown in Table 5.4, Se-FS released about 5.4 mM (about 34% of maximum possible release) of selenate after 1 month, and this concentration decreased to 4.2 mM after 3 months, indicating part of selenate released initially was removed again by the Se-FS. This trend was also observed for the Se-FS sample in the desorption test. By adding metasilicate and aluminate (Sample #4), the concentration of selenate released by Se-FS increased to 8.5 mM after 1 month and remained the same afterwards, suggesting that part of the selenate was replaced by silicate and aluminate within 1 month and no more selenate was replaced afterwards. The XRD patterns of Sample #4 after each month are shown in Figure 5.8a. Stratlingite was not observed during the first 2 months, but a small peak of stratlingite was observed after 3 months, suggesting the formation of aluminosilicate was a very slow process. Meanwhile, as the selenate concentration in Sample #4 remained at 8.5 mM, it was still only 53% of the theoretical maximum concentration of 15.9 mM if all

the selenate was released. Therefore, the transformation from Se-FS to stratlingite only caused partial desorption of selenate. The aluminosilicate ion increased the interlayer distance and created the space for other anions to intercalate. Once there were multiples types of anions existing inside the interlayers of the AFm phase, the structure became less crystalline and the XRD peak became weaker and broader. This also explains why the peak of as-prepared FS was much higher and sharper than the other peaks which correspond to the reacted FS samples.

For Cr-FS, about 2.6 mM (about 24% of the maximum possible desorption) of chromate was released after 1 month and remained the same afterwards (Sample #5). By adding metasilicate and aluminate (Sample #6), the concentration of chromate released by Cr-FS increased slightly to 3.3 mM after 1 month and decreased slightly afterwards. The constant concentration of chromate in Sample #5 agrees with the result from the Cr-FS sample in the desorption test (Figure 5.6b). The slight increase of chromate concentration in Sample #6 indicated that only a small amount of chromate was replaced, suggesting that chromate was more stable inside the interlayer than selenate. A similar conclusion was made previously in the test where both selenate and chromate were removed by FS simultaneously (Figure 5.3a-b). Also, in the sorption and desorption tests, a slow but continuous removal of selenate through interlayer anion exchange was observed (Figure 5.5a), whereas chromate concentration remained the same after the 1 hour (Figure 5.5b), suggesting that chromate is highly preferred inside the interlayer. The XRD patterns of Sample #6 after each month are shown in Figure 5.8b. Stratlingite was not observed throughout the 3 months period, which agreed with discussion above.

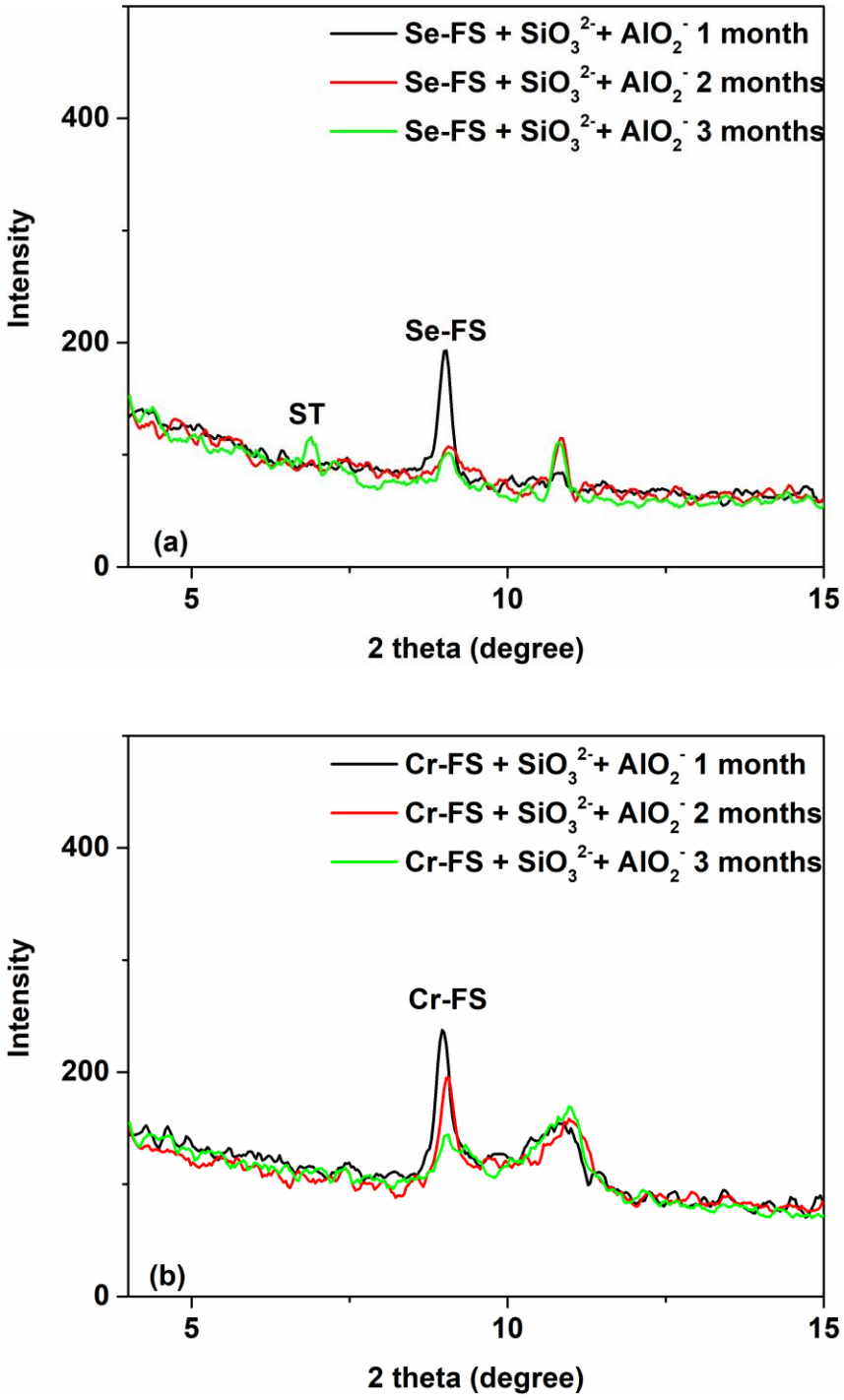

Figure 5.8. Transformation of (a) Se-FS and (b) Cr-FS to stratlingite.

5.5 CONCLUSIONS

The investigation of the effects of various anions on the removal of selenate and chromate have led to several new findings. At the same concentration with selenate or chromate, sulfate and carbonate exhibited stronger hindering effects than chloride and nitrate. Meanwhile, chromate was more favorable to be intercalated into the AFm phase of Friedel's salt than selenate. Once selenate and chromate were taken up by Friedel's salt, chromate-substituted Friedel's salt was more stable than selenate-substituted Friedel's salt. Transformation from Friedel's salt to stratlingite was observed when Friedel's salt was exposed to metasilicate and aluminate for a long period of 3 months. Selenate-substituted Friedel's salt also transformed into stratlingite, but chromate-substituted Friedel's salt did not. This transformation process did not significantly enhance the release of selenate because of the increased interlayer space. Based on the results of this study, applications using Friedel's for selenate and chromate removal should be cautious when the water contains high concentrations of sulfate and carbonate. The fate of AFm phase and the contaminant it captured over the long term should be also considered before application.

CHAPTER 6. CONCLUSIONS AND RECOMMANDATIONS

6.1 CONCLUSIONS

The results of this study show that the proposed ZLD method can successfully immobilize heavy metals and halides existed in both CFA and FGD wastewater brine. S/S solids made with SCFA perform well without further enhancement, while the performance of S/S solids made with BCFA could be enhanced by two approaches: pretreating the brine with a reduction process using ZVI or optimizing the mineralogy in the S/S solids by enhancing the formation of desired phases, especially AFm phases (e.g. Friedel's salt).

For the first aspect of this research in enhancing the performance of the ZLD method using a reduction process, the investigation of the removal of heavy metals by aged ZVI in concentrated FGD brines demonstrated that temperature and Mg^{2+} are the dominant factors that will enhance ZVI's reactivity for the removal of selenate, arsenate, cadmium, and chromate in brine matrices. At 80°C, other factors such as pH, TDS, nitrate and sulfate become negligible, and the Mg^{2+} can destruct the passive layer around the aged ZVI particles. Once the ZVI is corroded, the formation of green rust (GR) leads to the removal of selenate and chromium. Although GR is not stable in oxic conditions, the high temperature lowers the concentration of dissolved oxygen in the brine, thus improving the stability of GR. The longevity of ZVI depends on how fast the Fe(0) is depleted and the stability of GR.

Based on the results of this study, aged, micron-sized ZVI is an effective material for pretreating the hot FGD brine, and this pretreatment process can greatly enhance the overall

performance of the S/S process using BCFA. The reacted ZVI (with GR formation) not only reduces the heavy metals in the brine, but also those in the CFA when it is introduced into the S/S mixture.

For the second aspect of this research in enhancing the performance of the ZLD method by optimizing the mineralogy of S/S solids, this study demonstrated that enhancing the formation of Friedel's salt greatly reduced the leaching of contaminants (Se and chloride). In terms of enhancing the formation of Friedel's salt, aluminate addition along with an adequate amount of lime is most important. Gypsum addition enhances the formation of ettringite which does not improve the retainment of chloride and Se significantly but will improve the retainment of boron. The addition of hot brine, extra lime and aluminate could make the S/S slurry drier and harden faster. Therefore, the S/S solids generated under such conditions may be more porous and thus have a higher leaching potential for the contaminants. Although the addition of quick lime provides more alkalinity compared to the addition of hydrated lime (due to lower molecular weight of quick lime under the same mass amount addition), quick lime only slightly increases the percentage formation of Friedel's salt in the S/S solid, and thus has no significant impact on the overall contaminant leaching.

The stability of Friedel's salt in the S/S solids over the long-term leaching condition is also an important factor that needs to be considered. This study demonstrates that the transformation from FS to stratlingite is a possibility since the CFA can provide reactive silicate and aluminate which are required for this transformation to occur. Meanwhile, sulfate and carbonate in the matrix could compete with heavy metal oxyanions (e.g. selenate and chromate) for the uptake by Friedel's salt.

6.2 RECOMMANDATIONS

Based on the results of this study, aged, micron-sized ZVI is an effective material for treating hot FGD brine. Although the high temperature reaction condition makes this process energy intensive, the brine generated through thermal evaporation provides the high temperature condition. Hence, the ZVI treatment should be considered post evaporation of FGD wastewater. Magnetite as the final product could be easily removed magnetically to minimize the harms of heavy metals to the environment.

This work has also clearly demonstrated the importance of mineralogy of the S/S solids on the retainment of contaminants such as selenium and chloride. However, another important factor that must be considered as well is the permeability of the solids because permeability could govern the stability of the minerals inside the solids and the leaching of those free, unbounded contaminants (e.g. excess chloride). Regarding the influence of permeability, our preliminary results on a selected set samples have indicated that the long-term leaching of chloride may correlate more to the permeability of the solids, and less to the Friedel's salt formation, because most of the chloride in the S/S mixture remains as free chloride ions due to the very high concentration of chloride from the brine. Although the AFm phase is capable of binding chloride, the amount of Friedel's salt formed could only bind a small portion of the total chloride introduced from the brine. Meanwhile, the stability of the AFm phase can also affect the immobilization of the contaminants and should be considered. Once the S/S solids are exposed to the landfill conditions, rainwater and leachate may slowly penetrate the solids and the alkalinity could gradually be consumed or washed off. Preliminary analysis of the S/S solids generated in this study indicated a saturated hydraulic conductivity in the range of 10^{-7} to 10^{-9} cm/s which could be defined

as impervious. The long-term leaching tests (USEPA Method 1315) conducted in this study covered the span of nine weeks. For S/S solids to be disposed of in the landfill for years, a low permeability as well as the optimized mineralogy are critical for the immobilization of contaminants. Therefore, further research should be conducted on how to reduce the permeability while maintaining the desired mineralogy of the S/S solids.

For the applications using Friedel's for selenate and chromate removal, the matrix of wastewater must be carefully evaluated, especially when the wastewater contains high concentration of sulfate and carbonate. The fate of AFm phase and the contaminant it captured over the long term should be also considered before the application.

REFERENCES

1. Huang, Y. H.; Peddi, P. K.; Zeng, H.; Tang, C.; Teng, X., Pilot-scale demonstration of the hybrid zero-valent iron process for treating flue-gas-desulfurization wastewater: Part I. Water. Sci. Technol. 2013, 67, 16 - 23.

2. Fu, Y. Y.; Zhou, J. L.; Xiao, J. In the treatment and recycling of FGD waste, Adv. Mater.s Res., Trans. Tech. Publ.: 2014; pp 2901-2905.

3. Impact of air emissions controls on coal combustion products; 1015544; EPRI: Palo Alto, California, 2008.

4. USEPA, Steam electric power generation point source category: final detailed study report. Washington, DC, 2009.

5. Gingerich, D. B.; Sun, X.; Behrer, A. P.; Azevedo, I. L.; Mauter, M. S., Spatially resolved air-water emissions tradeoffs improve regulatory impact analyses for electricity generation. Proceedings of the National Academy of Sciences 2017, 114 (8), 1862-1867.

6. USEPA, Effluent limitations guidelines and standards for the steam electric power generating point source category; Final rule, 40 CFR Part 423, Federal Register. 2015, 80.

7. Pudvay, M.; Degremont, I., Operating experience on the treatment on FGD scrubber blowdown from existing generating stations. IWC, Richmoud: The international water assocation 2011, 21 (6), 05-69.

8. Layman, C. M., Navigating the new steam electric power effluent limitation guidelines. International Water Conference 2013, 174-187.

9. Cantafio, A. W.; Hagen, K. D.; Lewis, G. E.; Bledsoe, T. L.; Nunan, K. M.; Macy, J. M., Pilot-scale selenium bioremediation of San Joaquin drainage water with Thauera selenatis. Appl. Environ. Microb. 1996, 62 (9), 3298-3303.

10. Santos, S.; Ungureanu, G.; Boaventura, R.; Botelho, C., Selenium contaminated waters: an overview of analytical methods, treatment options and recent advances in sorption methods. Sci. Total. Environ. 2015, 521, 246-260.

11. Qiu, S. R., H.-F. La, M.J. Roberson, M.L. Hunt, C. Amrhein, L.C. Giancarlo, G.W. Flynn, and J.A. Yarmoff, Removal of contaminants from aqueous solution by reaction with iron surfaces. Langmuir 2000, 16, 2230-2236.

12. Mondal, K., G. Jegadeesan, and S.B. Lalvani, Removal of selenate by Fe and NiFe nanosized particles. Ind. & Eng. Chem. Res. 2004, 43, 4922-4934.

13. Zhang, Y., C. Amrhein, and W. T. Frankenberger, Effect of arsenate and molybdate on removal of selenate from an aqueous solution by zero-valent iron. Sci. Total. Environ. 2005, 350, 1-11.

14. Zhang, Y., J. Wang, C. Amrhein, and W.T. Frankenberger, Removal of selenate from water by zerovalent iron. J. Environ. Qual. 2005, 34, 487–495.

15. Huang, Y. H., P. K. Peddi, H. Zeng, C. Tang, and X. Teng, Pilot-scale demonstration of the hybrid zero-valent iron process for treating flue-gas-desulfurization wastewater: Part II. Water Sci. & Technol. 2013, 67, 239 - 246.

16. Huang, Y. H., P. K. Peddi, H. Zeng, C. Tang, and X. Teng, Pilot-scale demonstration of the hybrid zero-valent iron process for treating flue-gas-desulfurization wastewater: Part I. Water Sci. & Technol. 2013, 67, 16 - 23.

17. Peddi, P. K. Pilot-Scale Demonstration of hZVI Process for treating flue gas desulfurization wastewater at plant wansley, Carrolton, GA. Texas A&M University, Office of Graduate Studies, 2011.

18. Renew, J. E.; Huang, C.-H.; Burns, S. E.; Carrasquillo, M.; Sun, W.; Ellison, K. M., Immobilization of heavy metals by solidification/stabilization of co-disposed flue gas desulfurization brine and coal fly ash. Energ. Fuel. 2016, 30 (6), 5042-5051.

19. Huang, Y. H.; Peddi, P. K.; Tang, C.; Zeng, H.; Teng, X., Hybrid zero-valent iron process for removing heavy metals and nitrate from flue-gas-desulfurization wastewater. Sep. and Purif. Technol. 2013, 118, 690-698.

20. Peddi, P. Pilot-Scale Demonstration of hZVI Process for treating flue gas Desulfurization Wastewater at Plant Wansley, Carrollton, GA. 2011.

21. Huang, Y. H.; Peddi, P. K.; Zeng, H.; Tang, C.-L.; Teng, X., Pilot-scale demonstration of the hybrid zero-valent iron process for treating flue-gas-desulfurization wastewater: Part I. Water. Sci. & Technol. 2012, 67 (1), 16-23.

22. Huang, Y. H.; Peddi, P. K.; Zeng, H.; Tang, C.-L.; Teng, X., Pilot-scale demonstration of the hybrid zero-valent iron process for treating flue-gas-desulfurization wastewater: Part II. Water. Sci. & Technol. 2013, 67 (2), 239-246.

23. Sonstegard, J.; Pickett, T.; Harwood, J.; Johnson, D., Full scale operation of GE ABMet® biological technology for the removal of selenium from FGD wastewaters. IWC 2008, 8, 31.

24. Li, X.; Cao, J.; Zhang, W., Stoichiometry of Cr (VI) immobilization using nanoscale zerovalent iron (nZVI): a study with high-resolution X-ray photoelectron spectroscopy (HR-XPS). Ind. Eng. Chem. Res. 2008, 47 (7), 2131-2139.

25. Mohan, D.; Pittman, C. U., Activated carbons and low cost adsorbents for remediation of tri-and hexavalent chromium from water. J. of Hazard. Mater. 2006, 137 (2), 762-811.

26. Skovbjerg, L. L.; Stipp, S. L. S.; Utsunomiya, S.; Ewing, R., The mechanisms of reduction of hexavalent chromium by green rust sodium sulphate: Formation of Cr-goethite. Geochim. Cosmochim. Ac. 2006, 70 (14), 3582-3592.

27. Molin, M.; Ulven, S. M.; Meltzer, H. M.; Alexander, J., Arsenic in the human food chain, biotransformation and toxicology–Review focusing on seafood arsenic. J. Trace. Elem. Med. Bio. 2015, 31, 249-259.

28. Mohan, D.; Pittman Jr, C. U., Arsenic removal from water/wastewater using adsorbents—a critical review. J. Hazard. Mater. 2007, 142 (1-2), 1-53.

29. Waalkes, M. P., Cadmium carcinogenesis in review. J. Inorg. Biochem. 2000, 79 (1-4), 241-244.

30. Rao, K.; Mohapatra, M.; Anand, S.; Venkateswarlu, P., Review on cadmium removal from aqueous solutions. Inter. J of Eng., Sci. and Technol. 2010, 2 (7).

31. Huang, Y. H.; Tang, C.; Zeng, H., Removing molybdate from water using a hybridized zero-valent iron/magnetite/Fe (II) treatment system. Chem. Eng. J. 2012, 200, 257-263.

32. Liang, L.; Yang, W.; Guan, X.; Li, J.; Xu, Z.; Wu, J.; Huang, Y.; Zhang, X., Kinetics and mechanisms of pH-dependent selenite removal by zero valent iron. Water. Res. 2013, 47 (15), 5846-5855.

33. Wang, C.-B.; Zhang, W.-X., Synthesizing nanoscale iron particles for rapid and complete dechlorination of TCE and PCBs. Environ. Sci. & Technol. 1997, 31 (7), 2154-2156.

34. Zhang, P.; Tao, X.; Li, Z.; Bowman, R. S., Enhanced perchloroethylene reduction in column systems using surfactant-modified zeolite/zero-valent iron pellets. Environ. Sci. Technol. 2002, 36 (16), 3597-3603.

35. Zhang, Y.; Wang, J.; Amrhein, C.; Frankenberger, W. T., Removal of selenate from water by zerovalent iron. J. Environ. Qual. 2005, 34 (2), 487-495.

36. Xie, Y.; Cwiertny, D. M., Influence of anionic cosolutes and pH on nanoscale zerovalent iron longevity: time scales and mechanisms of reactivity loss toward 1, 1, 1, 2-tetrachloroethane and Cr (VI). Environ. Sci. Technol. 2012, 46 (15), 8365-8373.

37. Su, C.; Puls, R. W., Arsenate and arsenite removal by zerovalent iron: kinetics, redox transformation, and implications for in situ groundwater remediation. Environ. Sci. & Technol. 2001, 35 (7), 1487-1492.

38. Tyrovola, K.; Nikolaidis, N. P.; Veranis, N.; Kallithrakas-Kontos, N.; Koulouridakis, P. E., Arsenic removal from geothermal waters with zero-valent iron—effect of temperature, phosphate and nitrate. Water Res. 2006, 40 (12), 2375-2386.

39. Génin, J.-M.; Olowe, A.; Refait, P.; Simon, L., On the stoichiometry and pourbaix diagram of Fe (II)-Fe (III) hydroxy-sulphate or sulphate-containing green rust 2: An electrochemical and Mössbauer spectroscopy study. Corros. Sci. 1996, 38 (10), 1751-1762.

40. Refait, P.; Génin, J.-M., The oxidation of ferrous hydroxide in chloride-containing aqueous media and Pourbaix diagrams of green rust one. Corros. Sci. 1993, 34 (5), 797-819.

41. Refait, P.; Simon, L.; Génin, J.-M. R., Reduction of SeO42-anions and anoxic formation of iron (II)-iron (III) hydroxy-selenate green rust. Environ. Sci. Technol. 2000, 34 (5), 819-825.

42. Bernal, J.; Dasgupta, D.; Mackay, A., The oxides and hydroxides of iron and their structural inter-relationships. Clay. Miner. Bull. 1959, 4 (21), 15.

43. Hayashi, H.; Kanie, K.; Shinoda, K.; Muramatsu, A.; Suzuki, S.; Sasaki, H., pH-dependence of selenate removal from liquid phase by reductive Fe (II)–Fe (III) hydroxysulfate compound, green rust. Chemosphere 2009, 76 (5), 638-643.

44. Schellenger, A. E.; Larese-Casanova, P., Oxygen Isotope Indicators of Selenate Reaction with Fe (II) and Fe (III) Hydroxides. Environ. Sci. Technol. 2013, 47 (12), 6254-6262.

45. Myneni, S.; Tokunaga, T. K.; Brown, G., Abiotic selenium redox transformations in the presence of Fe (II, III) oxides. Science 1997, 278 (5340), 1106-1109.

46. Zingaro, R. A.; Carl Dufner, D.; Murphy, A. P.; Moody, C. D., Reduction of oxoselenium anions by iron (II) hydroxide. Environ. Int. 1997, 23 (3), 299-304.

47. Johnson, T. M.; Bullen, T. D., Selenium isotope fractionation during reduction by Fe (II)-Fe (III) hydroxide-sulfate (green rust). Geochim. Cosmochim. Ac. 2003, 67 (3), 413-419.

48. Williams, A. G.; Scherer, M. M., Kinetics of Cr (VI) reduction by carbonate green rust. Environ. Sci. Technol. 2001, 35 (17), 3488-3494.

49. Bond, D. L.; Fendorf, S., Kinetics and structural constraints of chromate reduction by green rusts. Environ. Sci. Technol. 2003, 37 (12), 2750-2757.

50. Legrand, L.; El Figuigui, A.; Mercier, F.; Chausse, A., Reduction of aqueous chromate by Fe (II)/Fe (III) carbonate green rust: kinetic and mechanistic studies. Environ. Sci. Technol. 2004, 38 (17), 4587-4595.

51. Loyaux-Lawniczak, S.; Refait, P.; Ehrhardt, J.-J.; Lecomte, P.; Génin, J.-M. R., Trapping of Cr by formation of ferrihydrite during the reduction of chromate ions by Fe (II)-Fe (III) hydroxysalt green rusts. Environ. Sci. Technol. 2000, 34 (3), 438-443.

52. Hansen, H. C. B.; Koch, C. B.; Nancke-Krogh, H.; Borggaard, O. K.; Sørensen, J., Abiotic nitrate reduction to ammonium: key role of green rust. Environ. Sci. Technol. 1996, 30 (6), 2053-2056.

53. Hansen, H. C. B.; Guldberg, S.; Erbs, M.; Bender Koch, C., Kinetics of nitrate reduction by green rusts—effects of interlayer anion and Fe (II): Fe (III) ratio. Appl. Clay. Sci. 2001, 18 (1), 81-91.

54. Erbs, M.; Bruun Hansen, H. C.; Olsen, C. E., Reductive dechlorination of carbon tetrachloride using iron (II) iron (III) hydroxide sulfate (green rust). Environ. Sci. Technol. 1999, 33 (2), 307-311.

55. Lee, W.; Batchelor, B., Abiotic reductive dechlorination of chlorinated ethylenes by iron-bearing soil minerals. 2. Green rust. Environ. Sci. Technol. 2002, 36 (24), 5348-5354.

56. O'Loughlin, E. J.; Kemner, K. M.; Burris, D. R., Effects of AgI, AuIII, and CuII on the reductive dechlorination of carbon tetrachloride by green rust. Environ. Sci. Technol. 2003, 37 (13), 2905-2912.

57. Zhang, Y.; Amrhein, C.; Frankenberger Jr, W. T., Effect of arsenate and molybdate on removal of selenate from an aqueous solution by zero-valent iron. Sci. of Total Environ. 2005, 350 (1), 1-11.

58. Gillham, R. W.; O'Hannesin, S. F., Enhanced degradation of halogenated aliphatics by zero‐valent iron. Groundwater 1994, 32 (6), 958-967.

59. Lo, I.; Lam, C. S.; Lai, K. C., Hardness and carbonate effects on the reactivity of zero-valent iron for Cr (VI) removal. Water. Res. 2006, 40 (3), 595-605.

60. Guan, X.; Sun, Y.; Qin, H.; Li, J.; Lo, I. M.; He, D.; Dong, H., The limitations of applying zero-valent iron technology in contaminants sequestration and the corresponding countermeasures: The development in zero-valent iron technology in the last two decades (1994–2014). Water Res. 2015, 75, 224-248.

61. WooáLee, J.; BináKim, S., Enhanced Cr (VI) removal using iron nanoparticle decorated graphene. Nanoscale 2011, 3 (9), 3583-3585.

62. Lv, X.; Xue, X.; Jiang, G.; Wu, D.; Sheng, T.; Zhou, H.; Xu, X., Nanoscale Zero-Valent Iron (nZVI) assembled on magnetic Fe 3 O 4/graphene for Chromium (VI) removal from aqueous solution. J. of Colloid Interf. Sci. 2014, 417, 51-59.

63. Liu, T.; Zhao, L.; Sun, D.; Tan, X., Entrapment of nanoscale zero-valent iron in chitosan beads for hexavalent chromium removal from wastewater. J. Hazard. Mater. 2010, 184 (1), 724-730.

64. Ahn, S. C.; Oh, S.-Y.; Cha, D. K., Enhanced reduction of nitrate by zero-valent iron at elevated temperatures. J. Hazard. Mater. 2008, 156 (1), 17-22.

65. Yoon, I.-H.; Kim, K.-W.; Bang, S.; Kim, M. G., Reduction and adsorption mechanisms of selenate by zero-valent iron and related iron corrosion. Appl. Catal. B: Environ. 2011, 104 (1), 185-192.

66. Qiu, S.; Lai, H.-F.; Roberson, M.; Hunt, M.; Amrhein, C.; Giancarlo, L.; Flynn, G.; Yarmoff, J., Removal of contaminants from aqueous solution by reaction with iron surfaces. Langmuir 2000, 16 (5), 2230-2236.

67. Morrison, S. J.; Metzler, D. R.; Dwyer, B. P., Removal of As, Mn, Mo, Se, U, V and Zn from groundwater by zero-valent iron in a passive treatment cell: reaction progress modeling. J. Contam. Hydrol. 2002, 56 (1), 99-116.

68. Kanel, S. R.; Greneche, J.-M.; Choi, H., Arsenic (V) removal from groundwater using nano scale zero-valent iron as a colloidal reactive barrier material. Environ. Sci. Technol. 2006, 40 (6), 2045-2050.

69. Jönsson, J.; Sherman, D. M., Sorption of As (III) and As (V) to siderite, green rust (fougerite) and magnetite: Implications for arsenic release in anoxic groundwaters. Chem. Geol. 2008, 255 (1-2), 173-181.

70. Su, C.; Puls, R. W., Significance of iron (II, III) hydroxycarbonate green rust in arsenic remediation using zerovalent iron in laboratory column tests. Environ. Sci. Technol. 2004, 38 (19), 5224-5231.

71. Randall, S. R.; Sherman, D. M.; Ragnarsdottir, K. V., Sorption of As (V) on green rust (Fe4 (II) Fe2 (III)(OH) 12SO4· 3H2O) and lepidocrocite (γ-FeOOH): Surface complexes from EXAFS spectroscopy. Geochim. Cosmochim. Ac. 2001, 65 (7), 1015-1023.

72. Li, X.-q.; Zhang, W.-x., Sequestration of metal cations with zerovalent iron nanoparticles a study with high resolution X-ray photoelectron spectroscopy (HR-XPS). J. Phys. Chem. C 2007, 111 (19), 6939-6946.

73. Su, Y.; Adeleye, A. S.; Huang, Y.; Sun, X.; Dai, C.; Zhou, X.; Zhang, Y.; Keller, A. A., Simultaneous removal of cadmium and nitrate in aqueous media by nanoscale zerovalent iron (nZVI) and Au doped nZVI particles. Water. Res. 2014, 63, 102-111.

74. Boparai, H. K.; Joseph, M.; O'Carroll, D. M., Kinetics and thermodynamics of cadmium ion removal by adsorption onto nano zerovalent iron particles. J. Hazard. Mater. 2011, 186 (1), 458-465.

75. O'Loughlin, E. J.; Kelly, S. D.; Kemner, K. M.; Csencsits, R.; Cook, R. E., Reduction of AgI, AuIII, CuII, and HgII by FeII/FeIII hydroxysulfate green rust. Chemosphere 2003, 53 (5), 437-446.

76. Batchelor, B., Overview of waste stabilization with cement. Waste Manage.2006, 26, 689–698.

77. Qian, G., Y. Cao, P. Chui, and J. Tay, Utilization of MSWI fly ash for stabilization/solidification of industrial waste sludge. J. Hazard. Mater. 2006, B129, 274-281.

78. Ramgobeen, D. "Preparation and testing of chloride & sulphate containing minerals from industrial wastes", solidification/stabilisation of chloride & sulphate ions from APC residues with calcium aluminate cements. University College of London, London, England, 2010.

79. 25 Pennsylvania Code Chapter 95: Wastewater treatment requirements. In 25 Pennsylvania Code Chapter 95 Board, T. E. Q., Ed. The Pennyslvania Bulletin: 2010.

80. Kumpienem, J., A. Lagerkvist, and C. Maurice, Stabilization of Pb- and Cu-contaminated soil using coal fly ash and peat. Environ. Pollut. 2007, 145, 365-373.

81. Keller, I. R. B. The immobilisation of heavy metals and metalloids in cement stabilised wastes: A study focusing on the selenium oxyanions SeO_3^{2-} and SeO_4^{2-}. Swiss Federal Institute of Technology, Zurich, Switzerland, 2002.

82. Kameswari, K. S. B., A.G. Bhole, and R. Paramasivam, Evaluation of solidification/stabilization (S/S) process for the disposal of arsenic-bearing sludges in landfill sites. Environ. Eng. Sci. 2001, 18, 167-176.

83. Kamon, M., T. Katsumi, and Y. Sano MSW Fly ash stabilized with coal ash for geotechnical application. J. Hazard. Mater. 2000, 76, 265-283.

84. Terzano, R., M. Spagnuolo, L. Medici, B. Vekemans, L. Vincze, K. Janssens, and P. Ruggiero, Copper stabilization by zeolite synthesis in polluted soils treated with coal fly ash. Environ.Sci. & Technol. 2005, 39, 6280-6287.

85. Singh, T. S., K. K. Pant, Solidification/stabilization of arsenic containing solid wastes using portland cement, fly ash and polymeric Materials. J. Hazard. Mater. 2006, B131, 29–36.

86. Mickley, M., Survey of high recovery and zero liquid discharge technologies for water utilities. Foundation, W. R., Ed. Water Reuse Foundation: Alexandria, Virginia, 2008.

87. Paria, S., and P. K. Yuet, Solidification-stabilization of organic and inorganic contaminants using portland cement: A literature review. Environ. Rev. 2006, 14, 217-255.

88. Yilmaz, O., K. Unlu, and E. Cokca, Solidification/dtabilization of hazardous eastes containing metals and organic contaminants. J. Environ. Eng. 2003, (129), 366-376.

89. Valls, S., and E. Vazquez, Leaching properties of stabilised/solidified cement-admixtures-sewage sludges systems. Waste Ma. 2002, 22, 37-45.

90. Su, D. C., and J. W. C. Wong, Chemical speciation and phytoavailability of Zn, Cu, Ni and Cd in soil amended with fly ash-stabilized sewage sludge. Environ.Inter. 2003, 29, 895– 900.

91. Solem-Tishmack, J. K., G. J. McCarthy, High-calcium combustion by-products: engineering properties, ettringite formation, and potential application in solidification and stabilization of selenium and boron. Cement Concrete Res. 1995, 25, 658-670.

92. Pereira, C. F., M. Rodriguez-Piñero, and J. Vale, Solidification/stabilization of electric arc furnace dust using coal fly ash analysis of the stabilization process. J. Hazard. Mater. 2001, B82, 183-195.

93. Moon, D. H., D. G. Grubb, and T. L. Reilly, Stabilization/solidification of selenium-impacted soils using portland cement and cement kiln dust. J. Hazard. Mater. 2009, 168, 944–951.

94. Mangialardi, T., A. E. Paolini, A. Polettini, and P. Sirini, Optimization of the solidification/stabilization process of MSW fly ash in cementitious matrices. J. Hazard. Mater. 1999, B70, 53-70.

95. Li, X. D., C. S. Poona, H. Suna, I. M. C. Lob, and D. W. Kirk, Heavy metal speciation and leaching behaviors in cement based solidified/stabilized waste materials. J. Hazard. Mater. 2001, A82, 215–230.

96. Akhter, H., F. K. Cartledge, A. Roy, and M. E. Tittlebaum, Solidification/stabilization of arsenic salts: Effects of long cure times. J. Hazard. Mater. 1997, 52, 247-264.

97. Singh, M., and M. Gart, Cementitious Binder from Fly ash and other industrial wastes. Cement and Concr. Res. 1999, 29, 309–314.

98. Mahlaba, J. S., E.P. Kearsley, and R. A. Kruger, Effect of fly ash characteristics on the behavior of paste prepared under varied brine conditions. Miner. Eng. 2011, 24, 1077-1081.

99. Mahlaba, J. S., E. P. Kearsley, R. A. Kruger, and P. C. Pretorius, Evaluation of workability and strength development of fly ash pastes prepared with industrial brines rich in SO_4^{2-} and Cl^- to expand brine utilization. Miner. Eng. 2011, 24, 1077-1081.

100. Mahlaba, J. S., E. P. Kearsley, and R. A. Kruger, Physical, chemical, and mineralogical characteristics of hydraulically disposed fine coal fly ash from SASOL synfuels. Mine. Eng. 2011.

101. Mahlaba, J. S., P. C. Pretorius, and M. P. Augustyn influence of admixtures on paste behaviour and the role of surface area on remobilization. In 11th International Seminar on Thickened Tailings and Paste, Botswana, 2006.

102. Mahlaba, J. S. Evaluation of paste technology to co-dispose of ash and brines sasol synfuels complex. University of the Witwatersrand, Johannesburg, South Africa, 2006.

103. Kaplan, D. I., K. Roberts, J. Coates, M. Siegfried, and S. Serkiz, Saltstone and concrete interactions with radionuclides: sorption (Kd), desorption, and reduction Capacity measurements. United States Department of Energy: Savannah River Site, Aiken, South Carolina, 2008.

104. Connor, J. R., and S. L. Hoeffner, A critical review of stabilization/solidification technology. Critical Rev. Environ. Sci. Technol. 1996, 28 (4), 397-462.

105. Dhir, R. K., and M.R. Jones Development of chloride resisting concrete using fly ash. Fuel 2006, 78, 137-142.

106. Kumpienem, J., A. Lagerkvist, and C. Maurice, Stabilization of Pb- and Cu-contaminated soil using coal fly ash and peat. Environ. Pollut. 2007, 145, 365-373.

107. Connor, J. R., Guide to improving the effectiveness of cement-based stabilization/solidification. Portland Cement Association: Skokie, Illinois, 1997.

108. Page, A.; Elseewi, A. A.; Straughan, I., Physical and chemical properties of fly ash from coal-fired power plants with reference to environmental impacts. In Residue Reviews, Springer: 1979; pp 83-120.

109. USEIA, Annual Coal Report. 2017.

110. Papadakis, V. G., Effect of fly ash on portland cement systems: Part II. High-Calcium Fly Ash. Cement Concrete Res. 2000, 30 (10), 1647-1654.

111. Dai, Y.; Qian, G.; Cao, Y.; Chi, Y.; Xu, Y.; Zhou, J.; Liu, Q.; Xu, Z. P.; Qiao, S., Effective removal and fixation of Cr (VI) from aqueous solution with Friedel's salt. J. Hazard. Mater. 2009, 170 (2), 1086-1092.

112. Wu, Y.; Chi, Y.; Bai, H.; Qian, G.; Cao, Y.; Zhou, J.; Xu, Y.; Liu, Q.; Xu, Z. P.; Qiao, S., Effective removal of selenate from aqueous solutions by the Friedel phase. J. Hazard. Mater. 2010, 176 (1), 193-198.

113. Baur, I.; Johnson, C. A., Sorption of selenite and selenate to cement minerals. Environ. Sci. Technol. 2003, 37 (15), 3442-3447.

114. Ke, X.; Bernal, S. A.; Provis, J. L., Uptake of chloride and carbonate by Mg-Al and Ca-Al layered double hydroxides in simulated pore solutions of alkali-activated slag cement. Cement Concrete Res. 2017, 100, 1-13.

115. Li, Z.; Jiang, Y.; Yang, X., Synthesis, characterization and formation mechanism of friedel's salt (FS: 3CaO· Al2O3· CaCl2· 10H2O) by the reaction of calcium chloride with sodium aluminate. J. Mater. Sci. 2015, 30 (1), 76-83.

116. Birnin-Yauri, U.; Glasser, F., Friedel's salt, Ca 2 Al (OH) 6 (Cl, OH)· 2H 2 O: its solid solutions and their role in chloride binding. Cement Concrete Res. 1998, 28 (12), 1713-1723.

117. Chrysochoou, M.; Dermatas, D., Evaluation of ettringite and hydrocalumite formation for heavy metal immobilization: literature review and experimental study. J. Hazard. Mater. 2006, 136 (1), 20-33.

118. Alpaslan, B.; Yukselen, M. A., Remediation of lead contaminated soils by stabilization/solidification. Water, Air, and Soil Pollut. 2002, 133 (1-4), 253-263.

119. Dermatas, D.; Meng, X., Stabilization/solidification (S/S) of heavy metal contaminated soils by means of a quicklime-based treatment approach. In stabilization and solidification of hazardous, radioactive, and mixed wastes: 3rd Volume, ASTM International: 1996.

120. Can, C.; Weiqiang, X.; Xiaoming, L.; Qi, Y.; Zhenyu, Z.; Xunfeng, C.; Yan, W.; Yu, Z., Solidification/stabilization treatment of Pb and Zn in tailing waste using cement, fly ash and quick lime. 2015.

121. Steam Electric Power Generation Point Source Category: Final Detailed Study Report. USEPA,Washington, DC, 2009.

122. Taylor, H. F., Cement chemistry. Thomas Telford: 1997.

123. Glasser, F., Chemistry of cement-solidified waste forms. Lewis Publishers: Boca Raton, FL: 1993; pp 1-39.

124. Gougar, M.; Scheetz, B.; Roy, D., Ettringite and CSH portland cement phases for waste ion immobilization: A review. Waste Manage. 1996, 16 (4), 295-303.

125. Matschei, T.; Lothenbach, B.; Glasser, F. P., The AFm phase in portland cement. cement concrete res. 2007, 37 (2), 118-130.

126. Wu, Y.; Chi, Y.; Bai, H.; Qian, G.; Cao, Y.; Zhou, J.; Xu, Y.; Liu, Q.; Xu, Z. P.; Qiao, S., Effective removal of selenate from aqueous solutions by the friedel phase. J. Hazard. Mater. 2010, 176 (1–3), 193-198.

127. Chrysochoou, M.; Dermatas, D.; Meng, X., Evaluation of ettringite and hydrocalumite formation for heavy metal immobilization: literature review and experimental study. J. Hazard. Mater. 2006, 136 (1), 20-33.

128. Goñi, S.; Guerrero, A.; Hernández, M. S., Spanish LLW and MLW Disposal: durability of cemented materials in (Na, K)Cl simulated radioactive liquid waste. Waste Manage. 2001, 21 (1), 69-77.

129. Lampris, C. Solidification/stabilisation of air pollution control residues from municipal solid waste incineration. Imperial College London, London, 2013.

130. Lampris, C.; Stegemann, J. A.; Cheeseman, C. R., Solidification/stabilisation of air pollution control residues using portland cement: physical properties and chloride leaching. Waste Manage. 2009, 29 (3), 1067-1075.

131. Ramgobeen, D. "Preparation and testing of chloride & sulphate containing minerals from industrial wastes", solidification/stabilisation of chloride & culphate ions from APC residues with calcium aluminate cements. University College of London, London, England, 2010.

132. Kellie, S.; Cao, Y.; Duan, Y.; Li, L.; Chu, P.; Mehta, A.; Carty, R.; Riley, J. T.; Pan, W., Factors affecting mercury speciation in a 100-MW coal-fired boiler with low-NO x burners. Energ. Fuel. 2005, 19 (3), 800-806.

133. Richardson, S. D.; Thruston, A. D.; Rav-Acha, C.; Groisman, L.; Popilevsky, I.; Juraev, O.; Glezer, V.; McKague, A. B.; Plewa, M. J.; Wagner, E. D., Tribromopyrrole, brominated acids, and other disinfection byproducts produced by disinfection of drinking water rich in bromide. Environ. Sci. Technol. 2003, 37 (17), 3782-3793.

134. Richardson, S. D., Disinfection by-products and other emerging contaminants in drinking water. TrAC Trends in Anal. Chem. 2003, 22 (10), 666-684.

135. Noda, N.; Ito, S.; Nunome, Y.; Ueki, Y.; Yoshiie, R.; Naruse, I., Volatilization characteristics of boron compounds during coal combustion. Proceedings of the Combustion Institute 2013, 34 (2), 2831-2838.

136. Davidson, G. R.; Bassett, R. L., Application of boron isotopes for identifying contaminants such as fly ash leachate in groundwater. Environ. Sci. Technol. 1993, 27 (1), 172-176.

137. Ruhl, L. S.; Dwyer, G. S.; Hsu-Kim, H.; Hower, J. C.; Vengosh, A., Boron and strontium isotopic characterization of coal combustion residuals: validation of new environmental tracers. Environ. Sci. Technol. 2014, 48 (24), 14790-14798.

138. Williams, L. B.; Hervig, R. L., Boron isotope composition of coals: a potential tracer of organic contaminated fluids. Appl. Geochem. 2004, 19 (10), 1625-1636.

139. Spivack-Brindorf, L.; Stewart, B. In Use of boron isotopes to track the interaction of coal utilization byproducts with water and the environment, The Geological Society of America, 2006 Philadelphia Annual Meeting, 2006.

140. Jankowski, J.; Ward, C. R.; French, D.; Groves, S., Mobility of trace elements from selected Australian fly ashes and its potential impact on aquatic ecosystems. Fuel 2006, 85 (2), 243-256.

141. Kaakinen, J. W.; Jorden, R. M.; Lawasani, M. H.; West, R. E., Trace element behavior in coal-fired power plant. Environ. Sci. Technol. 1975, 9 (9), 862-869.

142. Hansen, L. D.; Fisher, G. L., Elemental distribution in coal fly ash particles. Environ. Sci. Technol. 1980, 14 (9), 1111-1117.

143. Querol, X.; Fernández-Turiel, J.; López-Soler, A., Trace elements in coal and their behaviour during combustion in a large power station. Fuel 1995, 74 (3), 331-343.

144. Cox, J. A.; Lundquist, G. L.; Przyjazny, A.; Schmulbach, C. D., Leaching of boron from coal ash. Environ. Sci. Technol. 1978, 12 (6), 722-723.

145. Kitano, Y.; Okumura, M.; Idogaki, M., Coprecipitation of borate-boron with calcium carbonate. Geochem. J. 1978, 12 (3), 183-189.

146. Hollis, J.; Keren, R.; Gal, M., Boron release and sorption by fly ash as affected by pH and particle size. J. Environ. Qual. 1988, 17 (2), 181-184.

147. Solem-Tishmack, J.; McCarthy, G.; Docktor, B.; Eylands, K.; Thompson, J.; Hassett, D., High-calcium coal combustion by-products: engineering properties, ettringite formation, and potential application in solidification and stabilization of selenium and boron. Cement Concrete Res. 1995, 25 (3), 658-670.

148. Bothe, J. V.; Brown, P., Phase formation in the system $CaO–Al_2O_3–B_2O_3–H_2O$ at 23±1° C. J. Hazard. Mater. 1998, 63 (2), 199-210.

149. Zhang, M.; Reardon, E. J., Removal of B, Cr, Mo, and Se from wastewater by incorporation into hydrocalumite and ettringite. Environ. Sci. Technol. 2003, 37 (13), 2947-2952.

150. Clark, B.; Brown, P., The formation of calcium sulfoaluminate hydrate compounds: Part II. Cement Concrete Res. 2000, 30 (2), 233-240.

151. Clark, B.; Brown, P., The formation of calcium sulfoaluminate hydrate compounds: Part I. Cement Concrete Res. 1999, 29 (12), 1943-1948.

152. Baur, I.; Johnson, C. A., The solubility of selenate-AFt ($3CaO\cdot Al_2O_3\cdot 3CaSeO_4\cdot 37.5\ H_2O$) and selenate-AFm ($3CaO\cdot Al_2O_3\cdot CaSeO_4\cdot xH_2O$). Cement Concrete Res. 2003, 33 (11), 1741-1748.

153. Perkins, R. B.; Palmer, C. D., Solubility of chromate hydrocalumite ($3CaO\cdot Al_2O_3\cdot 3CaCrO_4\cdot nH_2O$) 5–75 C. Cement Concrete Res. 2001, 31 (7), 983-992.

154. Perkins, R. B.; Palmer, C. D., Solubility of $Ca_6[Al(OH)_6]$ $(CrO_4)_3 \cdot 26H_2O$, the chromate analog of ettringite; 5–75 C. Appl Geochem 2000, 15 (8), 1203-1218.

155. Damidot, D.; Glasser, F. P., Thermodynamic investigation of the $CaO \cdot Al_2O_3 \cdot 3CaSO_4 \cdot H_2O$ system at 50° C and 85° C. Cement Concrete Res. 1992, 22 (6), 1179-1191.

156. McCarthy, G. J.; Hassett, D. J.; Bender, J. A. In Synthesis, crystal chemistry and stability of ettringite, a material with potential applications in hazardous waste immobilization, MRS Proceedings, Cambridge Univ Press: 1991; p 129.

157. Klemm, W. A.; Bhatty, J. I.; Association, P. C., Fixation of heavy metals as oxyanion-substituted ettringites. Portland Cement Association: 2002.

158. Albino, V.; Cioffi, R.; Marroccoli, M.; Santoro, L., Potential application of ettringite generating systems for hazardous waste stabilization. J. Hazard. Mater. 1996, 51 (1), 241-252.

159. Ghosh, A.; Subbarao, C., Hydraulic conductivity and leachate characteristics of stabilized fly ash. J. Environ. Eng. 1998, 124 (9), 812-820.

160. Mahlaba, S. J., Evaluation of paste technology to co-dispose of ash and brines at Sasol Synfuels complex. 2006.

161. Bowders Jr, J. J.; Gidley, J. S.; Usmen, M. A., Permeability and leachate characteristics of stabilized class F fly ash. Transport. Res. Rec. 1990, (1288).

162. Shao, Y.; Zhou, M.; Wang, W.; Hou, H., Identification of chromate binding mechanisms in Friedel's salt. Constr. Build. Mater. 2013, 48, 942-947.

163. Zhang, D.; Jia, Y.; Ma, J.; Li, Z., Removal of arsenic from water by Friedel's salt (FS: 3CaO· Al2O3· CaCl2· 10H2O). J. Hazard. Mater. 2011, 195, 398-404.

164. Li, D.; Guo, X.; Tian, Q.; Xu, Z.; Xu, R.; Zhang, L., Synthesis and application of Friedel's salt in arsenic removal from caustic solution. Chem. Eng. J. 2017, 323, 304-311.

165. Yao, J.; Kong, Q.; Zhu, H.; Shen, D.; Zhang, Z., Adsorption properties of Friedel's salt for the nitrate in the landfill. Korean. J. Chem. Eng. 2016, 33 (2), 553-558.

166. Yao, J.; Kong, Q.; Zhu, H.; Long, Y.; Shen, D., Adsorption characteristics of nitrite on Friedel's salt under the landfill circumstance. Chem. Eng. J. 2014, 254, 479-485.

167. Matschei, T.; Lothenbach, B.; Glasser, F. P., Thermodynamic properties of Portland cement hydrates in the system $CaO–Al_2O_3–SiO_2–CaSO_4–CaCO_3–H_2O$. Cement Concrete Res. 2007, 37 (10), 1379-1410.

168. Shi, Z.; Geiker, M. R.; De Weerdt, K.; Østnor, T. A.; Lothenbach, B.; Winnefeld, F.; Skibsted, J., Role of calcium on chloride binding in hydrated Portland cement–metakaolin–limestone blends. Cement Concrete Res. 2017, 95, 205-216.

169. Saikia, N.; Kato, S.; Kojima, T., Thermogravimetric investigation on the chloride binding behaviour of MK–lime paste. Thermochim. Acta. 2006, 444 (1), 16-25.

170. USEPA, Method 1311. Toxicity Characteristic Leaching Procedure, 1990.

171. USEPA, Method 1313. Leaching Test (Liquid–Solid Partitioning as a Function of Extract pH) of Inorganic Species in Solid Materials Using a Parallel Batch Extraction Test, 2009.

172. USEPA, Method 1315. Mass Transfer Rates of Constituents in Monolithic or Compacted Granular Materials Using a Semi-Dynamic Tank Leaching Procedure, 2013.

173. USEPA, Effluent Limitations Guidelines and Standards for the Steam Electric Power Generating Point Source Category; Final Rule, 40 CFR Part 423, Federal Register. 2015.

174. Vollprecht, D.; Krois, L.-M.; Sedlazeck, K. P.; Müller, P.; Mischitz, R.; Olbrich, T.; Pomberger, R., Removal of critical metals from waste water by zero-valent iron. J. Clean. Prod. 2019, 208, 1409-1420.

175. Sarathy, V.; Tratnyek, P. G.; Nurmi, J. T.; Baer, D. R.; Amonette, J. E.; Chun, C. L.; Penn, R. L.; Reardon, E. J., Aging of iron nanoparticles in aqueous solution: effects on structure and reactivity. J. Phy. Chem. C 2008, 112 (7), 2286-2293.

176. Lewis, D. G., Factors influencing the stability and properties of green rusts. Catena Verlag: 1997.

177. Xiong, Z.; Zhao, D.; Pan, G., Rapid and complete destruction of perchlorate in water and ion-exchange brine using stabilized zero-valent iron nanoparticles. Water. Res. 2007, 41 (15), 3497-3505.

178. Hwang, Y.; Kim, D.; Shin, H.-S., Inhibition of nitrate reduction by NaCl adsorption on a nano-zero-valent iron surface during a concentrate treatment for water reuse. Environ. Technol. 2015, 36 (9), 1178-1187.

179. Müller, P.; Lorber, K.; Mischitz, R.; Weiß, C., Implementation of fluidized granulated iron reactors in a chromate remediation process. Sci. Total. Environ. 2014, 485, 748-754.

180. Huang, X.-y.; Ling, L.; Zhang, W.-x., Nanoencapsulation of hexavalent chromium with nanoscale zero-valent iron: High resolution chemical mapping of the passivation layer. J.Environ. Sci. 2018, 67, 4-13.

181. Zou, H.; Hu, E.; Yang, S.; Gong, L.; He, F., Chromium (VI) removal by mechanochemically sulfidated zero valent iron and its effect on dechlorination of trichloroethene as a co-contaminant. Sci. Total. Environ. 2019, 650, 419-426.

182. Das, S.; Lindsay, M. B.; Essilfie-Dughan, J.; Hendry, M. J., Dissolved selenium (VI) removal by zero-valent iron under oxic conditions: influence of sulfate and nitrate. ACS Omega 2017, 2 (4), 1513-1522.

183. Liu, T.; Li, X.; Waite, T. D., Depassivation of aged Fe0 by divalent cations: correlation between contaminant degradation and surface complexation constants. Environ. Sci. Technol. 2014, 48 (24), 14564-14571.

184. 2013 Coal Combustion Product (CCP) Production & Use Survey Report; American Coal Ash Association: 2013.

185. USEPA, Kingston TVA Project Completion Fact Sheet 2014.

186. Ruhl, L.; Vengosh, A.; Dwyer, G. S.; Hsu-Kim, H.; Deonarine, A.; Bergin, M.; Kravchenko, J., Survey of the potential environmental and health impacts in the immediate aftermath of the coal ash spill in Kingston, Tennessee. Environ. Sci. Technol. 2009, 43 (16), 6326-6333.

187. USEPA, Disposal of Coal Combustion Residuals from Electric Utilities, 2015.

188. Zou, Y.; Wang, X.; Khan, A.; Wang, P.; Liu, Y.; Alsaedi, A.; Hayat, T.; Wang, X., Environmental remediation and application of nanoscale zero-valent iron and its composites for the removal of heavy metal ions: a review. Environ. Sci. Technol. 2016, 50 (14), 7290-7304.

189. Zhang, W., Oswal, H., Renew, J., Ellison, K., Huang, C., Removal of heavy metals by aged zero-valenet iron in flue-gas-desulfurization brine under high salt and temperature conditions. J. Hazard. Mater. 2019.

190. Huang, C.; Renew, J. E. Immobilization of Heavy Metals by Solidification/stabilization in co-disposed coal fly ash and concentrated flue gas desulfurization wastewater brines; Environmental Research and Education Foundation Charlotte, North Carolina, 2016.

191. Renew, J. E.; Huang, C.-H.; Burns, S.; Carrasquillo, M., Immobilization of heavy metals by solidification / stabilization in co-disposed coal fly ash and concentrated flue gas desulfurization wastewater brines. In International Water Conference Orlando, Florida, 2013.

192. Renew, J. E.; Huang, C.-H.; Burns, B.; Carrasquillo, M., Immobilization of heavy metals by solidification / stabilization in co-disposed coal fly ash and concentrated flue gas desulfurization wastewater brines. In Power Plant Pollutant Control “MEGA” Symposium, Baltimore, Maryland, 2014.

193. Novotny, E. V., and H. G. Stefan, Projections of chloride concentrations in urban lakes receiving road de-icing salt. Water, Air, & Soil Pollut. 2010, 211, 261-271.

194. Boelter, A. M., F. N. Lamming, A. M. Farag, and H. L. Bergman, Environmental Effects of Saline Oil-Field Discharges on Surface Waters. Environ. Toxicol. and Chem. 1992, 11, 1187-1195.

195. Langen, T. A., M. Twiss, T. Young, K. Janoyan, J. C. Stager, J. Osso, H. Prutzman, and B. Green, Environmental impacts of winter road management at the cascade lakes and chapel pond; Clarkson Center for the Environment: Potsdam, New York, 2006.

196. Nelson, S. S.; Yongek, D. R.; Barber, M. E., Effects of road salts on heavy metal mobility in two eastern Washington soils. J.Environ.Eng. 2009, 135, 505-510.

197. Ma, J.; Li, Z.; Zhang, Y.; Demopoulos, G. P., Desilication of sodium aluminate solution by Friedel's salt (FS: $3CaO{\cdot}A1_2O_3{\cdot}CaCl_2{\cdot}10H_2O$). Hydrometallurgy 2009, 99 (3-4), 225-230.

198. Prasanna, S. V.; Kamath, P. V.; Shivakumara, C., Synthesis and characterization of layered double hydroxides (LDHs) with intercalated chromate ions. Mater. Res. Bull. 2007, 42 (6), 1028-1039.

199. Roeffaers, M. B.; Sels, B. F.; Loos, D.; Kohl, C.; Müllen, K.; Jacobs, P. A.; Hofkens, J.; De Vos, D. E., In situ space and time resolved sorption kinetics of anionic dyes on individual LDH crystals. Chemphyschem 2005, 6 (11), 2295-2299.

200. Glasser, F.; Kindness, A.; Stronach, S., Stability and solubility relationships in AFm phases: Part I. Chloride, sulfate and hydroxide. Cement Concrete Res. 1999, 29 (6), 861-866.

201. Marcus, Y., Ionic radii in aqueous solutions. Chem. Rev. 1988, 88 (8), 1475-1498.